Cytochrome *c* release from brain mitochondria in response to respiratory inhibition

Rebecca Clayton

A thesis submitted as partial fulfilment for the degree of Doctor of Philosophy in the Faculty of Science at the University of London

September 2003

Department of Molecular Neuroscience
Division of Neurochemistry
Institute of Neurology
Queen Square
London
WC1N 3BG

ProQuest LLC
789 East Eisenhower Parkway
P.O. Box 1346
Ann Arbor, MI 48106-1346

Abstract

Apoptosis is the programmed cell death mechanism responsible for regulation of cell number during tissue development and maturity. However, dysregulation of apoptosis has pathological consequences, particularly in the brain, where 'inappropriate' apoptosis leads to neurodegeneration.

Neuronal apoptosis is primarily initiated by release of the respiratory protein cytochrome *c* from mitochondria, the organelles responsible for aerobic respiration. Considerable interest has been focussed on the mechanism of cytochrome *c* release, but surprisingly little on the nature of the cytochrome *c* signal itself. It has been claimed that release is all-or-none, however this is inconsistent with accumulating evidence of cytosolic mechanisms for 'buffering' cytochrome *c*.

This study has addressed two primary methodological weaknesses in the field, by modelling an underlying disease pathology, rather than artificially inducing apoptosis, and by using a truly quantitative assay for measuring cytochrome *c* concentration. These experimental advantages have yielded the first demonstration that cytochrome *c* is released in proportion to the severity of pathological insult. The model adopted was reduced activity of the mitochondrial NADH:ubiquinone oxidoreductase, a recognised feature of Parkinson's disease, induced in this case by rotenone titration.

The controlled, proportional release observed invited the hypothesis that a low level of cytochrome *c* release is insufficient to induce apoptosis. In support of this suggestion, the mechanism of release was determined to be conducive to cell survival

given hypothetical 'sub-threshold' release. It was also demonstrated that release is likely to be induced following mitochondrial generation of reactive oxygen species, of which there is believed to be a constitutive basal level. Finally it was established that in primary cortical neurons, respiratory inhibition can induce cytochrome *c* release which is sub-threshold for induction of apoptosis.

The study has generated considerable support for therapeutic exploitation of the cytosolic 'Inhibitor of Apoptosis Proteins', for delaying progression of Parkinson's and other neurodegenerative diseases.

Acknowledgements

This project was enabled by the generous financial support of The Brain Research Trust.

I have been lucky enough to produce this thesis in a laboratory full of encouraging, and selfless people. I could not have hoped for a more understanding, patient and respected Head of Department and supervisor than Professor John Clark. His encouragment and apparent confidence in me have been so reassuring. This helped me through the departure of my second supervisor, Dr. Tim Bates, from whom I had learnt a great deal. At this point, I was lucky enough to 'adopt' Dr. Martyn Sharpe in his place. He has readily given help whenever I have asked, but also allowed me the freedom to address my own curiosities during the project. I am extremely grateful to Professor Clark and Dr. Sharpe, and hope that they are pleased with the result.

I am also indebted to my fellow students, two of which deserve particular mention. Claudie Hooper taught me all I know about Western blotting, and I am extremely grateful to her for her time and advice. I would also like to extend a special thank you to Susan Griffin, without whom my cell culture work would probably not have happened. She has been a third supervisor to me, and is undoubtedly the most dedicated student I have ever met.

Finally, thank you to my family and to Matt, for their continual support, encouragement and taxi services! I hope you are proud of the result.

"Writing is like getting married. One should never commit oneself until one is amazed at one's luck." - Iris Murdoch

For my fiancé, Matt and for the real Doctors Clayton

Contents

List of figures

(NSM indicates non-synaptic mitochondria, SM indicates synaptic mitochondria)

List of tables

(NSM indicates non-synaptic mitochondria, SM indicates synaptic mitochondria)

Abbreviations

ADP	-	adenosine diphosphate
AIF	-	apoptosis inducing factor
AK	-	adenylate kinase
AMP	-	adenosine monophosphate
ANT	-	adenine nucleotide translocator
Apaf-1	-	apoptosis protease activating factor-1
ATP	-	adenosine triphosphate
BIRP	-	baculovirus IAP repeat-containing protein
BSA	-	bovine serum albumin (fatty acid free)
CARD	-	caspase recruitment domain
CCHL	-	cytochrome *c* heme lyase
CCR	-	cytochrome *c* release
CoQ_1	-	coenzyme Q_1 (ubiquinone 5)
CS	-	citrate synthase
CsA	-	cyclosporin A
dADP	-	deoxyadenosine diphosphate
DAPI	-	4',6-diamidino-2-phenylindole
dATP	-	deoxyadenosine triphosphate
DIABLO	-	direct IAP binding protein with low pI
DNA	-	deoxyribonucleic acid
DNAse	-	deoxyribonuclease type I
DTNB	-	5,5'-dithiobis(2-nitrobenzoic acid)
DTT	-	dithiothreitol
EBSS	-	Earle's balanced salt solution

EDTA	-	ethylenediaminetetraacetic acid
EGTA	-	ethylene glyco-bis-(beta-aminoethylether)-tetraacetic acid
ELISA	-	enzyme-linked immunosorbent assay
ETC	-	electron transport chain
FAD	-	flavin adenine dinucleotide
FBS	-	foetal bovine serum
FITC	-	fluoresceineisothiocyanate
FMN	-	flavin mononucleotide
GFP	-	green fluorescent protein
GPx	-	glutathione peroxidase
GSH	-	glutathione, glutamylcysteinylglycine
GSSG	-	glutathione disulphide
HBSS	-	Hank's balanced salt solution
HPLC	-	high performance liquid chromatography
HRP	-	horseradish peroxidase
Hsp	-	heat shock protein
IAP	-	inhibitor of apoptosis protein
IC_{50}	-	inhibitory concentration 50%
IM	-	inner membrane
IMAC	-	inner membrane anion channel
IMS	-	intermembrane space
kDa	-	kiloDaltons
KPa	-	Konig's Polyanion
LDH	-	lactate dehydrogenase
LEHD	-	Leu-Glu-His-Asp peptide

MDa	-	megaDaltons
MEM	-	minimal essential medium
MPP^+	-	1-methyl-4-phenylpyridinium ion
MPT	-	mitochondrial permeability transition
NADH	-	nicotinamide adenine dinucleotide
NAIP	-	neuronal apoptosis inhibitor protein
NGF	-	nerve growth factor
OD	-	optical density units
OM	-	outer membrane
PBR	-	peripheral benzodiazepine receptor
PEP	-	phosphoenolpyruvate
P_i	-	inorganic phosphate
PK	-	pyruvate kinase
PTP	-	permeability transition pore
PVDF	-	polyvinylidene fluoride
RCR	-	respiratory control ratio
ROS	-	reactive oxygen species
SDS	-	sodium decyl sulphate
SEM	-	standard error of the mean
SIMP	-	soluble intermembrane protein
Smac	-	second mitochondrial activator of apoptosis
SOD	-	superoxide dismutase
TBS	-	tris buffered saline
TCA	-	tricarboxylic acid
TMPD	-	N,N,N',N'-tetramethyl-*p*-phenylenediamine

TNFR	-	tumour necrosis factor receptor
TOM	-	translocator outer membrane
TPP^+	-	tetraphenylphosphonium ion
TTBS	-	tris buffered saline with 0.5% Tween-20
UQ	-	ubiquinone
UV	-	ultraviolet
VDAC	-	voltage dependent anion channel
$\Delta\psi_m$	-	membrane potential

CHAPTER 1

General Introduction

1.1 Mitochondria

1.1.1 *Origin*

Mitochondria are discrete organelles found in the cytosol of most eukaryotic cells. They are thought to have evolved from free-living bacteria. These early prokaryotes are suggested to have been engulfed by larger cells, with which they forged a symbiotic relationship. Now dependent on their host cells, mitochondria still display evidence to suggest a former prokaryotic existence, for instance retaining their own DNA and bacteria-like ribosomes. This 'Endosymbiont Hypothesis' was popularised by Lynn Margulis (1981) and is now widely accepted.

1.1.2 *Respiratory function*

Mitochondria have evolved to contribute the facility of aerobic respiration in eukaryotic cells. They are contained within two membranes, an outer (OM) and an inner (IM) membrane. The OM is permeable to molecules of less than 10kDa, due to the presence of porin channels within the phospholipid bilayer. This means that ATP, ADP and ions (plus other small proteins) can all freely translocate between the 'inter-membrane space' (IMS) and the cytosol. The IM, in contrast, is impermeable to most ions and solutes, except through specific carriers, eg. the adenine nucleotide translocator (ANT) which allows ADP and ATP to move between the matrix and the IMS. The IM is highly invaginated, with folds organised into layers known as cristae. The IM therefore has a much larger surface area than the OM. It also has a significantly greater protein concentration. In addition to requiring numerous

transporter proteins, the IM also encompasses the machinery required for 'oxidative phosphorylation', the process which underlies aerobic respiration (reviewed by Scheffler, 1999).

This machinery makes up the 'Electron Transport Chain', or ETC. This is a series of anchored protein complexes and mobile electron carriers, which together serve to create a proton electrochemical gradient. This has two components: a pH difference and a membrane potential ($\Delta\psi_m$) which is due to charge separation. Dissipation of this 'proton motive force' can be used to power the phosphorylation of ADP to form ATP (Mitchell, 1961). The components of the ETC are used in order of increasing reduction potential, such that an electron flows spontaneously through the chain (see Figure 1.1). Electrons are accepted initially from NADH and succinate, and at the site of the final complex in the chain, donated to molecular oxygen to form water. In three of the four complexes of the ETC, electron transfer is coupled to movement of protons from the matrix to the IMS. This leads to generation of the proton motive force across the IM. Experimentally, this gradient can be approximated to $\Delta\psi_m$, and it is this parameter which is generally referred to in the literature.

Movement of protons back down the gradient via the ATP synthase provides energy for the phosphorylation of ADP to ATP, at the expense of $\Delta\psi_m$. In addition, protons appear to 'leak' back down the gradient, crossing the IM by a means other than the ATP synthase (reviewed by Kadenbach, 2003). This leak reduces the efficiency of oxidative phosphorylation.

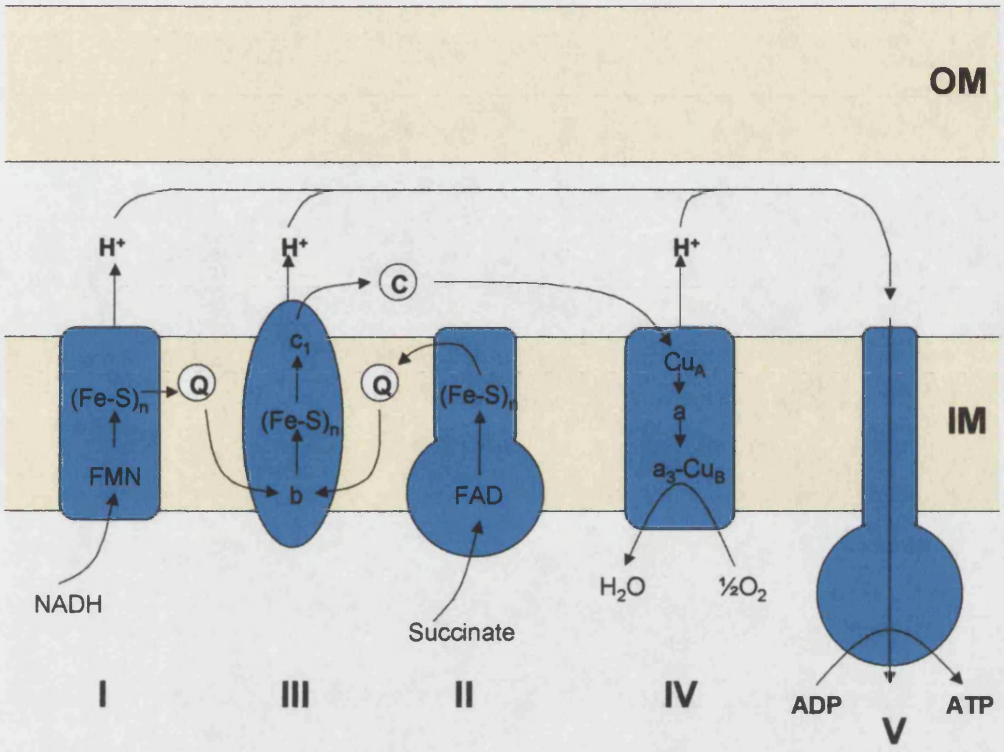

Figure 1.1

Schematic diagram of the mitochondrial ETC. Electrons, donated by nicotinamide adenine dinucleotide (NADH) and succinate, pass down a series of protein complexes and electron carriers of increasing reduction potential. The passage of electrons is coupled to the generation of a proton gradient (extrusion of protons is coupled to electron transfer through complexes I, III and IV), which can be used to power the ATPase, also known as complex V of the ETC. Electrons are donated to molecular oxygen at the end of the chain, forming water.

The individual complexes will now be described in more detail (general references Heales *et al*, 2002, Lehninger *et al*, 1993) with particular emphasis on complexes I and IV, which will feature most prominently in this study. A number of universal electron carriers are also used in the ETC. In addition to NADH, flavin mononucleotide (FMN) and flavin adenine dinucleotide (FAD) can both act as electron acceptors and donators. They shuttle electrons in pairs (as $FMNH_2$ and $FADH_2$), using 'semiquinone' forms as intermediates (FMNH and FADH). Fe-S centres, in contrast, are single electron carriers, containing Fe and S atoms in 1:1 stoichiometry. Their function relies on the single electron oxidation or reduction of the Fe ions.

1.1.2.1 Complex I (EC 1.6.5.3)

Complex I is commonly known as the NADH dehydrogenase or NADH:ubiquinone oxidoreductase. It is the largest of the ETC enzyme complexes, the mammalian enzyme comprising 45 subunits (Carroll *et al*, 2002). It contains two types of prosthetic groups: an FMN group and at least 6 Fe-S centres. It is thought to exist as a dimer. The complex has an L formation, with a short arm (the NADH dehydrogenase) extending into the matrix and a long arm (the ubiquinone hydrogenase) which is largely held within the IM. The two are connected by a narrow stalk.

The process of electron transport through complex I is shown schematically in Figure 1.3. Electrons are donated by NADH, which is present in the matrix as a product of the TCA cycle. NADH produced by glycolysis is imported from the cytosol by the malate-aspartate shuttle (primary mechanism in liver, kidney and heart mitochondria),

and the glycerol-3-phosphate shuttle (primary mechanism in brain and skeletal muscle mitochondria). The FMN group of complex I accepts hydrogen atoms from NADH, and is reduced to $FMNH_2$. This species is recycled to the oxidised form, donating two electrons to the Fe-S cluster, and releasing two protons back into the matrix. The Fe-S cluster donates the two electrons to ubiquinone (UQ), which on accepting two protons from the matrix along with the electrons, becomes reduced to ubiquinol (UQH_2), via a semiquinone intermediate (UQH). The UQ in this stage of the pathway is anchored within complex I. UQH_2 then donates the two electrons to a second cluster of Fe-S groups, releasing the two associated protons into the IMS. Now in the ubiquinone hydrogenase region of the complex, electrons are passed from the Fe-S centres onto UQ, which in this case is freely mobile within the IM. Once again, via a UQH intermediate, the electron carrier is reduced to UQH_2, taking up two protons from the matrix in the process. UQH_2 then migrates through the IM and passes on the two electrons to complex III.

The net reaction catalysed by complex I is:

$$NADH + UQ + 5H^+_i \longrightarrow NAD^+ + UQH_2 + 4H^+_o$$

where H^+_i are internal protons, ie. in the matrix, and H^+_o are external protons, ie. in the IMS. Therefore there is a net extrusion of four protons per NADH oxidised. This contributes to the generation of $\Delta\psi_m$ across the IM.

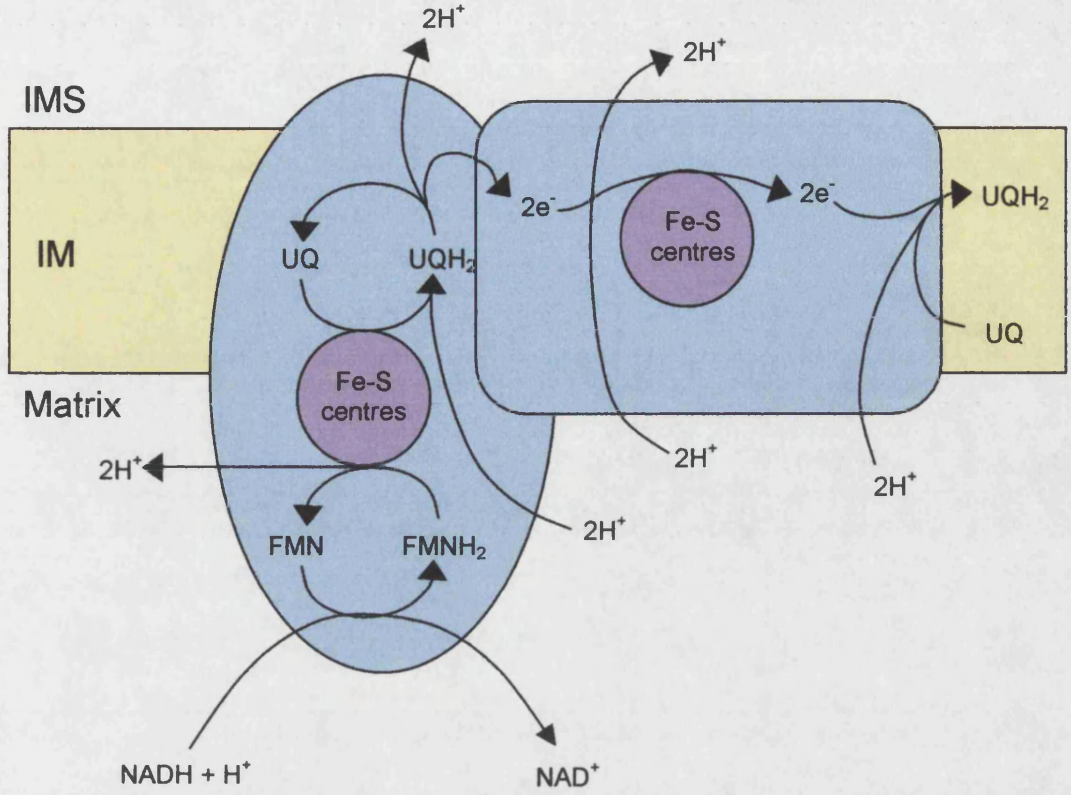

Figure 1.2

Schematic diagram to demonstrate the structure and function of complex I (NADH dehydrogenase). Electrons are donated by NADH in the matrix, and via FMN, clusters of Fe-S centres and anchored ubiquinone, are ultimately passed on to ubiquinone in the IM to form ubiquinol, which can then diffuse from the complex. There is a net translocation of four protons from the matrix to the IMS for every NADH oxidised.

Complex I can be inhibited using a variety of compounds. The most commonly used of these experimentally is rotenone, a commercially used pesticide, whose structure is shown in Figure 1.3. Rotenone is a 'class II' inhibitor of complex I, meaning that it inhibits in a non-competitive manner (as opposed to 'class I' inhibitors such as piericidin A, which are partially competitive with UQ). Like all other known inhibitors of complex I, rotenone acts on the matrix-embedded long arm of the complex, arresting electron transfer from the Fe-S cluster to the free UQ in the IM (Friedrich *et al*,1994).

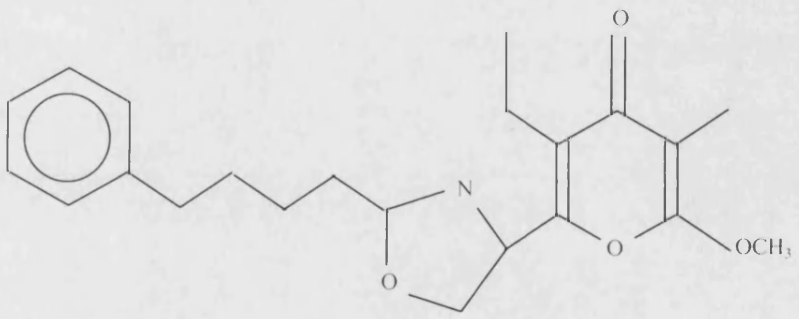

Figure 1.3

The structure of rotenone, class II inhibitor of complex I.

1.1.2.2 Complex II (EC 1.3.5.1)

Complex II is commonly known as succinate dehydrogenase or succinate:ubiquinone oxidoreductase. In addition to its role in the ETC, this enzyme complex also functions in the TCA cycle upstream of oxidative phosphorylation.

Complex II is composed of four subunits, and contains two types of prosthetic groups: a covalently bound FAD and Fe-S centres. The enzyme can accept electrons from succinate via the FAD group. The electrons are then passed through the Fe-S centres and donated to free UQ in the IM to form UQH_2.

The net reaction catalysed by complex II is:

$$\text{succinate} + UQ \longrightarrow \text{fumarate} + UQH_2$$

and there is no net transfer of protons from the matrix to the IMS.

UQH_2 migrates to complex III, where it donates a pair of electrons and is therefore oxidised.

Complex II can be inhibited using malonate.

1.1.2.3 Complex III (EC 1.10.2.2)

Complex III is also known as the cytochrome bc_1 complex, or ubiquinone-cytochrome *c* oxidoreductase. It exists as a homodimer and is composed of eleven

subunits. Complex III contains two types of prosthetic groups: hemes and Fe-S centres. The cytochrome *b* proteins (b_{562} and b_{566}) span the IM, while cytochrome c_1 and the Fe-S centre are localised to the IMS face of complex III.

Electrons are donated by UQH_2, which enters a 'Q cycle' within the enzyme complex. This is as a result of the Fe-S centre being only a single electron carrier. Following acceptance of one electron from UQH_2, the Fe-S centre cannot be further reduced. The resulting UQH is therefore forced into donating the second electron to the heme *b* group. UQ can then re-enter the soluble membrane pool. Meanwhile, within complex III, the electron is passed onto a second heme *b* group, which can reduce UQ from the membrane pool back to semiquinone. When a second electron is passed through the system, this UQH can be reduced to UQH_2 and returned to the membrane pool. The effect of this Q cycle is to enable the net efflux of four protons into the IMS for every UQH_2 which is oxidised. This again contributes to generation of $\Delta\psi_m$ (Reviewed by Hunte *et al*, 2003).

The net reaction catalysed by complex III is therefore:

$$UQH_2 + 2\text{cyt } c^{3+} + 2H^+_i \rightleftharpoons UQ + 2\text{cyt } c^{2+} + 4H^+_o$$

Cytochrome *c* is released from complex III in the reduced form, and migrates to complex IV, where it is oxidised.

Complex III can be inhibited using myxothiazol or antimycin A.

1.1.2.4 Complex IV (EC 1.9.3.1)

Complex IV is commonly known as cytochrome *c* oxidase. The mammalian enzyme is composed of thirteen subunits, and contains two types of prosthetic groups: hemes and copper ions. The hemes are incorporated within cytochromes *a* and a_3. Both of these cytochromes are in rapid redox equilibrium with a copper centre (Cu_A and Cu_B, respectively). Electrons are donated by reduced cytochrome *c* (which has migrated from complex III) and are passed, via the two bimetallic redox centres, to oxygen. A simplified diagram of the currently understood mechanism of electron transfer through complex IV is shown in Figure 1.4.

The mechanism by which electrons are transferred through complex IV has been the subject of considerable interest. In particular, the role of the bimetallic Cu-cytochrome a_3 centre in causing the four-electron reduction of oxygen has been investigated. A basic scheme for this process is shown in Figure 1.5. The process is suggested to create a kind of 'oxygen trap'. As soon as the heme is reduced (ie. Fe^{3+} reduced to Fe^{2+}), oxygen can be bound. On binding, the reduced heme and Cu centres very rapidly donate an electron to each of the oxygen atoms, themselves being oxidised back to Fe^{3+} and Cu^{2+} respectively. Once this rapid phase has been completed, the reaction is irreversible, therefore the process effectively 'traps' oxygen.

The net reaction catalysed by complex IV is:

$$4\text{cyt } c^{2+} + 8H^+_i + O_2 \longrightarrow 4\text{cyt } c^{3+} + 4H^+_o + 2H_2O$$

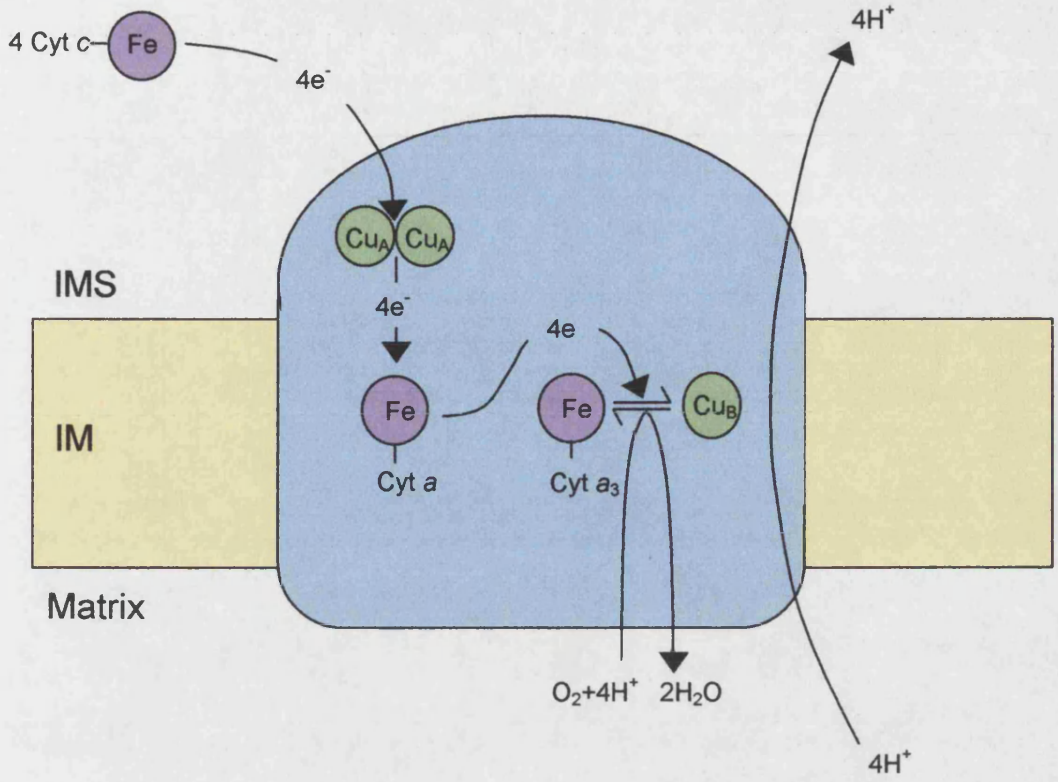

Figure 1.4

Schematic diagram to demonstrate the structure and function of complex IV (cytochrome *c* oxidase). Electrons are donated by cytochrome *c*, and ultimately passed on to oxygen in the matrix to form water. This is the point of oxygen consumption during mitochondrial respiration. There is a net translocation of one proton from the matrix to the IMS for every cytochrome *c* oxidised, and a further proton is consumed chemically.

There is a net efflux of one proton per cytochrome *c* oxidised. However, due to the influx of one electron, there is a net two charge transfer per cytochrome *c* oxidised. Complex IV is therefore the third complex able to contribute to the generation of $\Delta\psi_m$.

Complex IV can be inhibited experimentally using cyanide. Nitric oxide and carbon monoxide are also recognised inhibitors. The inhibition of complex IV by cyanide is not fully understood. It appears that the CN^- ion may bridge the heme a_3-Cu_B bimetallic centre in its fully oxidised form, thus forming a Fe^{3+}-CN^--Cu^{2+} moiety (Gardner *et al*, 1996). Assuming that this complex has a lower reduction potential than the bimetallic centre alone, then electron transfer through complex IV and therefore the generation of $\Delta\psi_m$ would be inhibited.

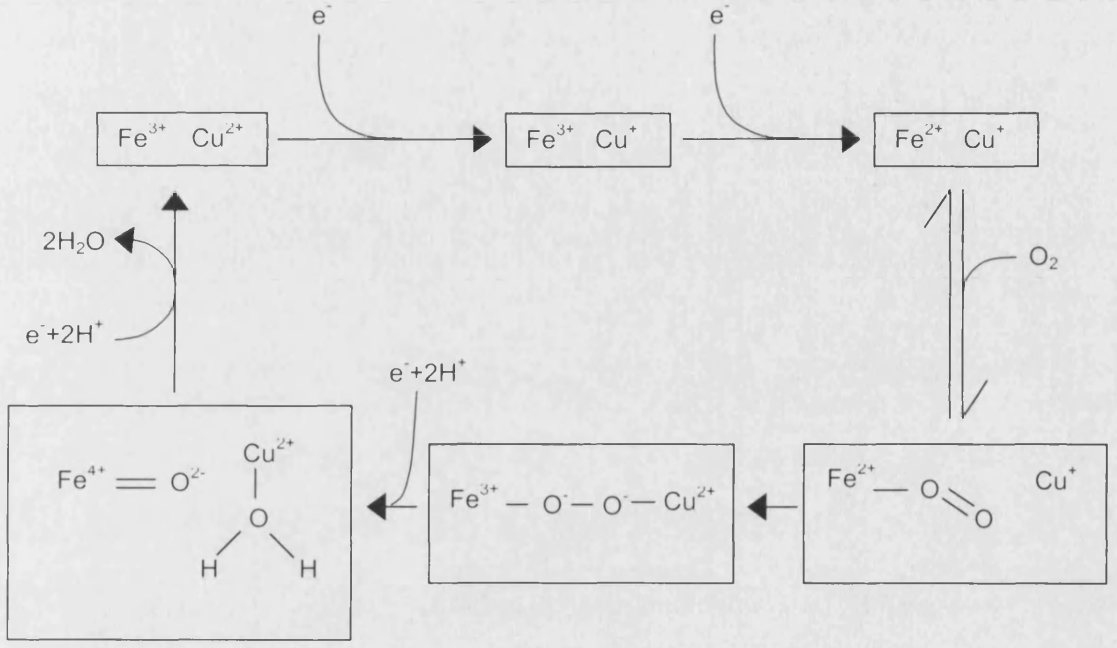

Figure 1.5

Schematic diagram to demonstrate the mechanism utilised by complex IV to complete the four-electron reduction of oxygen to water without the generation of free radical intermediates. This is achieved by the bimetallic Fe-Cu group. (Adapted from Babcock & Wikstrom, 1992).

1.1.2.5 Complex V

Complex V is more commonly known as the ATP synthase. Structurally, the enzyme contains two major sectors, F_1 and F_o. F_o is a transmembrane complex spanning the IM, is composed of four polypeptides and forms the channel for proton translocation. The '$_o$' notation refers to the sensitivity of this region to oligomycin. F_1 projects into the matrix, and contains the catalytic machinery for ATP synthesis.

Functionally, the complex is tripartite. The first region to act is a motor or turbine which converts the energy generated from the flow of protons through F_1 down the gradient into rotational energy. Following this, a 'rotating transmission device' transmits the rotational energy to the catalytic sites. Finally, there are three catalytic sites which transform rotational energy into the chemical energy required for formation of the bond between ADP and P_i.

The ATP synthase enzyme can function in reverse to hydrolyse ATP at the expense of $\Delta\psi_m$. It has been proven that this function is associated with subunit rotation within the complex. It is believed that the reverse rotation mediates the phosphorylation of ADP.

1.1.3 *The ETC and reactive oxygen species*

The ETC is a site where oxygen and unpaired electrons are permanently in close proximity. Incomplete reduction of molecular oxygen results in the generation of reactive oxygen species (ROS) instead of water. It is perhaps not surprising, therefore, that an estimated 1 – 3% of the total oxygen consumed at the ETC is

converted to ROS (Boveris *et al*, 1972). Monoelectronic reduction of oxygen yields the superoxide radical ($O_2^{\bullet -}$). Complexes I and III are thought to be the major sites of production of superoxide in the ETC. It has been suggested that if generated at complex I, superoxide is released on the matrix side of the IM (St-Pierre *et al*, 2002). Either the Fe-S centres (Genova *et al*, 2001) or the active site flavin (Liu *et al*, 2002) are thought to be the major site of electron leak to oxygen within complex I. Conversely, complex III is thought to release superoxide on the cytosolic face of the IM. The UQH in the Q cycle of complex III (see 1.1.2.3) is thought to be the primary site of electron leak to oxygen within complex III (Turrens *et al*, 1985).

The role of reduced intermediates in the mitochondrial generation of superoxide may be an explanation for the observed dependence of the process on $\Delta\psi_m$. It has been suggested that dissipation of $\Delta\psi_m$, and therefore maximal oxidation of electron carriers such as UQ, reduces the potential for reduction of oxygen to superoxide (Skulachev, 1996). Indeed in Drosophila mitochondria, a 10% decrease in $\Delta\psi_m$ was sufficient to abolish approximately 70% of the ROS generation by reverse electron flow through complex I (Miwa & Brand, 2003). The relationship has been specifically demonstrated in brain mitochondria, where ROS generation is decreased by opening the mitochondrial ATP-sensitive K^+ channel (and therefore reducing $\Delta\psi_m$) (Ferranti *et al*, 2003).

Superoxide is rapidly converted to hydrogen peroxide (H_2O_2), a reaction accelerated by four orders of magnitude by superoxide dismutase (SOD). H_2O_2 can then be oxidised to water by glutathione peroxidase, using reduced glutathione (γ-glutamylcysteinylglycine, GSH) as an electron donor. As a result, GSH is oxidised to

glutathione disulphide (GSSG) but can be recycled to GSH via the glutathione reductase reaction. Alternatively, H_2O_2 can be oxidised to water and molecular oxygen in a reaction catalysed by catalase (see Figure 1.6).

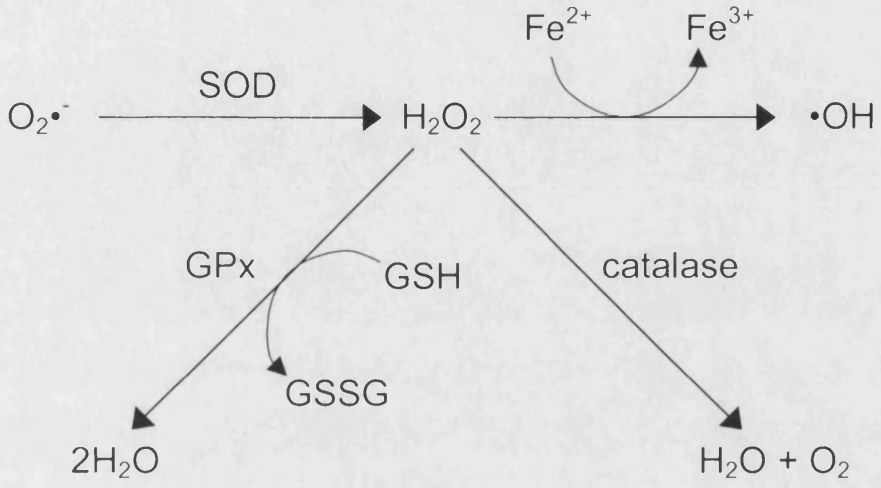

Figure 1.6

Cellular disposal of superoxide. Superoxide is rapidly converted to hydrogen peroxide in the presence of superoxide dismutase. This may then be reduced to water either by glutathione peroxidase (GPx) or catalase. Alternatively, hydrogen peroxide can form the hydroxyl radical via a Fenton reaction. This is one of a number of possible alternative fates; reactions with other proteins or iron in heme proteins can also occur.

1.1.4 *Brain mitochondria*

1.1.4.1 Mitochondrial heterogeneity

Mitochondria differ in their properties depending on the tissue from which they originate. Indeed in some regions there is variation within one tissue type and even within one cell. The brain is an example of a tissue in which such diversity in mitochondrial properties is observed. Brain mitochondria differ from those from heart, liver, muscle, kidney etc. in many ways, eg. susceptibility for calcium-induced damage (Kristiàn *et al*, 2000), extent of ROS generation and antioxidant capacity (Liu *et al*, 2000), and proton leak (Rolfe *et al*, 1994). Further to this, discrepancies in mitochondrial function have been observed between different regions and cell types of the brain eg. in sensitivity to calcium (Brustovetsky *et al*, 2003a), response to oxygen and glucose deprivation (Almeida *et al*, 2002), ETC complex activities (Battino *et al*, 1991) and other enzyme activities (Lai *et al*, 1994).

1.1.4.2 Experimental isolation of brain mitochondria

The heterogeneity of brain mitochondria is taken into account when isolating these organelles for experimentation. Methods have been developed by Lai and Clark (1989) for the isolation of both 'non-synaptic' and 'synaptic' brain mitochondria. Mitochondria classified as non-synaptic are more plentiful in the brain, since the term encompasses all brain mitochondria excepting those from the synaptic terminals of neurons. This excluded population are the synaptic mitochondria, of which the yield is relatively much smaller per unit mass of brain.

The isolation procedure involves a series of centrifugation steps, including an ultracentrifugation of a density gradient, which is used to separate myelin, synaptosomes (from which synaptic mitochondria can be released) and 'free' (or non-synaptic) mitochondria. Throughout the preparation, yield is sacrificed for purity. Brain tissue has a particularly high lipid content. The presence of lipids such as myelin during the mitochondrial preparation allows vesicle formation during homogenisation, which contaminates a preparation of otherwise isolated mitochondria. Due to the need to eliminate non-mitochondrial material, the isolation of brain mitochondria is a process of longer duration than that for their heart or liver counterparts, for example. The yield is also much lower per unit mass of original tissue. This would explain the relative lack of literature concerning isolated brain mitochondria as compared to those from other sources.

However, as described, there are important differences in properties between mitochondria from different tissues, hence the importance of using the relevant source. The isolation of synaptic mitochondria is an even more arduous procedure than that of non-synaptic mitochondria, involving a larger number of centrifugation steps including two density gradient ultracentrifugation spins. Of those isolated mitochondria studies which use brain mitochondria, a low percentage of this subset are of synaptic origin. The understanding that synaptic mitochondria have distinctive properties (Almeida *et al*, 1995; Davey *et al*, 1998) and their particular importance in the pathology of neurodegeneration underlie the need to make more frequent use of them as an experimental tool.

1.1.4.3 Brain mitochondria in neurodegenerative disease

As described later (1.3.3), mitochondria have an important role in initiating cell death. This implicates the organelles in the neuronal loss observed in neurodegenerative disease. However, there is a more clinically recognised link between brain mitochondria and neurodegenerative pathologies which relates to the activities of the ETC enzyme complexes. The majority of neurodegenerative diseases are associated with reduced activity of at least one of the complexes. For example, complex I activity is reduced in the brains of patients with Parkinson's disease (Schapira, 1990), Alzheimer's disease and Down syndrome (Kim *et al*, 2001), complex II/III deficiency is detected in Huntington's disease brain (Gu *et al*, 1996), and complex IV deficiency in brain tissue from Leigh disease patients (Cacic *et al*, 2001).

1.2 Cytochrome c

This study will focus on the particularly important and contradictory roles of the electron carrier cytochrome *c* (see 1.2.3).

1.2.1 *Structure*

Cytochrome *c* is a 12.1kDa protein consisting of a single polypeptide chain of 104 amino acids, covalently attached to a heme group. It is one of a family of cytochromes, all of which are iron-containing electron transfer proteins. The three classes of cytochromes within this family, *a*, *b* and *c*, are defined by their light

absorption spectra. The longest wavelength absorption band is approximately 600nm for type *a*, 560nm for type *b* and 550nm for type *c* cytochromes.

The redox properties are afforded by the heme group which is present in all cytochromes. The heme group is a porphyrin ring structure, composed of four, smaller, nitrogen containing rings. The porphyrin ring is centred around an Fe ion, which can exist in the oxidised (or ferricytochrome *c*, Fe^{3+}) or reduced (or ferrocytochrome *c*, Fe^{2+}) state, hence the redox properties of the cytochrome. Each class of cytochrome has a different form of heme. Cytochrome *c*, which contains heme C, is unique within the family in its covalent attachment to the heme group; cytochromes *a* and *b* form tight but non-covalent associations with heme A and heme B, respectively.

The amino acid sequence of cytochrome *c* has been determined in a wide range of species, including human (Matsubara & Smith, 1962) and rat (Scarpulla *et al*, 1981). The structure of heme C is shown in Figure 1.7.

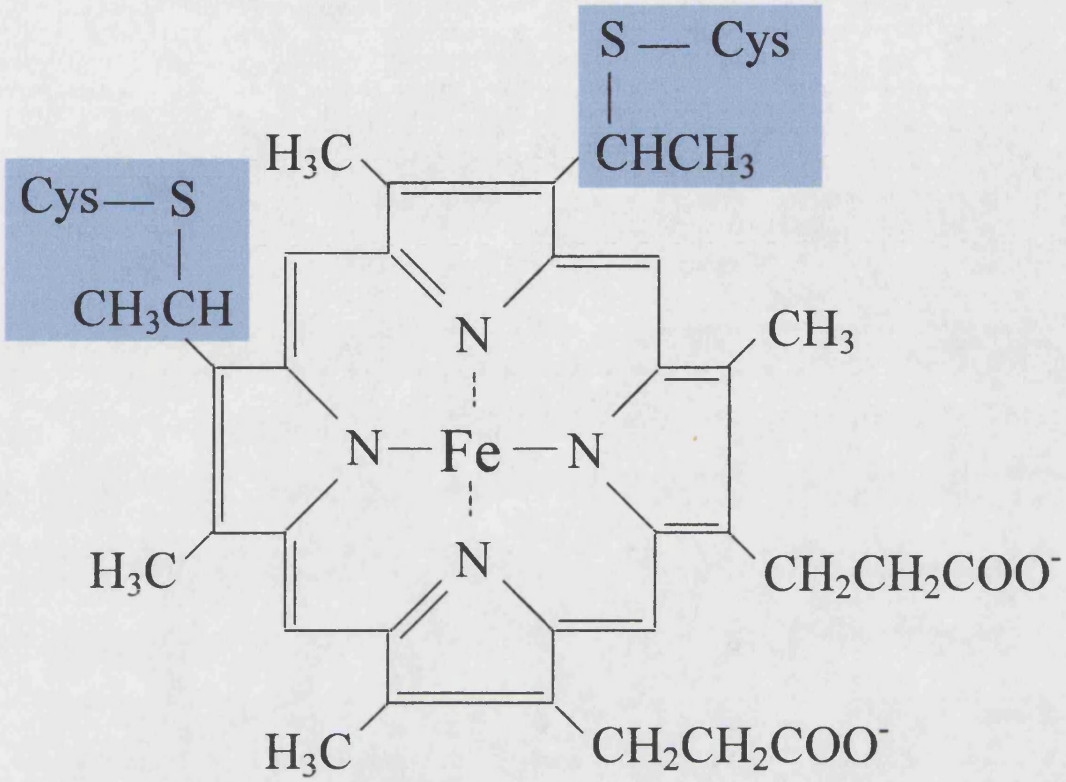

Figure 1.7

Structure of heme C. The areas shaded in blue are the sites of covalent attachment with the cytochrome protein. Thioether bonds are formed with the two cysteine residues.

1.2.2 *The biometabolism of cytochrome c*

1.2.2.1 Synthesis

Cytochrome *c* is encoded by nuclear DNA. However, it is constitutively localised to the IMS and IM of mitochondria (or the lumen of chloroplasts or outside the cytoplasmic membrane in bacteria, depending on the system). A crucial factor in the biogenesis of cytochrome *c* is therefore its translocation to the target location. It is understood that cytochrome *c* is synthesised at the site of cytosolic ribosomes as 'apocytochrome *c*', which is the protein without the heme moiety. Apocytochrome *c* is converted to 'holocytochrome *c*' (or simply cytochrome *c*) by ligation of heme at the site to which it has been targeted. The heme ligation process varies depending on the system (ie. mitochondria, chloroplast or bacteria). Of interest in this study is cytochrome *c* which is located at the IMS and IM of eukaryotic mitochondria, therefore this is the system which will be described.

Apocytochrome *c*, having been synthesised on cytosolic ribosomes as described, translocates to mitochondria due to an internal (rather than N-terminal) targeting sequence. It is 'trapped' in the IMS of mitochondria by the enzyme cytochrome *c* heme lyase (CCHL). The action of the enzyme, as the name suggests, is to attach the heme group onto the apo-protein. Prior to the association of heme, apocytochrome *c* has a protease-sensitive unfolded conformation. This may be a crucial factor in the import process across the OM (Jordi *et al* 1992). However, once heme has been covalently attached via the CCHL, cytochrome *c* adopts a protease-resistant, folded form, which is then released from CCHL into the IMS. It then appears to exist in dynamic equilibrium between freely soluble and IM-associated states (1.2.2.2).

Generally, mitochondrial proteins which are encoded by the nucleus, and therefore synthesised in the cytosol, require the translocase of the mitochondrial OM, known as the TOM complex (Lill & Neupert, 1996) or other protease-sensitive OM components for targeting and import into the mitochondria. It has been claimed that activity of the CCHL enzyme on the peripheral surface of the OM is sufficient to cause import of apocytochrome *c* into the IMS (Mayer *et al*, 1995), independently of the TOM complex. This is disputed by Diekert *et al* (2001), who claim that the TOM complex is in fact required for import of cytochrome *c*. Aside from this debate, it is accepted that cytochrome *c* appears to employ a unique import pathway.

It should be noted that the initial and final stages of heme biosynthesis take place in the mitochondrial matrix. The last stage of the heme synthesis process is the insertion of ferrous iron into the protoporphyrin ring by ferrochelatase (reviewed by Ferreira, 1995). Heme must be in the reduced form during covalent attachment to apocytochrome *c*, therefore heme must be maintained in this ferrous form. Yet to be identified are the components of the heme translocation and membrane transport processes and the IMS mechanisms for maintenance of the reduced form of heme.

1.2.2.2 Constitutive localisation

Following heme attachment, it is recognised that cytochrome *c* is constitutively localised to the IMS. However, it has become increasingly apparent that there is a certain extent of anchoring of cytochrome *c* to the IMS face of the IM. This may be mediated by the IM phospholipid cardiolipin (Cortese *et al*, 1998; Nicholls, 1974). It is thought that the varying levels of association of cytochrome *c* with the IM via

cardiolipin have important implications for the susceptibility of the protein to be released into the cytosol (see 1.3.5.3).

1.2.2.3 Degradation

Cellular proteins which are constitutively localised to the cytosol or nucleus are generally degraded in the cytosol by the action of the proteasome. Prior to this process, proteins are attached to a 76-residue ubiquitin protein via an isopeptide bond. Ubiquitination signals that the bound protein should be targeted for degradation by the proteasome. Mitochondria, however, do not express the proteasome. Nonetheless, proteins which are constitutively localised to the mitochondrial matrix can be degraded in the same compartment, by a variety of ATP-dependent and ATP-independent proteases (reviewed by Bota and Davies, 2001).

There is, however, very little information available in the literature on the fate of IMS proteins with respect to degradation. Bearing in mind the limited permeability of the IM, it would appear more likely that IMS proteins would be subject to cytosolic, rather than matrix-based degradation. In accordance with this, it has been shown that yeast cytochrome *c*, in either the oxidised or reduced form, readily undergoes ubiquitination *in vitro* (Sokolik & Cohen, 1992). It appears that the understanding of cytochrome *c* degradation has not progressed from this point. It is possible that the cytochrome *c* protein is degraded by the proteasome, and that the heme groups are excreted. However, it is unclear whether there are specific protective mechanisms in place to prevent cytochrome *c* which is released from mitochondria for the purpose of degradation from exhibiting its pro-apoptotic role (as described in 1.3.3.1).

1.2.3 *Roles of cytochrome c*

1.2.3.1 Electron carrier in the ETC

The longest established role of cytochrome *c* is as an electron carrier in the mitochondrial ETC. This chain of enzyme complexes was described in 1.1.2. Cytochrome *c* accepts an electron from complex III (ubiquinone:cytochrome *c* oxidoreductase), and is released as ferrocytochrome *c*. On encountering complex IV (cytochrome *c* oxidase), cytochrome *c* donates the electron, thus returning to the ferri form.

1.2.3.2 Pro-apoptotic signalling protein

Relatively recently, cytochrome *c* has been exposed to have somewhat of a "Jekyll and Hyde" character. In addition to its vital role in the ETC, it has become apparent that cytochrome *c* can actively initiate the programmed cell death mechanism known as apoptosis (see 1.3.3.1) (Liu *et al*, 1996). If released from the IMS into the cytosol of the host cell, cytochrome *c* induces an amplifying cascade of proteolytic enzyme activity, which ultimately is fatal to the cell. (Importantly, this capacity is limited to holocytochrome *c* – apocytochrome *c* has no pro-apoptotic properties - Yang *et al,* 1997). The apoptotic process is an essential part of development and physiological regulation of cell number, however dysregulation can have pathological consequences such as tumourigenesis and neurodegeneration.

1.2.3.3 Anti-oxidant

The two main roles of cytochrome *c* are described above. However, it is also recognised that cytochrome *c* has anti-oxidant properties. It has been known for some

time that cytochrome *c* can oxidise superoxide back to oxygen (Nakano, 1990). An intriguing study by Korshunov and co-workers (1999) demonstrates that submicromolar concentrations of cytochrome *c* external to the mitochondria are capable of inhibiting ROS generation at complex I.

1.3 Apoptosis

1.3.1 *The definition of apoptosis*

Apoptosis is a term coined in 1972 by Kerr, Wyllie and Currie. In contradiction to the title of this much-cited paper, the process is far from basic. It describes a form of cell death which can be seen as suicide. In response to a pro-apoptotic stimulus, a cell undergoes a controlled sequence of events, depending on the presence of sufficient ATP, culminating in chromatin condensation, nuclear fragmentation, cell shrinkage and plasma membrane blebbing. The cell carefully packages its contents into small, membrane-bound vesicles, which can then be phagocytosed. By committing itself to death in this way, the cell prevents the generalised release of its contents, including lysosomal enzymes etc., to the extracellular environment. The process does not initiate any localised inflammation (Arends & Wyllie, 1991). This is in contrast to necrotic cell death, where massive and uncontrolled membrane breakdown leads to non-specific release of potentially dangerous cellular contents into the surroundings of neighbouring cells. Death by apoptosis provides significant 'damage limitation' with respect to the remaining cells.

1.3.2 *Physiological versus pathological apoptosis*

This 'damage limitation' aspect of apoptotic cell death is crucial to its role as a mechanism of regulating cell number during development and, in some tissues, during maturity also. The brain is a particular example of the physiological role of apoptosis in development. As the brain develops, neurons are vastly overproduced. As connections form between the more active neurons, cells which remain latent can be removed via apoptosis to shape the developed brain structure (Oppenheim, 1991).

Apoptosis also has important physiological roles long into maturity. Organs or tissues in which cells are rapidly proliferating, eg. the liver and the skin, use apoptosis as a means of regulating cell number while new cells are produced. However, failure of apoptosis-mediated regulation of cell number is the basis of a tumour. Cancerous cells display a resistance to undergo apoptosis (reviewed by Igney & Krammer, 2002). Many lines of investigation for cancer therapy aim to exploit the apoptotic machinery (Jansen *et al*, 1998; Keane *et al*, 1999 among many others).

A second route via which apoptosis can exert pathological effects is in the brain. In this organ, once maturity is reached, the cells are not turned over as in the liver, for example. The complement of neurons at maturity is, for the most part, not replenished (although it has been suggested that regeneration of pyramidal neurons in the hippocampus is possible – Nakatomi *et al*, 2002). If neurons are lost through apoptosis or any other form of death, they are unlikely to be replaced.

Apoptotic cell death is thought to be a major mechanism of cell loss during neurodegenerative disease (Hirsch *et al*, 1999; Smale *et al,* 1995; Thomas *et al*, 1995 and reviewed by Yuan *et al*, 2000). Inappropriate apoptosis in response to genetic or environmental factors can lead to the loss of adult neurons, which may never be replaced. In addition to neuronal loss during disease, a gradual decline in neuronal number due to apoptosis with evidence of oxidative stress is suggested to be a major factor contributing to aging (Anglade *et al*, 1997).

This particular feature of mature brain tissue is a very good example of a reason for studying brain mitochondria. Given the role of mitochondria in initiating apoptosis (1.3.3) and the unique implications of apoptosis for neurons in mature brain, the features of brain mitochondria with respect to apoptotic induction may be highly individual.

1.3.3 *Initiation of apoptosis*

There are two major routes by which apoptosis may be triggered in a cell. The first is via receptors on the surface of the cell membrane. These 'death receptors' are members of the tumour necrosis factor receptor (TNFR) family, whose major role aside from the induction of apoptosis is in regulating the function of the immune system. Ligands of these receptors, either soluble or membrane-bound, can provide 'communication' between cells, passing on the message to commit to apoptosis. This process is tightly regulated. Specific criteria might exist for the conformation of a pro-apoptotic ligand, with respect to the extent of homopolymerisation for example.

In addition, soluble or membrane-bound 'decoy' receptors can quench the pro-apoptotic signal.

The second route appears to be the dominant one for neuronal apoptosis (Pettmann & Henderson, 1998) and is the process of interest in this study. Relatively recently, it was found that mitochondria, in addition to being the 'powerhouse' of the eukaryotic cell, could also actively trigger its death (Newmeyer *et al*, 1994). Mitochondria can provide a pro-apoptotic signal to the host cell, and importantly, are then required to provide sufficient ATP for the apoptotic program to be completed. This signal, as was indicated in 1.2.3.2 is the redox protein cytochrome *c*, more commonly associated with electron transport in the ETC.

There are other IMS proteins which, when released from mitochondria, have pro- or anti-apoptotic influences on the cytochrome *c*-mediated pathway (1.3.6). One, however, appears to induce apoptosis in a manner independently of cytochrome *c*. Apoptosis Inducing Factor (or AIF) is a flavoprotein which, when present in the cytosol, can induce the same apoptotic endpoint as cytochrome *c* (chromatin condensation, DNA fragmentation, etc.) (Candé *et al*, 2002). However, it bypasses the proteolytic enzyme cascade which is a feature of cytochrome *c*-induced apoptosis (1.3.3.1, 1.3.4). The relative importance of AIF-induced apoptosis is not yet determined, but it appears that it may be required for death occurring in response to some stimuli (Joza *et al*, 2001).

1.3.3.1 Induction of apoptosis by cytochrome *c*

Under physiological conditions, the OM is impermeable to the 12.1kDa cytochrome *c*. However, certain insults experienced by the mitochondria can cause cytochrome *c* to be released from the IMS, where a proportion of the protein is freely mobile, to the cytosol (Yang *et al*, 1997). It has been estimated that the cytochrome *c* concentration of an apoptotic cell could range from 5 to 150μM (Waterhouse *et al*, 2001). Once in the cytosol, cytochrome *c* is potentially lethal (Liu *et al*, 1996).

Although there are protective mechanisms in place (see 1.3.6), the pro-apoptotic target of cytochrome *c* in the cytosol is a soluble cytosolic protein of approximately 130kDa called Apaf-1 (Apoptosis Protease Activating Factor-1). The association of these two proteins forms a complex known as the 'apoptosome'. Binding of cytochrome *c* increases the affinity of Apaf-1 for 2' deoxyATP (dATP) (Jiang and Wang, 2000).[1]

Binding of dATP to the apoptosome causes the complex to oligomerise. A non-hydrolysable analogue of dATP appears sufficient to exert the same effect as dATP (Jiang & Wang, 2000), likewise dADP can substitute (Liu *et al*, 1996). It therefore appears to be the binding of dATP which promotes assembly of the apoptosome, rather than the hydrolysis of dATP. There is debate as to whether ATP can substitute for dATP and initiate apoptosis via the apoptosome (Liu *et al*, 1996; Zou *et al*, 1999).

[1] This is the deoxynucleoside triphosphate which incorporates 2' deoxyribose, and is used in the composition of the DNA backbone. This form of dATP is therefore present in viable cells, unlike 3' deoxyATP, which is the 'mimic' nucleoside, unable to be incorporated into DNA. This latter can be used to treat diseases such as AIDS and chicken pox, by halting DNA synthesis.

The oligomerised apoptosome complex is then responsible for the activation of a cascade of protease activity which executes the apoptotic program. These aspartate-specific cysteine proteases are known as caspases. They operate in a hierarchical sequence, with 'initiator' caspases responsible for the activation of their downstream 'effector' counterparts. Prior to activation, they exist in zymogen form, ie. inactive pro-enzymes. The zymogen comprises a prodomain with two catalytic subunits. It is generally considered that release of the catalytic subunits by cleavage at the site of aspartic acid residues is required in order for the caspase to be activated (Thornberry & Lazebnik, 1998), with the notable exception of caspase-9 (Stennicke *et al*, 1998).

The death receptor pathway resulting from extrinsic signals, as described above (1.3.3), is generally initiated by caspase 8 (Boldin *et al*, 1996). Apoptosis which occurs via the mitochondrial pathway, in contrast, utilises caspase-9 at the head of the 'caspase cascade'. This caspase is the exception to the general rule of activation by cleavage. A study by Stennicke *et al* (1999) demonstrated that the activity of caspase-9 was primarily mediated not by proteolytic processing, but by the presence of cytosolic factors. Recombinant caspase-9 (the 'activated', cleaved form) was found to be maximally active (2000-fold increase) in cells when in the presence of cytochrome *c* and dATP. Mutated recombinant procaspase-9 which could not be proteolytically cleaved was able to support apoptosis with 'equal vigour' to the wild-type protein, providing that cytosolic factors were present.

The reliance on cytosolic factors for the activation of procaspase-9 is explained by the function of the apoptosome complex. Procaspase-9 is recruited to the oligomerised apoptosome, where it associates and appears to stimulate further or stabilise existing

dATP binding. It is docked by the N-terminal 1 – 97 amino acids of Apaf-1, which form a CARD domain (caspase recruitment domain, a recognised sequence common to several caspases and adaptor proteins which activate them – Hofmann *et al*, 1997). The association is of a homophilic nature, since procaspase-9 also has a CARD region. The CARD domain on Apaf-1 appears to remain inaccessible to procaspase-9 except in the presence of dATP and cytochrome *c*, which promote conformational changes in Apaf-1 (Li *et al*, 1997). It is believed that the WD repeat domain at the C-terminal of Apaf-1 is responsible for blocking the CARD domain, and that interaction of the WD repeat region (which is thought to be involved in protein-protein interactions – Komachi *et al*, 1994) with cytochrome *c* and dATP induces this conformational change.

Procaspase-9 is thought to associate in a 1:1 stoichiometry with Apaf-1, forming a 1.4MDa complex, with eight Apaf-1 subunits per apoptosome (Zou *et al*, 1999,). However, a smaller, 700kDa complex can also be detected and appears to be more active (Cain *et al*, 2000). Procaspase-9 is seldomly detected when associated with the apoptosome complex. It is thought that the zymogen is rapidly processed on recruitment, and that perhaps clustering of the zymogen allows autoactivation by proteolytic cleavage (Srinivasula *et al*, 1998).

However, caspase-9 appears to be unique within the family in that it does not require proteolytic processing in order to be activated (Stennicke *et al*, 1999). Active caspase-1 and -3 are composed of two catalytic subunits, thought to arise from dimerization of monomeric zymogens (Stennicke & Salveson, 1998). It is suggested therefore that the apoptosome could induce proximity of procaspase-9 zymogens,

driving homodimerization of monomers and therefore activation without proteolytic cleavage (Stennicke *et al*, 1999).

It has been determined that caspase-9 is only active when associated with the apoptosome (Rodriguez & Lazebnik, 1999), and it has been suggested that the complex may not only serve to activate the zymogen, but also to recruit previously activated caspase-9 in order that it may be functional (Cain *et al*, 2002).

It has been suggested that other CARD-containing caspases, eg. -1, -2, -4, -8 and -10, may be able to substitute for caspase-9 in the apoptosome if their level of expression is sufficient (Li *et al*, 1997). However, Pan *et al* (1998) have used an *in vitro* system to demonstrate that this is not the case, and that the apoptosome-mediated activation of caspase-9 appears to be specific for that enzyme.

1.3.4 *The caspase cascade*

There are at least 14 mammalian caspases recognised to date (2003). Whilst it was assumed that caspase-9 was responsible for the activation of downstream caspases, a study by Slee *et al* (1999) simply but elegantly demonstrated that this was the case using caspase inhibitors and immunodepletion in cell free extracts. This approach enabled the authors to deduce the order of activation of caspases in response to cytochrome *c*. Not only did they demonstrate a hierarchy of caspase activity (reproduced in Figure 1.8), but they also confirmed that caspase-9 was indispensable for cytochrome *c*-initiated triggering of the death program, a conclusion consistent with the claim of Pan *et al* (1998) as mentioned above (1.3.3.1).

The branched sequential nature of the cascade results in considerable amplification between activation of procaspase-9 and the terminal effector caspases. This amplification is augmented by the postulated positive feedback by active caspase-3 onto the upstream activation of procaspase-9. This feature of the apoptotic program emphasises the importance of the cytochrome *c*-mediated formation of the apoptosome complex. It highlights the necessity to buffer 'accidental' cytochrome *c* release, potential mechanisms for which are described in 1.3.6.

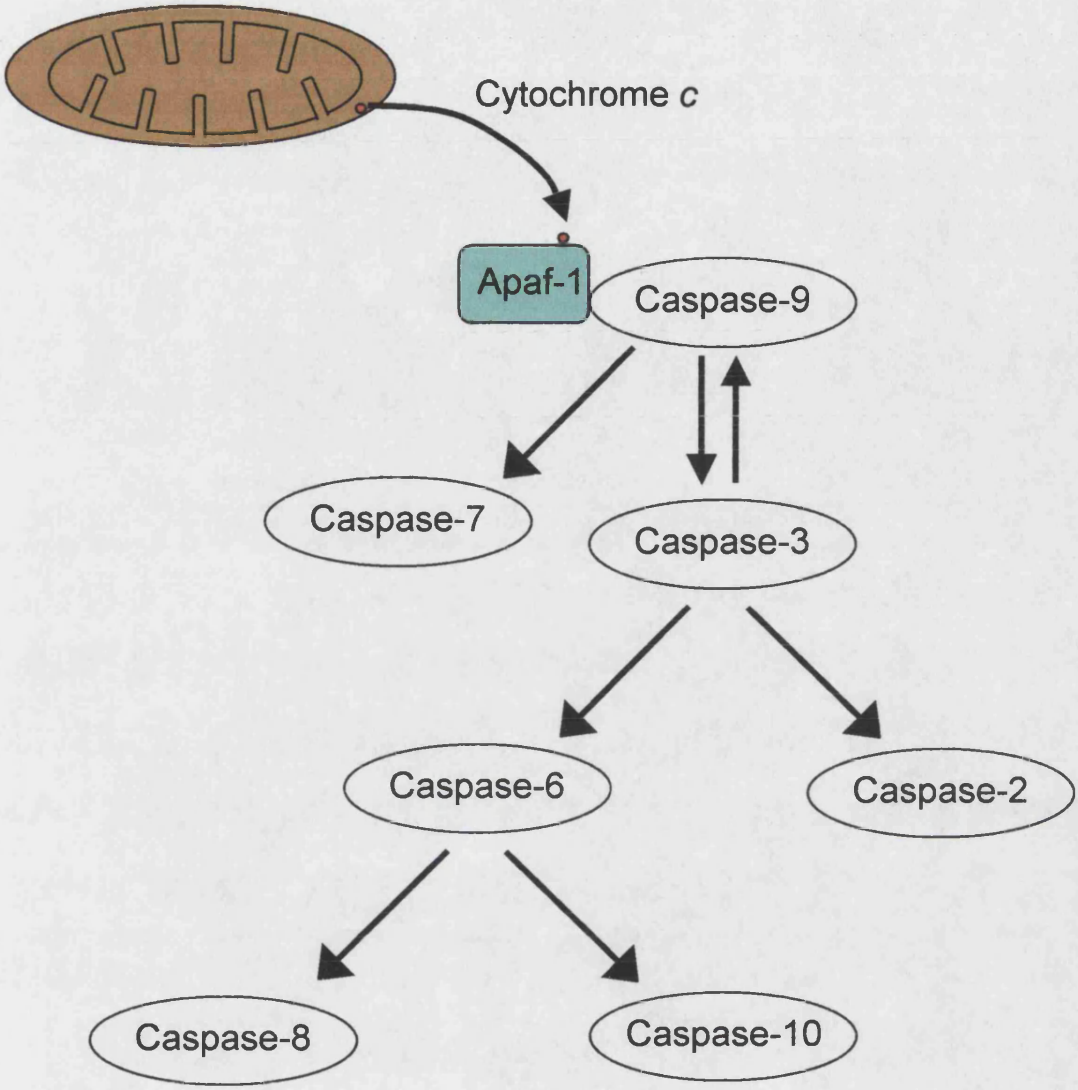

Figure 1.8

The postulated caspase cascade, reproduced from Slee *et al* (1999). The cascade is branched, with at least one feedback loop – caspase-3 activity provides positive feedback to the activation of caspase-9. It is interesting to note that caspase-8 features as an effector caspase in this pathway, bearing in mind the initiator role it plays in the death receptor-mediated apoptosis (1.3.3).

1.3.5 *Mechanisms of release of cytochrome c*

In order for cytochrome *c* to bind to Apaf-1 and trigger the events described above, it must be present in the cytosol, which clearly necessitates the release of cytochrome *c* from its IMS location, through the OM. Apocytochrome *c* is not able to substitute for the holo- form (Yang *et al,* 1997), therefore release of the mature protein is required. The mechanism by which cytochrome *c* release (CCR) occurs has been the subject of huge debate, not least due to the clinical implications of determining the mechanisms of apoptosis and how they might be exploited.

1.3.5.1 Swelling-dependent release mechanisms

As the importance of the CCR event emerged, there was renewed interest in the description by Hunter and Haworth in (1979) of a large proteinaceous pore which spanned the IM and OM of mitochondria, and whose opening rendered the membrane envelope permeable to solutes with a molecular mass below approximately 1.5kDa. It became apparent that this 'permeability transition pore' (PTP) could cause CCR. Opening of the PTP leads to influx of solutes and water into the mitochondrial matrix, and therefore swelling of the matrix contents. This forces the IM outwards. Since the surface area of the IM is greater than that of the OM, the outward force exerted by the former causes generalised rupture of the latter. As a result, IMS proteins such as cytochrome *c* can be released in a non-specific manner.

Evidence for occurrence of this 'Mitochondrial Permeability Transition' (MPT) was found in many cases of CCR (Borutaite *et al*, 2003; Yang & Cortopassi, 1998; Zhu *et al*, 2002; among others). Much interest was invested in determining the structure of

the PTP, with clinical exploitation in mind. There have been numerous proposed components, although three proteins are most commonly associated with the megachannel. The first is the OM 'voltage dependent anion channel', or VDAC. Also known simply as 'porin', this channel has a physiological role in regulating metabolite flow across the OM. However, it is also thought to associate with other proteins to form the major OM component of the PTP. The adenine nucleotide translocator (ANT) is thought to constitute the primary IM component of the PTP, in addition to its role as the translocator of ADP and ATP across the IM. The third PTP protein is cyclophilin *d*, found in the matrix. Aside from a role in apoptosis, cyclophilin *d* belongs to a family of molecular chaperones, capable of peptidyl-prolyl isomerase mediated protein folding.

In addition to these three main components, other postulated players are the peripheral benzodiazepine receptor (PBR, McEnery *et al*, 1992) and mitochondrial hexokinase (Beutner *et al*, 1996). A role is also suggested for the Bcl-2 family of proteins. This group includes both pro- and anti-apoptotic members. Pro-apoptotic Bax (Marzo, 1998) is thought to be a peripheral pore component, rendering the MPT sensitive to inhibition by anti-apoptotic family members (Narita *et al*, 1998).

The inclusion of cyclophilin *d* in the PTP is widely accepted, and it is this protein which confers sensitivity of MPT to the immunosuppressive drug cyclosporin A. (CsA). This drug is widely used as an experimental tool to identify occurrence of the MPT. However, it has numerous targets other than the PTP-associated cyclophilin *d* (Capano *et al*, 2002; Kim *et al*, 2003; Sanchez *et al*, 2003; among others). The

effects of the drug are therefore notoriously non-specific and must be interpreted with caution.

A further feature of MPT often used as a tool for its detection is the dissipation of $\Delta\psi_m$. Loss of the integrity of the IM inevitably causes a loss of ability to support a proton gradient.

Another major experimental tool for detection of MPT is the monitoring of mitochondrial volume. Evidence of mitochondrial swelling is usually taken as indication of MPT. However, there is another, less recognised, 'swelling-dependent' CCR mechanism which leads to generalised OM rupture. Vander Heiden & Thompson (1999) report that inappropriate closure of the VDAC (described in 1.3.5.1) can also mediate CCR. Closure of this channel leads to a defect in the exchange of ATP and ADP across the OM. As ADP levels in the matrix decline, ADP becomes less available as a substrate for the ATP synthase (complex V). In fact, if the ATP:ADP ratio increases sufficiently within the matrix, the ATP synthase can function in reverse, catalysing the dephosphorylation of ATP to ADP (Oster & Wang, 2000). In contrast to the dissipation of $\Delta\psi_m$ associated with the MPT, the effect of this dysregulation is to hyperpolarize the $\Delta\psi_m$. It is claimed by the authors that this hyperpolarisation leads to matrix swelling and non-specific OM rupture as described for the MPT. However, the authors did not provide justification for their suggested link between hyperpolarisation of $\Delta\psi_m$ and matrix swelling.

1.3.5.2 Swelling-independent release mechanisms

Whilst non-specific rupture of the OM would inevitably cause CCR (at least of the proportion which is freely soluble in the IMS – see 1.2.2.2), a major discrepancy has arisen in recent years. An increasing number of studies are reporting CCR in the absence of any detectable swelling of the mitochondria. There is little argument that MPT would lead to CCR, but it would appear that it is not the sole mechanism capable of doing so.

It has been claimed that MPT is in fact a reversible event, with 'flickering' opening of the PTP occurring prior to the permanent loss of membrane integrity described above (1.3.5.1). This has been suggested as a possible reconciliation of swelling-independent CCR with MPT as the mechanism (Scarlett & Murphy, 1997). However, there has been no explanation of how the IMS cytochrome *c* could be liberated by a channel which spans both the IM and OM, and has a permeability limit of 1.5kDa (note that cytochrome *c* is 12.1kDa). The crucial event in the MPT theory of CCR was rupture of the OM, which is inextricably linked to matrix swelling.

Attention has switched, therefore, to potential CCR mechanisms which leave the IM unperturbed, but instead rely on permeability changes in the OM alone. This approach has identified a number of channels in the OM which may be implicated in CCR. One of these is the postulated OM component of the PTP, the VDAC. This channel is constitutively present as an OM channel, as described (1.3.5.1). It has however been identified as a potential route by which CCR may occur (Madesh & Hajnoczky, 2001). The argument has been put forward, however, that the pore diameter of this channel is insufficient to permit CCR (Mannella, 1998). This led to a

new line of investigation involving the Bcl-2 family of proteins, referred to in 1.3.5.1. One pro-apoptotic member in particular has been implicated. Bax has been seen to translocate through the cytosol to the mitochondrial OM during apoptosis (Wolter *et al*, 1997; Zhang *et al*, 1998) and has sequence homology with known channel-forming proteins (Montessuit *et al*, 1999). It is subject to regulation by heterodimerisation with anti-apoptotic members of the Bcl-2 family, which are thought to be constitutively present in the OM. However, providing that these regulatory systems allow, Bax is now thought to be able to form OM channels of sufficient pore diameter to permit CCR (Antonsson *et al*, 2000).

In order to reconcile this data with reports of VDAC being required for CCR, work has been carried out into the possible association of Bax and VDAC. It has been demonstrated that Bax can coimmunoprecipitate with VDAC (Narita *et al*, 1998), and modulate its permeability (and a Bax-VDAC channel is now considered a strong candidate for a swelling-independent CCR channel (Shimizu *et al*, 2000)). It is possible that there may be substitution of Bax by other pro-apoptotic Bcl-2 family members in some cases (Brustovetsky *et al*, 2003b).

A third possible OM channel hypothesis also implicates Bax. It has been shown that Bax can cause membrane instability by reducing the linear tension of phospholipid bilayers (Basanez *et al*, 1999). It has been suggested that this induced instability could lead to the formation of lipidic pores or lipid-protein complexes which could permit CCR. However, this hypothesis has attracted significantly less interest to date.

A summary of the major recognised swelling-dependent and swelling-independent CCR mechanisms can be seen in Figure 1.9.

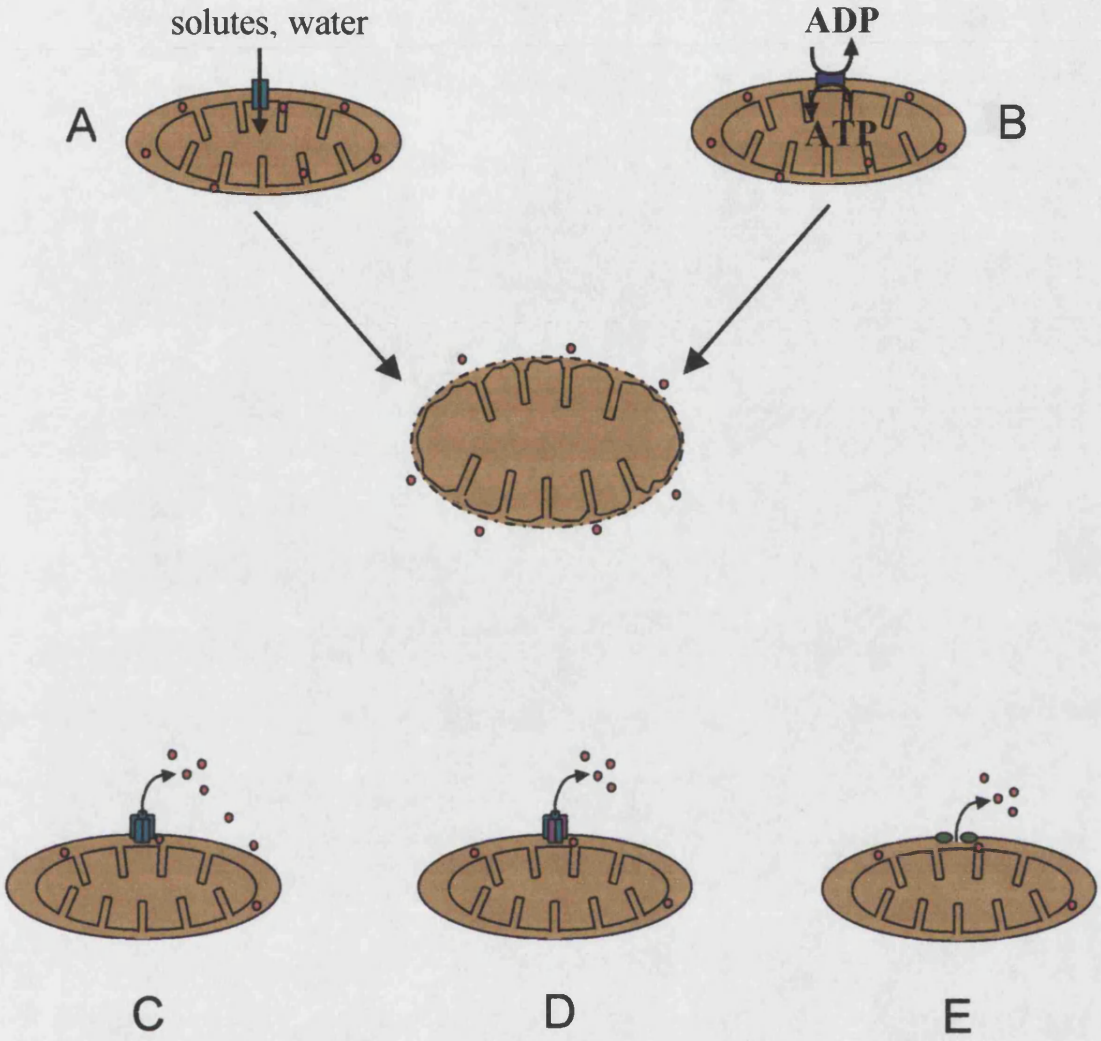

Figure 1.9

Summary of the currently recognised possible CCR mechanisms. A and B show swelling-dependent release mechanisms, due to opening of the PTP and closure of the VDAC, respectively. C, D and E demonstrate swelling-independent mechanisms, caused by Bax oligomerisation, Bax oligomerisation and association with VDAC, and Bax-mediated lipidic pore formation, respectively. For details, see text.

1.3.5.3 Implications of the release mechanism

Due to the implications of the suggested CCR mechanisms, swelling-independent processes are gaining support. The recognised apoptotic program is energy-dependent. The loss of IM integrity associated with swelling-dependent CCR mechanisms, and inevitable dissipation of $\Delta\psi_m$ are inconsistent with the sustained generation of ATP required for apoptosis. It is possible that there are releasable and non-releasable pools of cytochrome *c*, and that sufficient cytochrome *c* is retained in the event of MPT to support the apoptotic program. It is also suggested that released cytochrome *c* may be capable of maintaining $\Delta\psi_m$ and ATP production (Waterhouse *et al*, 2001). However, as Crompton alludes to in his 2000 review, this highly disruptive process appears poorly matched with the tightly regulated apoptotic program, designed to tidily package cellular contents so as to prevent further damage (see 1.3.1).

There has been discussion of the apoptosis and necrosis programs not being independent events, but rather that cell death occurs by mechanisms which fall along a continuum between the two extremes (Zeiss, 2003). It is possible that MPT is associated with more necrotic forms of cell death, where the energy requirement is reduced.

One recent study has suggested a very interesting possible reconciliation of the MPT with swelling-independent apoptosis. De Giorgi *et al* (2002) report that 'flickering' openings of the PTP can signal for the redistribution of Bax to the mitochondrial OM. Bax oligomerisation at the OM then allows CCR as described in 1.3.5.2. In this

sense, the PTP is not an intrinsic component of the CCR machinery, but an upstream trigger which can induce release by another means.

The mechanism responsible for CCR during apoptosis has implications other than simply allowing the redistribution of cytochrome *c*. Downstream of CCR, defence mechanisms exist in the cytosol to prevent 'inappropriate' apoptosis. If the death program is to be arrested at a 'post-mitochondrial' stage, the extent of disruption afforded by the CCR mechanism becomes vitally important. It is essential for cell survival that it retains energetic viability (highly dependent on the functional capacity of the mitochondria). Preservation of mitochondrial respiratory function is of particular importance in neurons, which have limited glycolytic capacity (Walz & Mukerji, 1988). Therefore disruptive release mechanisms such as MPT render the post-mitochondrial defence processes somewhat redundant.

1.3.6 *Post-mitochondrial regulation of apoptosis*

It would appear that even following activation of the caspase cascade, a cell has not reached the 'point of no return' in its survival. A number of mechanisms have been identified whereby apoptosis can be prevented at a stage downstream of CCR.

1.3.6.1 IAPs

Inhibitor of apoptosis ('IAP') proteins belong to a family known as the BIR-containing proteins ('BIRPs'). The BIR domain is the 'baculovirus IAP repeat', and is essential to the anti-apoptotic properties of IAPs (Duckett *et al*, 1998). Some IAPs

also contain a zinc-binding 'ring finger' domain (Verhagen *et al*, 2001). Since the discovery of the first IAP in 1993 (Crook *et al*, 1993), eight human IAPs have been identified: XIAP, ILP-2, c-IAP1, c-IAP2, ML-IAP, NAIP, survivin and apollon. The best characterised of these, and apparently the most potent (Deveraux *et al*, 1999) is XIAP. From the study of this protein, understanding has grown about how IAPs act to regulate apoptosis by direct inhibition of caspases.

XIAP is thought to regulate at least seven caspases, however a detailed understanding of the mechanism of inhibition only exists at present for its interaction with caspases –3, -7 and –9. Interestingly, although proteolytic cleavage of procaspase-9 is not required for its activation (Stennicke *et al*, 1999), only the cleaved form is subject to regulation by XIAP (Srinivasula *et al*, 2001). XIAP binds directly via its BIR3 domain to the smallest cleavage product of caspase-9. In contrast, caspases-3 and –7 are inhibited by steric occlusion by XIAP following binding of the caspase by a region adjacent to BIR2 (Riedl *et al*, 2001).

Other IAPs most likely operate by similar mechanisms, although no other IAP has as large a repertoire of recognised target caspases as XIAP. Interestingly, there is an IAP specific to neuronal cells, NAIP (neuronal apoptosis inhibitory protein). To date, NAIP is only thought to regulate the activities of caspases-3 and –7 (Maier *et al*, 2002), but bearing in mind the sequential, non-redundant nature of the caspase cascade, this inhibition may still be significant. With respect to the role of apoptosis in neurodegeneration (1.3.2), it has been shown that NAIP levels are decreased in adult patients with Down syndrome and Alzheimer's disease (Seidl *et al*, 1999). It

has also been demonstrated that NAIP has a protective role in an *in vivo* model of Parkinson's disease (Crocker *et al*, 2001).

1.3.6.2 Smac

The 'second mitochondria-derived activator of caspase' (Smac) protein was identified in 2000 by Du *et al* (and also concurrently by Verhagen *et al*, who named the protein 'direct IAP binding protein with low pI', or DIABLO). The name assigned by the latter group reveals the role of Smac in the regulation of apoptosis. It serves as an inhibitor of the IAP proteins described above (1.3.6.1), and therefore by a disinhibition mechanism, promotes apoptosis:

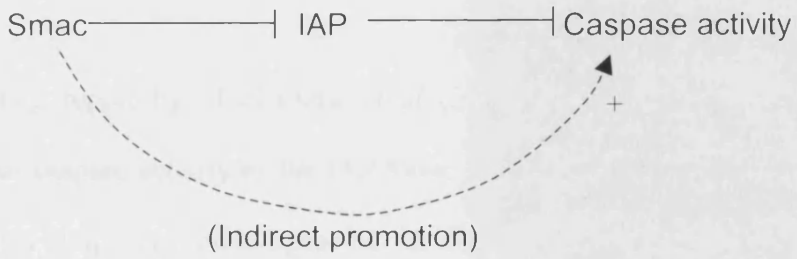

Smac was found to be a 23-25kDa protein which co-localised with cytochrome *c* under normal conditions. It was identified in several tissue types, although interestingly was only present at low levels in brain (Verhagen *et al*, 2000). It was found to be synthesised with an N-terminal mitochondrial targeting sequence, which was cleaved off to form the mature protein. It has been repeatedly proven that Smac is an IMS protein, released to the cytosol during apoptosis (Adrain *et al*, 2001; Deng *et al*, 2002; Rehm *et al*, 2003; among others). This is clearly reminiscent of cytochrome *c*, however it appears that the two proteins are not necessarily released by the same mechanism during apoptosis (Kandasamy *et al*, 2003; Rehm *et al*, 2003).

In the study by Verhagen *et al* (2000), Smac interacted with all of the IAPs tested (XIAP, c-IAP1, c-IAP2 and the baculoviral OpIAP). It is likely therefore that the interaction is mediated by the conserved BIR domains and that Smac will inhibit any IAP family member.

Smac will therefore potentiate the pro-apoptotic effects induced by cytochrome *c*. Clearly, it is not required for the activation of procaspase-9 by the apoptosome system (Liu *et al*, 1996). However, it has been claimed by Deshmukh *et al* (2002) that Smac release is required for the full apoptotic program to be completed in primary neurons. As yet, there are no reports which confirm the repeatability of this finding.

An interesting report by MacFarlane *et al* (2002) lends added complexity to the regulation of caspase activity by the IAP/Smac system. The authors claim that XIAP functions as a ubiquitin-protein ligase for the ubiquitination and therefore subsequent degradation of Smac. Therefore, XIAP creates a form of negative feedback loop on the pro-apoptotic Smac, overall strengthening its own anti-apoptotic capacity.

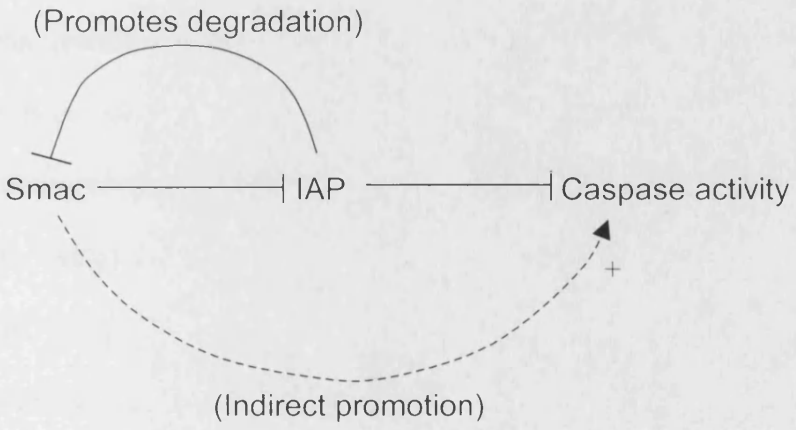

1.3.6.3 Omi

Omi, also known as HtrA2 (Gray *et al*, 2000), is very similar in localisation and role to Smac. Although the bacterial homologue HtrA has roles as a protease and as a chaperone, the proven role of mammalian Omi lies in its ability to inhibit IAPs (Suzuki *et al*, 2001). The mature Omi is a 37kDa protein, synthesised, like Smac, with a mitochondrial targeting sequence which is cleaved off upon mitochondrial transport. It is released from mitochondria during apoptosis, and via inhibition of IAPs potentiates the other pro-apoptotic signals (van Loo *et al*, 2002). Unlike Smac, Omi does not interact with all the IAPs tested (Verhagen *et al*, 2002), however it does appear to have a more ubiquitous expression pattern than Smac (Gray *et al*, 2000). There is evidence that Omi exerts a more severe inhibition of IAPs than Smac, by catalysing their irreversible catalytic cleavage (Yang *et al*, 2003). The serine protease activity of Omi is also thought to induce an atypical caspase-independent form of cell death (van Gurp *et al*, 2003).

1.3.6.4 Hsps

The cytosolic heat shock proteins (Hsps) have been known for some time to have anti-apoptotic properties (Jaattela *et al*, 1992; Mosser *et al*, 1997). It has now been revealed that this effect is, at least in part, due to the capacity of Hsps to chaperone Apaf-1 in the cytosol. Both Hsp70 (Saleh *et al*, 2000) and Hsp90 (Pandey *et al*, 2000) have been shown to sequester Apaf-1, preventing the formation of the oligomerised apoptosome. This in turn prevents association with and activation of procaspase-9. Saleh *et al* (2000) demonstrate that the association of Hsp70 with Apaf-1 occurs via the CARD domain on Apaf-1 (1.3.3.1). It is suggested that Hsp-mediated inhibition of apoptosome oligomerisation may be due to a conformational

change in the dATP-binding site on Apaf-1. Pandey *et al* (2000) demonstrated that a range of DNA-damaging agents relieved the protective effects of Hsp90 by dissociating the Hsp90-Apaf-1 complex.

1.3.6.5 GSH

It has been suggested that only ferricytochrome *c* is capable of initiating apoptosis (Hancock *et al*, 2001). Provided that cytosolic GSH levels (1.1.3) are sufficient, cytochrome *c* released into the cytosol would be rapidly reduced to the ferro form, and therefore according to the theory of Hancock *et al* (2001) be prevented from activating caspase-9. However, if either the cytosolic cytochrome *c* concentration rises high enough, or the GSH concentration falls low enough, there will be an increasing presence of ferricytochrome *c*.

1.3.6.6 Potassium

It has been reported that physiological concentrations of intracellular K^+ inhibit cytochrome *c*-dependent caspase activation (Hughes *et al*, 1997). A mechanism of this inhibition has since been determined by Cain *et al* (2001). It appears that K^+ can inhibit the binding of cytochrome *c* to Apaf-1, and therefore the formation of the active 700kDa apoptosome complex. Clearly, this will prevent activation of caspase-9 and the subsequent caspase cascade. It is suggested that this may be a protective mechanism employed by the cell to prevent inappropriate apoptosis resulting from accidental release of small quantities of cytochrome *c*. Interestingly, the inhibition is antagonised in a concentration-dependent manner by cytochrome *c*, although the kinetics of K^+ mediated inhibition are not truly competitive with the pro-apoptotic protein. It has been reported that intracellular levels of K^+ are reduced during

apoptosis (Hughes *et al*, 1997). This would lower the threshold cytochrome *c* concentration required for apoptosis to proceed.

Regulation of the cytosolic K^+ concentration would therefore appear to be a very important post-mitochondrial control mechanism for protection against apoptosis.

1.3.6.7 Phosphorylation

It has been noted that cells in which activity of the protein kinase Akt is increased by transfection show reduced susceptibility to apoptosis (Nakashio *et al*, 2000). Cytosolic extracts from such cells are resistant to cytochrome *c*-induced caspase activation (Cardone *et al*, 1998). These authors determined that the Akt-mediated protection from apoptosis is due to phosphorylation of both procaspase-9 and active caspase-9. It is hypothesised that Akt-induced phosphorylation of either form results in blocking of the Apaf-1 binding site by a non-cleavable zymogen (in the case of procaspase-9) or a cleaved but inactive enzyme (in the case of caspase-9). This would reduce the availability of the site to non-phosphorylated procaspase-9 or caspase-9, thus inhibiting apoptosis.

1.3.6.8 Ubiquitination

The conjugation of ubiquitin to a protein leads in the majority of cases to degradation by the proteasome (see 1.2.2.3). Ubiquitin-mediated degradation and change in activity of proteins involved in the apoptotic machinery are thought to be important *in vivo* mechanisms of regulating the death process (Yang & Yu, 2003). Regulation of the activity of caspases (Chen *et al*, 2003) and Bcl-2 proteins (Marshansky *et al*, 2001) by ubiquitination has been reported. It has even been suggested that

degradation of IAPs via ubiquitination might be essential for apoptosis to proceed (Yang *et al*, 2000).

An interesting twist to the regulation of apoptosis is that the IAPs which have the carboxy-terminal ring finger motif (1.3.6.1) have E3 activity. E3 is the enzyme responsible for recognising target proteins and transferring activated ubiquitin to them (reviewed by Pickart, 2001). As a result, these IAPs can catalyse their own autoubiquitination (Yang *et al*, 2000) as well as the ubiquitination of other players in the apoptotic program such as caspases (Huang *et al*, 2000; Suzuki *et al*, 2001b) and Smac (MacFarlane *et al*, 2002). Interestingly it has been suggested that Smac may in return be capable of catalysing the ubiquitination of XIAP (Yang & Yu, 2003).

Proteasome-mediated degradation of ubiquitinated proteins therefore has considerable influence over the pro/anti-apoptotic balance within the cytosol.

CHAPTER 2

Materials and Methods

2.1 Materials

2.1.1 *Chemicals and reagents*

Ficoll 400 was purchased from Amersham Pharmacia Biotech (Bucks., UK). Deoxyribonuclease type I (DNAse, EC 3.1.21.1, from bovine pancreas), cytochrome *c* (from horse heart), pyruvate kinase (PK, EC 2.7.1.40, from rabbit muscle) and lactate dehydrogenase (LDH, EC 1.1.1.27, from rabbit muscle) were purchased from Roche Diagnostics (East Sussex, UK). L-valine based minimal essential medium (MEM), neurobasal medium, foetal bovine serum (FBS) and B27 with antioxidants were purchased from Gibco BRL (Renfrewshire, UK). Anti-Bak (rabbit polyclonal G-23), anti-Smac (goat polyclonal V-17), anti-AIF (goat polyclonal D-20) and the secondary anti-goat horseradish peroxidase-conjugated antibody were purchased from Santa Cruz Biotechnology Inc. (Heidelberg, Germany). Adenosine 5'-diphosphate (ADP, potassium salt) and cyclosporin A (from *Tolypocladium inflatum*) were purchased from Merck Biosciences Ltd. (Nottingham, UK). Anti-tubulin (mouse monoclonal TU-20) was purchased from AbCam (Cambridge, UK). The secondary anti-mouse FITC-conjugated antibody was purchased from Molecular Probes Europe BV (Leiden, The Netherlands). All other chemicals and reagents were of analytical grade and purchased from Sigma-Aldrich (Poole, UK).

2.1.2 *Assay kits*

The rat/mouse Quantikine M Immunoassay kit for cytochrome *c* and the colorimetric caspase-9 assay kit were purchased from R&D Systems (Abingdon, UK). The

Detergent Compatible Protein Assay reagents were purchased from Bio-Rad (Herts., UK).

2.1.3 *Equipment*

Sterile six-well culture plates (for neuronal cultures) were purchased from Costar (Corning Costar, High Wycombe, UK). Sterile 80cm^2 flasks (for astrocytic cultures) were purchased from Nalge Nunc International (Naperville, IL, USA). Glass coverslips were purchased from Chance-Proper (Smethwick, UK). Microscope slides (1-1.2mm super premium) and 50ml screw-top centrifuge tubes were purchased from BDH Laboratory Supplies (Poole, UK). 96-well microtiter plates were purchased from Thermo LabSystems (Vantaa, Finland). Ultra-Clear centrifuge tubes for ultracentrifugation were purchased from Beckman Instruments (CA, USA). The oxygen electrode was purchased from Rank Bros. (Cambridge, UK). The TPP^+ electrode was purchased from World Precision Instruments (Herts., UK).

2.1.4 *Animals*

Rats used for isolated mitochondria preparations were male, approximately 250g and of the Wistar strain. Embryonic day 17 Wistar rat pups were used for primary neuronal culture, and 1-2 day old neonates used for the astrocyte primary culture. All animals were purchased from A.J. Tuck & Son Ltd. (Rayleigh, Essex, UK). Animals were kept under 12 hour light/dark cycles, fed a stock laboratory diet and provided with water *ad libitum*.

2.2 Preparation of sample material

2.2.1 *Isolation of brain mitochondria from adult rat whole brain*

2.2.1.1 Preparation of Ficoll gradients

The isolation of mitochondria from whole brain tissue requires that contaminating subcellular elements be removed. A series of simple centrifugation steps yields a crude mitochondrial pellet, but separation by density gradient is required in order to remove contaminating myelin and to distinguish the synaptosomal fraction from the non-synaptic mitochondria.

Traditionally, this density gradient separation was achieved using sucrose solutions (Gray & Whittaker, 1962; Blokhuis & Veldstra, 1970). However, this involved subjecting the mitochondria to extremely hypertonic sucrose concentrations, and centrifugation was at very high speed and of long duration. These factors had detrimental effects on the metabolic activity of mitochondria isolated in this manner.

A preferable alternative is now available. Ficoll 400 (Amersham Pharmacia Biotech, Bucks, UK) is a high molecular mass (average M_R 400g.mol^{-1}) polymerised sugar. Since its molecular mass is significantly greater than that of sucrose, Ficoll solutions of the same concentration (in g per unit volume) have relatively lower osmolarity (since a lower number of moles per unit volume is required). Consequently, the use of Ficoll allows contaminating elements such as myelin to be filtered out whilst not exerting osmotic stress on organelles such as mitochondria.

Ficoll 400 was prepared for use in mitochondrial isolation procedures as follows. Ficoll was dissolved in deionised water at a concentration of $500g.l^{-1}$. This solution was dialysed against deionised water overnight at 4°C. The specific gravity of the dialysed Ficoll was then measured. Using the manufacturer's standard curve, this specific gravity was then used to determine the Ficoll concentration. The volume of deionised water required to reduce this concentration to 20% (w/v) was calculated and the necessary dilution made.

10% and 7.5% Ficoll solutions were prepared by dilution of the 20% solution using isolation medium, to give final concentrations 10% or 7.5% (w/v) Ficoll, 0.32M sucrose, 50μM K^+EDTA, 10mM Tris-HCl pH 7.4.

6% and 4.5% Ficoll solutions were prepared by dilution of the 20% solution using modified isolation medium, to give final concentrations 6% or 4.5% (w/v) Ficoll, 0.24M mannitol, 60mM sucrose, 50μM K^+EDTA, 10mM Tris-HCl pH 7.4.

3% Ficoll was prepared by diluting 6% Ficoll (made as above) 1:1 with deionised water.

All Ficoll solutions were brought to pH 7.4 immediately prior to use with HCl and Tris.

Gradients were made up by slow layering of Ficoll in Beckman Ultra-Clear Centrifuge Tubes (Beckman Instruments Ltd, California). The first gradient consisted

of 18ml 10% Ficoll, 9ml 7.5% Ficoll and 9ml isolation medium. The second gradient (synaptic preparation only) consisted of 9ml 6% Ficoll, 4.5ml 4.5% Ficoll and 3ml 3% Ficoll. Visible clear interfaces provided verification of discrete density layers.

The procedure for separation by the first gradient (10% / 7.5% / isolation medium) differed between the non-synaptic and the synaptic mitochondria isolation protocol (see Figure 2.1). For the former, a 'spin-down' method was used. This means that the homogenate to be separated is suspended in the top layer, ie. the isolation medium. Centrifugation results in the required fraction (the non-synaptic mitochondria) passing down through the gradient. The parameters of the spin are such that some non-synaptic mitochondria remain in the synaptosomal layer, but no synaptosomes reach the pellet. Thus yield is sacrificed for purity.

For the isolation of synaptic mitochondria, a 'spin-up' method is used. The homogenate to be separated is this time resuspended in the bottom layer. The volume of homogenate is known exactly, and used to dilute a 12% Ficoll solution to 10% (w/v). This mixture is then used as the bottom layer of the gradient, and the top layer is isolation medium alone. The centrifugation then results in the required fraction (the synaptosomes) passing up through the gradient. Again, yield is sacrificed for purity, as the spin-up process leaves some residual synaptosomes in the pellet, but avoids contamination of the synaptosomal layer by non-synaptic mitochondria.

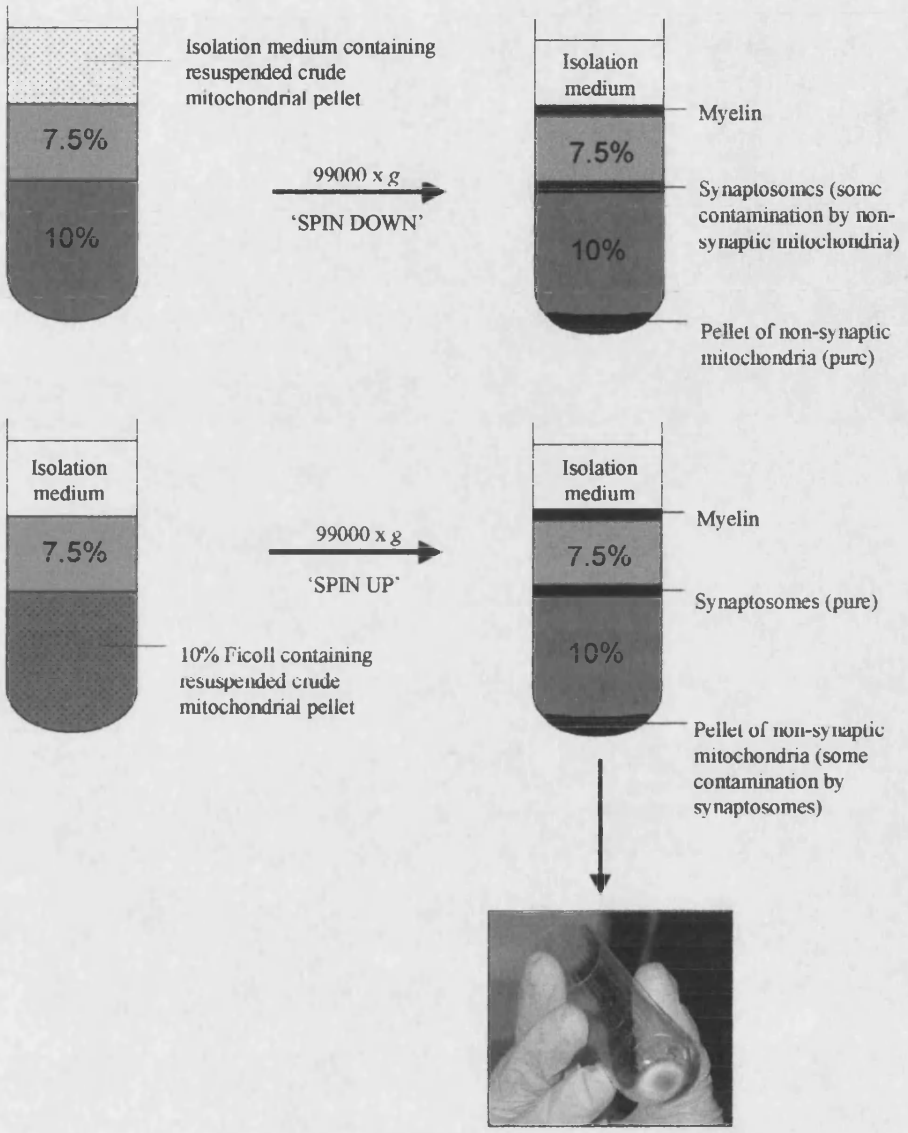

Figure 2.1

Schematic diagram to demonstrate the advantages of 'spin down' and 'spin up' techniques for density gradient separation of non-synaptic and synaptic mitochondria, respectively. Photograph shows contamination of non-synaptic mitochondrial pellet with white synaptosomes following 'spin-up' procedure.

2.2.1.2 Isolation of non-synaptic rat brain mitochondria

The isolation of non-synaptic rat brain mitochondria was carried out according to the method of Lai and Clark (1989), which is demonstrated schematically in Figure 2.2. Three male Wistar rats were killed by cervical dislocation and decapitated. The whole brains were removed and placed in approximately 30ml isolation medium (0.32M sucrose, 1mM K^+EDTA, 10mM Tris-HCl, pH 7.4) at 4°C. From this point the isolation procedure was carried out at this temperature. The brains were rapidly chopped manually. The tissue was allowed to settle and the isolation medium was gently poured away and replaced with fresh medium. This was repeated three times to remove as much contaminating blood as possible.

The chopped brain tissue was then diluted 1:10 with isolation medium in a Dounce homogeniser. The suspension was homogenised using eight up-and-down strokes. The resulting homogenate was centrifuged in two tubes at 1500x*g* for 3 minutes in a pre-cooled Beckman J2-21M/E centrifuge (Beckman RIIC Ltd., High Wycombe, UK) with a Beckman JA-20 fixed angle rotor. The supernatants were decanted off into clean centrifuge tubes. Isolation medium was added to the pellets, and these were homogenised in the Dounce homogeniser using four up-and-down strokes. The resulting homogenate was centrifuged for a second time under the conditions above. Again, the supernatants were decanted off into clean tubes.

The pellets were discarded, and the pooled supernatants centrifuged at 17000x*g* for 10 minutes in the pre-cooled Beckman J2-21M/E centrifuge. The supernatants were this time discarded, and the 'crude mitochondrial pellets' resuspended in a total of

18ml isolation medium. The pellets were resuspended by five up-and-down strokes in a Potter homogeniser.

Ficoll gradients of 18ml 10% Ficoll and 9ml 7.5% Ficoll were set up in two Beckman Ultra-Clear Centrifuge Tubes. 9ml of the mitochondrial homogenate was layered gently onto each of these gradients (as described in 2.2.1.1). The two tubes were then placed into matched rotor buckets from a Beckman SW28 swing-out rotor. Isolation medium was used to bring the two buckets to equal mass, as determined by a digital balance. The buckets were attached to the rotor, and the tubes centrifuged at 99000x*g* for 30 minutes in a pre-cooled Beckman L8-70M ultracentrifuge. The layers of Ficoll and the myelin and synaptosomal bands were removed carefully by pipetting. (see Figure 2.1). The mitochondrial pellet was washed very gently with isolation medium.

The pellet was then resuspended in approximately 1ml isolation medium by five up-and-down strokes in a 2ml Potter homogeniser. The homogenate was centrifuged in a 1.5ml eppendorf tube in a pre-cooled centrifuge (Sigma Laborzentrifugen 3K10, Osterode, Germany) at 9800x*g* for 10 minutes. This process allowed removal of any residual Ficoll. The supernatant was discarded, and the pellet resuspended in isolation medium to a concentration of approximately 15mg.ml^{-1} (determined by observation) using 3 up-and-down strokes in the 2ml Potter homogeniser. The final mitochondrial suspension was stored on ice in a 1.5ml eppendorf tube prior to experimentation.

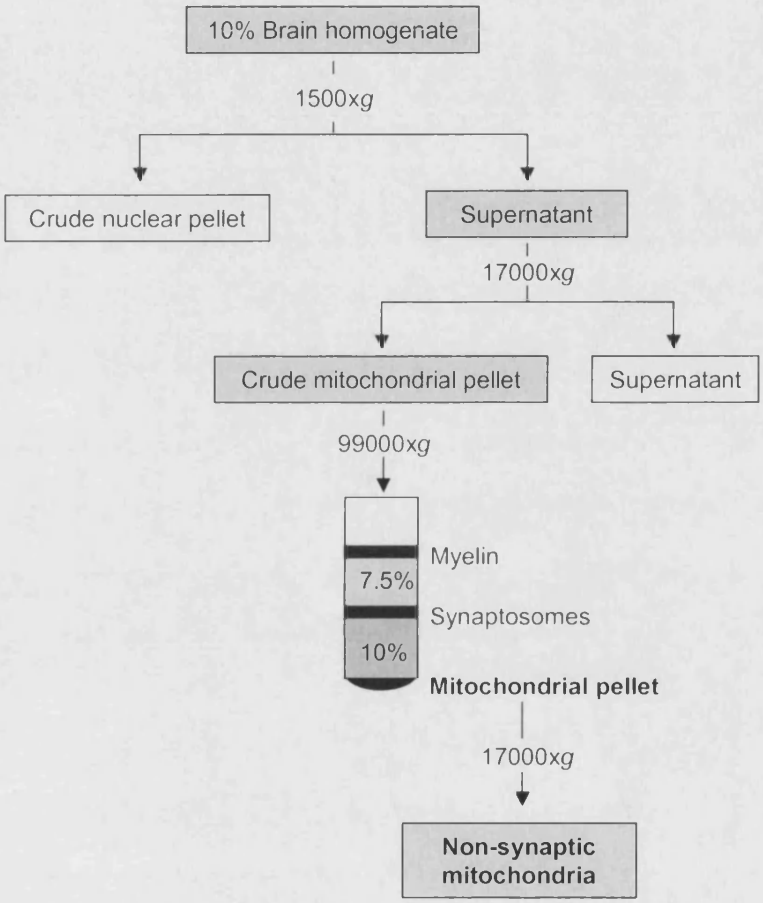

Figure 2.2

Schematic diagram to demonstrate the procedure for isolating non-synaptic mitochondria from whole rat brains.

2.2.1.3 Isolation of synaptic rat brain mitochondria

The isolation procedure for synaptic rat brain mitochondria is the same as for the non-synaptic population to the point of obtaining the crude mitochondrial pellet. However, due to the relatively poor yield of synaptic mitochondria, it was necessary to use whole brains from four, instead of three, animals. The whole procedure is demonstrated schematically in Figure 2.3.

On obtaining the four crude mitochondrial pellets, 6ml isolation medium was used to pool them. This was then homogenised together with some of a 30ml volume of 12% Ficoll, using five up-and-down strokes in a Potter homogeniser. This homogenate was then transferred to a 50ml falcon tube, and mixed thoroughly with the remaining 12% Ficoll to make 36ml of a 10% (w/v) Ficoll / mitochondrial suspension. 18ml of this was used in each of two ultra-clear tubes as the bottom layer of the gradient, and 9ml 7.5% Ficoll and 9ml isolation medium gently layered on top (as described in 2.2.1.1). The samples were prepared for ultracentrifugation as in the non-synaptic preparation.

After the 30 minute spin at 99000x*g*, the top two layers of Ficoll and the myelin band were carefully removed. The synaptosomal band was then decanted using a Pasteur pipette. The synaptosomal layers from both tubes were pooled in a clean centrifuge tube and diluted 1:3 with isolation medium. This was then centrifuged at 18500x*g* for 10 minutes in the pre-cooled Beckman J2-21M/E centrifuge, using the Beckman JA-20 fixed angle rotor. The supernatant was removed, and 10ml 6mM Tris-HCl (pH 8.1) was added to lyse the synaptosomes. The pellet was resuspended in the aqueous Tris solution using four up-and-down strokes in a small Dounce homogeniser. 20ml

additional 6mM Tris-HCl (pH 8.1) was then added, and the suspension mixed gently. It was then centrifuged at 11800x*g* for 10 minutes. The supernatant was very carefully decanted off, ensuring that the loose pellet was not disturbed. 10ml 6mM Tris-HCl (pH 8.1) was added to the pellet, and again resuspension was achieved by four up-and-down strokes in the small Dounce homogeniser. The homogenate was centrifuged at 8300x*g* for 10 minutes. The supernatant was then sharply decanted, so that the loose white part of the pellet was lost.

The remaining darker pellet was resuspended using a pipette in 6ml 3% Ficoll. 3ml of this mixture was layered onto each of two gradients of 9ml 6% and 4.5ml 4.5% Ficoll. These tubes were prepared for ultracentrifugation as before, and centrifuged in the pre-cooled Beckman L8-70M ultracentrifuge using the Beckman SW28 swing-out rotor at 11300x*g* for 30 minutes. After separation, the top fraction was carefully removed using a Pasteur pipette. The band between the 6% and 4.5% Ficoll layers was removed from each tube, pooled in a clean centrifuge tube and diluted 1:3 with isolation medium. This was centrifuged at 12000x*g* for 10 minutes.

The pellet from this spin, along with the two pellets from the ultracentrifugation were pooled in approximately 1ml isolation medium and resuspended in a 2ml Potter homogeniser. This suspension was centrifuged in a 1.5ml eppendorf at 9800x*g* for 10 minutes in a pre-cooled centrifuge (Sigma Laborzentrifugen 3K10, Osterode, Germany). The supernatant was removed, and the pellet resuspended in isolation medium to a concentration of approximately 10mg.ml^{-1} (determined by observation) using the 2ml Potter homogeniser. The final mitochondrial suspension was stored on ice in a 1.5ml eppendorf tube prior to experimentation.

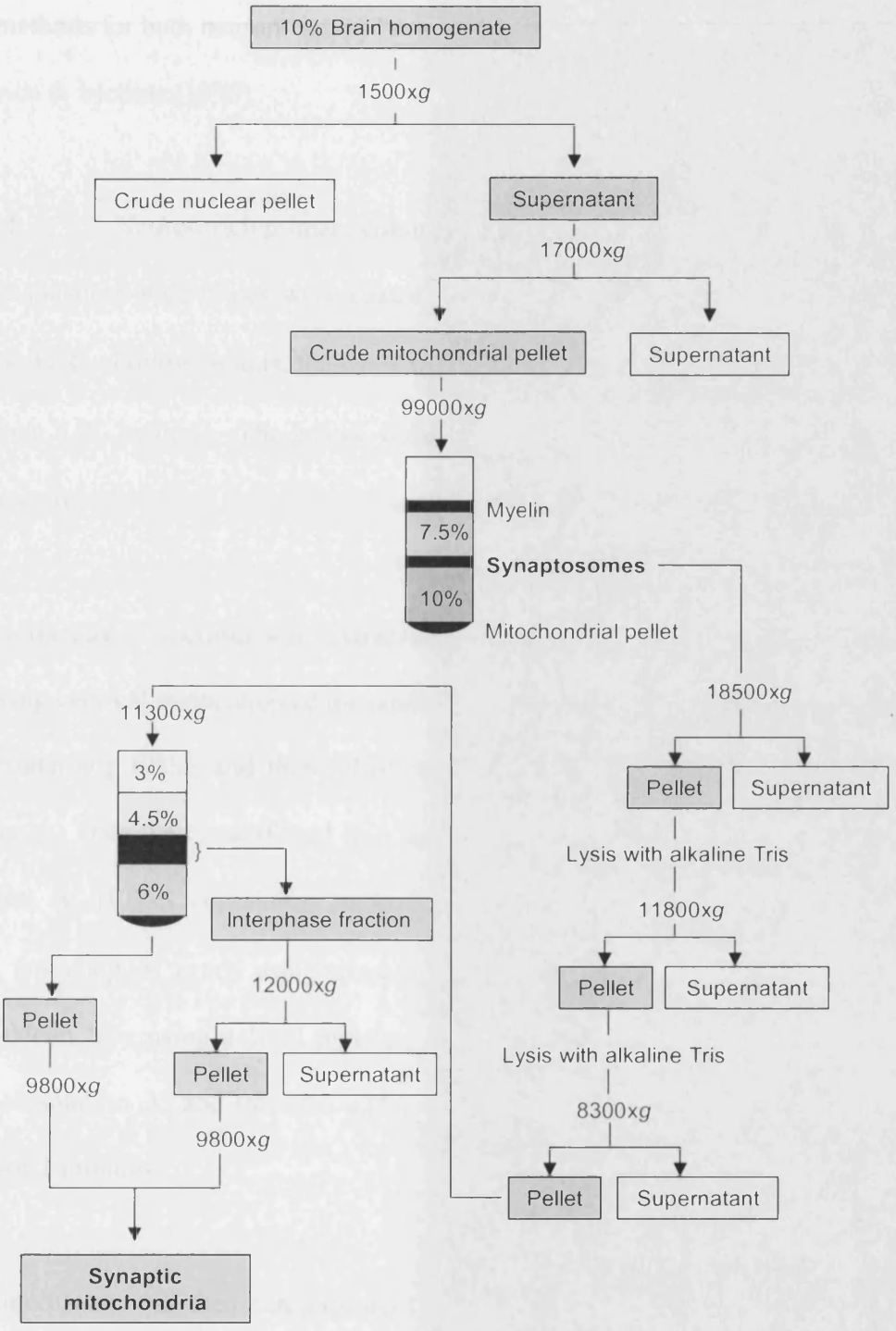

Figure 2.3

Schematic diagram to demonstrate the procedure for isolating synaptic mitochondria from whole rat brains.

2.2.2 *Cell culture*

The methods for both neuron-rich and astrocyte-rich cultures were adapted from Almeida & Medina (1998).

2.2.2.1 Neuron-rich primary culture from foetal rat cortex

Sterile plastic 6-well plates were coated with poly-L-ornithine and incubated for 1 hour at 37°C. Following this, the wells were washed twice with sterile distilled water and then UV treated. The plates were then incubated at 37°C during the cell preparation.

Embryonic day 17 foetuses were extracted from the uterus of a time-mated Wistar rat following cervical dislocation of the adult. The cortices were dissected out in a petri dish containing EBSS and then rolled on a sterile piece of filter paper to remove meninges. They were transferred to a small petri dish containing 10ml of neuronal 'solution A' (EBSS containing 26.5μg.ml^{-1} DNAse and 3mg.ml^{-1} fatty acid free BSA), and chopped gently using scissors. The contents of the dish were moved to a 50ml falcon tube using a 10ml pipette. The dish was then washed using a further 10ml of solution A, and this also added to the falcon tube. The tissue was left to settle for 2 minutes.

The supernatant was then carefully decanted off, and replaced with 10ml neuronal 'solution B' (EBSS containing 3.25mg.ml^{-1} fatty acid free BSA, 66.25μg.ml^{-1} DNAse and 250μg.ml^{-1} trypsin). This was incubated at 37°C for 15 minutes. After this time,

1ml cold (4°C) FBS was added to arrest the trypsinisation. The tissue was again allowed to settle for 2 minutes.

The supernatant was carefully removed and replaced with 12ml solution A. The tissue was gently triturated 5 times using a P1000 Gilson pipette and then a P200 Gilson pipette. The mixture was allowed to settle for 4 minutes. The supernatant was moved to a clean tube, ensuring that the pellet was not disturbed. 12ml solution A was added to the pellet and the trituration procedure repeated. After letting the mixture settle for 4 minutes once more, the supernatant was removed and combined with the first. This solution was then centrifuged at 500x*g* for 5 minutes at 4°C.

The supernatant was removed and the pellet resuspended in 1ml neuronal media (neurobasal media containing 1% (v/v) antibiotic-antimycotic solution, 2mM glutamine, 25μM glutamate and 2% (v/v) B27 with antioxidants). The cell suspension was passed through a pre-wetted nylon mesh strainer (pore size 100μm) and the volume brought to 3ml with neuronal media.

The cells were then counted. This was done by adding 10μl cell suspension to 40μl trypan blue and 30μl HBSS, and then applying 10μl of this mixture to a haemocytometer (Weber Scientific International, Middlesex, UK). The number of cells able to extrude trypan blue from their cytosol was counted over 4 separate grid sections, and the overall number of cells in 3ml media counted. Neuronal media was added to the suspension to bring it to 10^6 cells.ml^{-1} media. The cells were then seeded onto the poly-L-ornithine coated plates at a density of 2 x 10^6 cells.well^{-1}, ie.

2ml.well^{-1}. The plates were placed in an incubator (B5060EK/CO_2, Heraeus Instruments, Hanau, Germany) at 37°C with 5% CO_2/95% air and >90% humidity.

Taking the day of the preparation as Day 0, on Day 3, 1ml of the media in each well was substituted for conditioned media (see below) containing 20μM cytosine arabinoside (so final concentration in each well of 10μM) to prevent growth of dividing cells. The cells were treated on Day 6. Neurons at this stage are shown in Figure 2.4.

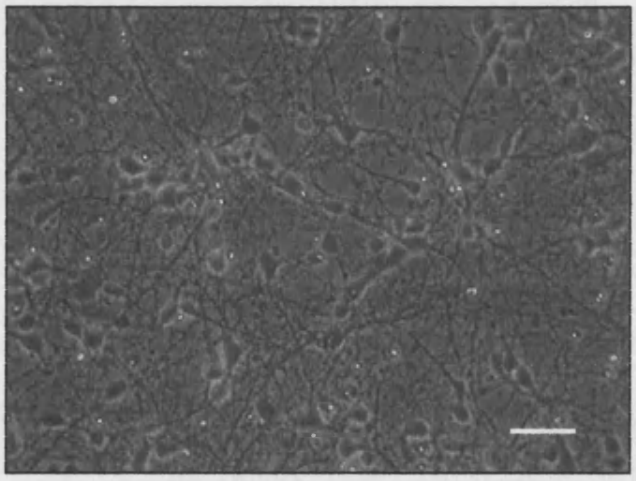

Figure 2.4

Primary cortical neurons at day 6 of culture. Phase contrast micrograph, X20 objective. Scale bar represents 40μm.

2.2.2.2. Astrocyte-rich primary culture from neonatal rat cortex

It is now well recognised that interaction with surrounding glia is an important aspect of the physiology of neurons *in vivo* (reviewed by Hatton, 2002), and it is therefore somewhat artificial to culture neurons in isolation. Co-culture systems can be used, but it is difficult to regulate the ratio of astrocytes to neurons over any significant period of time due to the constant proliferation of the glia. An alternative is to 'condition' the neuronal media by exposing it to astrocytes prior to use on the neurons. Neurobasal media supplemented with 1% (v/v) antibiotic-antimycotic solution, 2mM glutamine and 2% B27 with antioxidants was therefore added onto confluent astrocyte cultures (12ml per $80cm^2$ flask) and incubated for 24 hours. This was then used on Day 3 of the neuronal culture, supplemented with cytosine arabinoside (see 2.2.2.1).

The astrocyte-rich primary culture was prepared as follows. 1-2 day old Wistar rat pups were decapitated. The cortices were dissected out in a petri dish containing EBSS and then rolled on a sterile piece of filter paper to remove meninges. They were transferred to a petri dish containing 10ml of astrocytic 'solution A' (EBSS containing $20\mu g.ml^{-1}$ DNAse and $3mg.ml^{-1}$ fatty acid free BSA), and chopped gently using scissors. The tissue was triturated using a P1000 Gilson pipette, then moved to a 50ml falcon tube using a 10ml pipette. The petri dish was washed with a further 10ml solution A and this added to the falcon tube. The tube was then centrifuged at 500x*g* for 5 minutes at 4°C.

The supernatant was carefully removed, and replaced with 20ml astrocytic 'solution B' (EBSS containing $3mg.ml^{-1}$ fatty acid free BSA, $0.1mg.ml^{-1}$ DNAse and

0.25mg.ml^{-1} trypsin). The mixture was incubated for 10 minutes at 37°C. Towards the end of this incubation, the tissue was triturated using a P1000 and then a P200 Gilson pipette. 1ml cold (4°C) FBS was then added to arrest the trypsinisation. The mixture was centrifuged at 500x*g* for 5 minutes at 4°C.

The supernatant was removed and the pellet resuspended in 10ml solution A. The tissue was allowed to settle for 2 minutes. The supernatant was carefully decanted, and then centrifuged at 500x*g* for 5 minutes at 4°C.

The supernatant was removed and the pellet resuspended in astrocyte media (L-valine based MEM containing 1% (v/v) antibiotic-antimycotic solution, 10% (v/v) FBS and 2mM glutamine). The cells were then plated into 80cm^2 plastic flasks, and the volume of media brought to 10ml in each. The number of flasks was equated to the number of neonates dissected. The flasks were incubated at 37°C as described in 2.2.2.1.

The media was completely changed every 3 days. Once the astrocytes reached confluency (approximately 6 or 7 days after the preparation), they were exposed for 24 hours to 12ml neurobasal media per flask. After this time, the cells were removed from the flasks by trypsinisation and re-plated in double the number of flasks. The cells were allowed to proliferate and the media changed every 3 days as before. Once the cells achieved confluency for a second time, neurobasal media was once again conditioned. After this treatment, the astrocytes were discarded.

Astrocytes at confluency are shown in Figure 2.5.

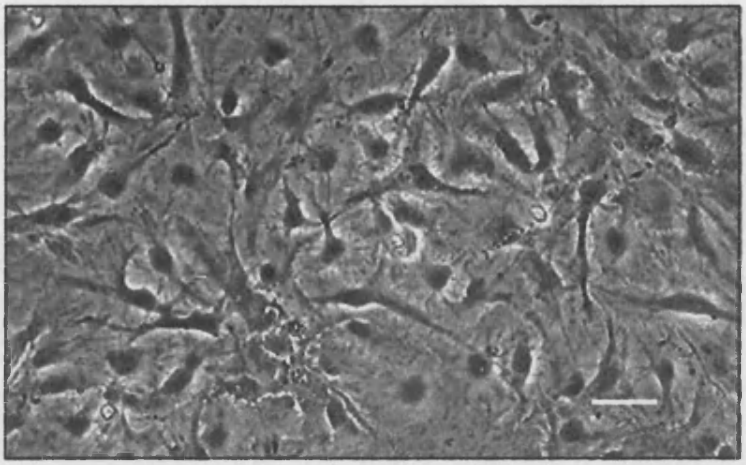

Figure 2.5

Primary cortical astrocytes at confluency. Neurobasal media was conditioned by 24 hours exposure to astrocytes at this stage. Phase contrast micrograph, X20 objective. Scale bar represents 40μm.

2.3 Measurement of mitochondrial respiratory function

2.3.1 *Mitochondrial incubations*

An 800µl glass chamber with a Clark-type oxygen and TPP^+ electrode with silver/silver chloride reference were used for determination of the respiratory parameters oxygen consumption rate and $\Delta\psi_m$. A schematic diagram of the chamber and electrode arrangement is shown in Figure 2.6.

2.3.1.1 Measurement of oxygen consumption rate

The oxygen electrode detects the falling oxygen concentration in the electrode chamber as mitochondria consume oxygen for the process of oxidative phosphorylation. A silver/silver chloride reference anode and a platinum cathode are immersed in a concentrated potassium chloride solution, which is separated from the mitochondria suspension by a thin Teflon membrane. The oxygen tension in the mitochondrial suspension equilibrates across the membrane. Oxygen is then reduced at the cathode:

$$4H^+ + 4e^- + O_2 \quad 2H_2O$$

The electrons for this reaction are produced at the anode, to which chloride ions migrate and are oxidised:

$$4Ag + 4Cl^- \quad 4AgCl + 4e^-$$

The current generated by this electron movement is measured, and is directly proportional to the oxygen tension. The rate of reduction in this current therefore represents the rate of oxygen consumption by the mitochondria.

The electrode must be calibrated before use at the temperature at which experiments will be carried out so that the measured current can be converted to absolute oxygen consumption rate. The current detected by the oxygen electrode is directly proportional to the oxygen tension in the mitochondrial suspension. Because of this linear relationship, only two calibration points are necessary - zero and 100%. In order to do this, aerated respiration buffer alone was added to the electrode chamber, which was maintained at 37°C. The steady state electrode reading at this point was taken as 100%. 1mM sodium dithionite was added to the chamber, and the oxygen concentration allowed to rapidly fall to zero. This reading was taken as 0%. 199 nmoles $O_2.ml^{-1}$ was taken as the partial pressure of oxygen at saturation point in buffer at 37°C (Chappell, 1964). This calibration therefore established two known oxygen concentrations (0 and 199 nmoles $O_2.ml^{-1}$), from which all subsequent recorded consumption rates could be calculated.

Each experiment yielded a straight line trace during state 3 respiration, the gradient of which represented the rate of oxygen consumption. The rate of oxygen consumption before the addition of mitochondria was subtracted in each case to correct for background signal. The resulting corrected reading was converted to nmoles $O_2.min^{-1}.mg^{-1}$, by means of the calibration points described above.

2.3.1.2 Measurement of mitochondrial membrane potential

ψ_m was measured using a tetraphenylphosphonium ion (TPP^+) electrode. The principle of the technique is that TPP^+ is taken up by mitochondria as a function of ψ_m. The electrode itself consists of an inert tube containing 10mM TPP^+, separated from the surrounding chamber by a membrane. 4μM TPP^+ is added to the respiration medium in the chamber. The concentration gradient of the charged ion between the inside and outside of the electrode (across the membrane) causes a potential difference, and this is the parameter which is measured (in mV) with respect to a silver/silver chloride electrode.

Prior to each experiment which involved measurement of ψ_m, three calibration curves were created. Each of these involved adding TPP^+ in 1μM increments between 0 and 6μM. The signal in mV resulting from each [TPP^+] was recorded. This was repeated for all three calibration curves, and the mean of the three readings calculated. This mean signal was then plotted against [TPP^+], and a second order polynomial equation was fitted to the resulting curve (since the relationship between [TPP^+] and measured voltage is non-linear). This equation could then be used to convert mV signals to [TPP^+] (μM).

It was necessary to correct for background binding of TPP^+ to mitochondria which was independent of ψ_m. In order to do this, before each experiment mitochondria were incubated with BSA in aerated respiration buffer in the electrode chamber at 37°C. (The BSA used throughout is fatty acid free. It is included for the purpose of binding free fatty acids in the incubation medium, which have mitochondrial

uncoupling properties (Samartsev *et al*, 2000)). State 3 respiration was induced by the addition of excess substrates and ADP, and the mitochondria allowed to consume all of the oxygen present. ψ_m was taken to be zero after an anaerobic state was reached. The signal in mV at this point was translated to $[TPP^+]$ using the best fit polynomial equation described above. This $[TPP^+]$ was the maximum possible free $[TPP^+]$, and was always slightly lower than 4μM due to the background binding.

Signals in mV from the experimental traces were converted to $[TPP^+]$ in the same way. They were then expressed as ψ_m (mV) by applying the following adaptation of the Nernst Equation:

$$\psi_m = (2.3RT)/nF \times \log_{10}(\Delta[TPP^+_{out}] / \Delta[TPP^+_{in}])$$

ie. $$\psi_m = -61.5 \times \log_{10}([TPP^+] / ([TPP^+]_{corr} - [TPP^+]) \times 2650)$$

where $[TPP^+]$ is the measured parameter for each experiment and $[TPP^+]_{corr}$ is the maximum possible free $[TPP^+]$ corrected for background binding as described above. The volume of mitochondria is estimated as being 2650 (derived from $0.755\mu l.mg^{-1}$, Brand, 1995) times smaller than the volume of the buffer in which it is suspended. The '$([TPP^+]_{corr} - [TPP^+]) \times 2650$' term of the equation therefore estimates the change in $[TPP^+]$ inside the mitochondria, given the measured change outside.

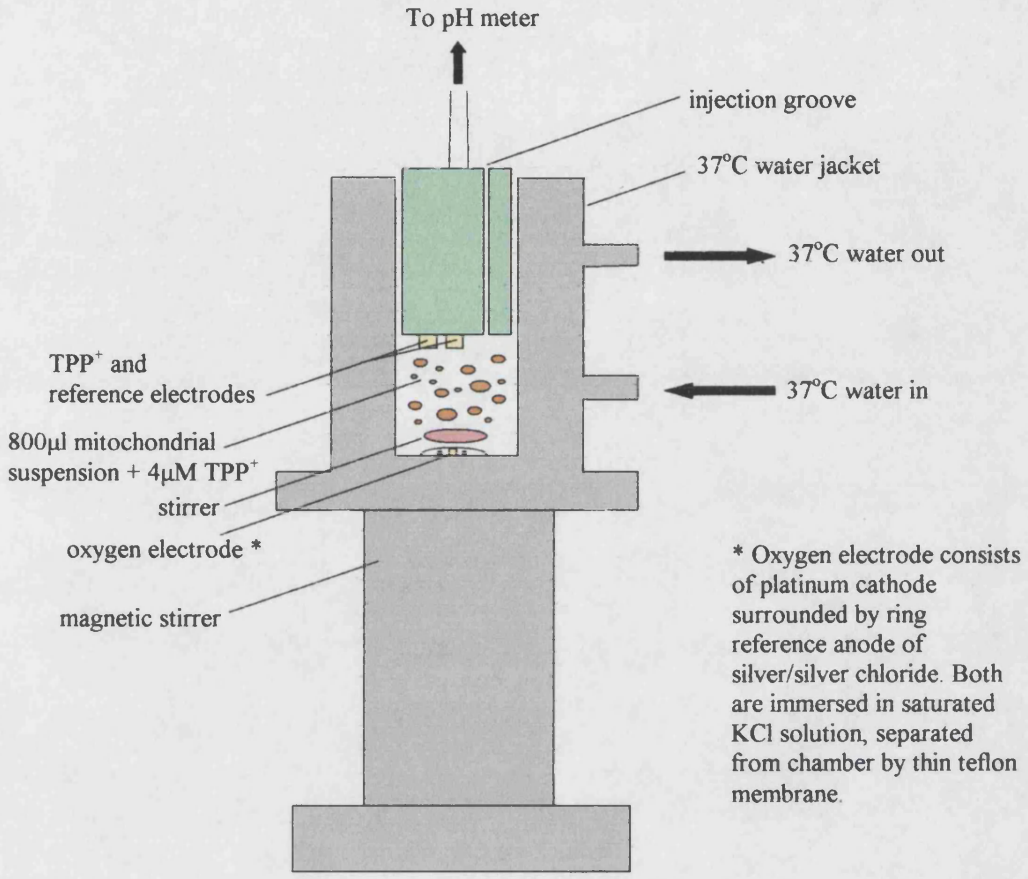

Figure 2.6

Schematic diagram to show the arrangements of oxygen and TPP^+ electrodes with the glass chamber.

2.3.1.3 Incubation schemes

All respiration experiments were carried out according to one of three 'incubation schemes'. These involve the addition of mitochondria to respiration buffer (100mM KCl, 75mM mannitol, 25mM sucrose, 10mM Tris-HCl, 50μM K^+EDTA, 10mM phosphate-Tris (pH 7.4)) at 37°C containing BSA (2mg.mg^{-1} protein). They allow a period of equilibration for the mitochondrial sample, before the later addition of substrates and ADP to induce state 3 respiration. Sufficient time was also allowed during the incubations for inhibitors to exert their effect before respiration was induced (Davey & Clark, 1996). A longer incubation time was provided where the series of experiments was to involve an antibody as the inhibitor (Brustovetsky *et al*, 2003b).

0 mins	**Respiration buffer** (37°C) **Fatty acid free BSA** (2mg.mg^{-1} mitochondrial protein) **TPP^{+}** (4μM) **Isolated mitochondria** (0.5mg.ml^{-1}) (Buffer volume corrected to give total volume 800μl)
2 mins	**Rotenone** (0 – 0.45nmoles.mg^{-1} protein for non-synaptic mitochondria, 0 – 0.25nmoles.mg^{-1} protein for synaptic mitochondria) or **KCN** (0-400nmoles.mg^{-1} protein for non-synaptic mitochondria)
7 mins	**Glutamate** (10mM) **Malate** (2.5mM) **Pyruvate** (10mM) **ADP** (2mM)
10 mins	Remove aliquots to be assayed

Table 2.1

The protocol for Incubation Scheme 1, as referred to in the text.

0 mins	**Respiration Buffer** (37°C) **Fatty acid free BSA** (2mg.mg^{-1} mitochondrial protein) **Inhibitor** (given concentration) **Isolated mitochondria** (0.5mg.ml^{-1}) (Buffer volume corrected to give total volume 800µl)
10 mins	**Rotenone** (0 or 0.375nmoles.mg^{-1} protein)
15 mins	**Glutamate** (10mM) **Malate** (2.5mM) **Pyruvate** (10mM) **ADP** (2mM)
18 mins	Remove aliquots to be assayed

Table 2.2

The protocol for Incubation Scheme 2, as referred to in the text.

0 mins	**Respiration Buffer** (37°C) **Fatty acid free BSA** (2mg.mg^{-1} mitochondrial protein) **Isolated mitochondria** (0.5mg.ml^{-1}) (Buffer volume corrected to give total volume 800µl)
10 mins	Remove aliquots to be assayed

Table 2.3

The protocol for Incubation Scheme 3, as referred to in the text.

2.3.2 *Respiratory enzyme complex assays*

2.3.2.1 Complex I assay

NADH ubiquinone oxidoreductase (complex I; EC 1.6.99.3) activity was measured using a method adapted from Ragan *et al* (1987). As Complex I serves to accept reducing equivalents from NADH and donate them to ubiquinone, its activity can be measured by monitoring the loss of NADH. This was done by determining the loss of absorbance at 340nm in a Uvikon 940 spectrophotometer (Kontron Instruments Ltd., Watford, UK).

The assay was carried out in 1ml of 25mM potassium phosphate buffer with 10mM $MgCl_2$, 1mM KCN, and 2.5mg.ml^{-1} fatty acid free BSA at 30°C and pH 7.2. 5mM NADH was added to the cuvette. The mitochondrial sample was frozen (in liquid nitrogen) and thawed three times and then 10μg protein added into the cuvette. The cuvette was placed in the spectrophotometer and allowed to equilibrate to 30°C. After two minutes, the reaction was initiated by the addition of 50μM CoQ_1. The absorbance at 340nm was read against blank cuvettes (identical except CoQ_1 omitted). 10μM rotenone was added after a further five minutes, and the absorbance monitored for a further five minutes.

The rotenone-inhibited rate of change of absorbance was subtracted from the initial rate. This rotenone-sensitive component was then converted to Complex I activity in nmoles.min^{-1}.mg^{-1} using the Beer-Lambert Law and an extinction coefficient of 6.81

x 10^3 $M^{-1}.cm^{-1}$ for NADH. (The generally accepted value for the extinction coefficient of NADH at 340nm is 6.22 x 10^3 $M^{-1}.cm^{-1}$. However, in the presence of CoQ_1, this is shifted to the value used in this case (Ragan *et al*, 1987)).

2.3.2.2 Complex IV assay

Cytochrome *c* oxidase (complex IV; EC 1.9.3.1) was measured using the method of Wharton & Tzagoloff (1967). As Complex IV serves to accept reducing equivalents from reduced cytochrome *c* and donate them to molecular oxygen to form water, its activity can be measured by monitoring the rate of oxidation of cytochrome *c*. This was done by determining the loss of absorbance at 550nm in a Uvikon 940 spectrophotometer (Kontron Instruments Ltd., Watford, UK).

For this assay, reduced cytochrome *c* is required as a reagent. A 10mg.ml^{-1} solution of oxidised cytochrome *c* was initially reduced by adding approximately 5mg sodium ascorbate. In order to remove the ascorbate from the solution, the reduced cytochrome *c* was then passed down a PD_{10} gel filtration column. The concentration of this reduced cytochrome *c* solution was then determined by measuring the absorbance at 550nm against cytochrome *c* which was fully oxidised by the addition of 100μM potassium ferricyanide. The Beer Lambert Law was applied to this absorbance difference, using the extinction coefficient for reduced cytochrome *c* 19.2 x 10^3 $M^{-1}cm^{-1}$.

The assay for Complex IV activity was then carried out in 1ml of 10mM potassium phosphate buffer with 50μM reduced cytochrome *c* at 30°C and pH 7.0. The cuvette was placed in the spectrophotometer and allowed to equilibrate for 2 minutes. The mitochondrial sample was frozen (in liquid nitrogen) and thawed three times and then 10μg protein added to the cuvette. The absorbance at 550nm was measured against a cuvette containing no sample but with the reduced cytochrome *c* fully oxidised by the addition of 100μM potassium ferricyanide.

The rate of change of absorbance at 550nm is non-linear. The reaction shows first order dependence on the concentration of reduced cytochrome *c*. By plotting the natural log of absorbance over time for each sample, a straight line relationship was obtained. The gradient of each the line was taken as the first order rate constant , and the activity of Complex IV expressed as $k min^{-1}.mg^{-1}$.

2.4 Assay of mitochondrial proteins

2.4.1 *Cytochrome c concentration*

Cytochrome *c* concentration can be measured accurately and quantitatively by immunoassay. The Quantikine M Rat/Mouse Cytochrome *c* Immunoassay kit from R&D Systems (Abingdon, UK) was used for this purpose. The assay works by a 'sandwich' method, immobilising a labelled monoclonal antibody by attachment to a second antibody, via mutual binding to cytochrome *c*. The mechanism is explained in Figure 2.7.

All reagents were brought to room temperature before use, having been stored at 4°C. 75µl of the conjugate monoclonal antibody was added to each of the wells, which had been pre-coated with a non-labelled monoclonal antibody. Samples were diluted according to their estimated cytochrome *c* concentration, in order that they should fall within the limits of the standard curve (0.78 - 25ng/ml). 50µl of sample or standard were added to the wells. A known mass of cytochrome *c* was also dissolved in deionised water and assayed in the same way as a control. The well contents were then mixed by gently tapping the plate for 1 minute. The plate was covered and incubated for 2 hours at room temperature to allow the antibodies to bind any cytochrome *c* present. The wells were then washed thoroughly 5 times, ensuring that wells were emptied completely each time. The plate was inverted and blotted against clean paper towels. 100µl substrate solution (H_2O_2 + tetramethylbenzidine) was added to each well, and the plate incubated at room temperature in the dark for 30 minutes. After this time, 100µl stop solution (dilute HCl) was added to each well. The plate was tapped gently to ensure thorough mixing. The absorbance of each well was determined at 450nm and 540nm in a plate-reading spectrophotometer (SpectraMaxPlus, Molecular Devices, Sunnyvale, CA). The latter was subtracted from the former to correct for background absorbance.

A standard curve was plotted as log([cyt *c*]) versus log(A_{450} - A_{540}). The linear equation of best fit was used to translate the absorbance readings obtained from the samples to concentrations of cytochrome *c*. Finally, these were corrected for the

initial dilution factor, and expressed as nmoles.mg^{-1} mitochondrial protein. A typical standard curve is shown in Figure 2.8.

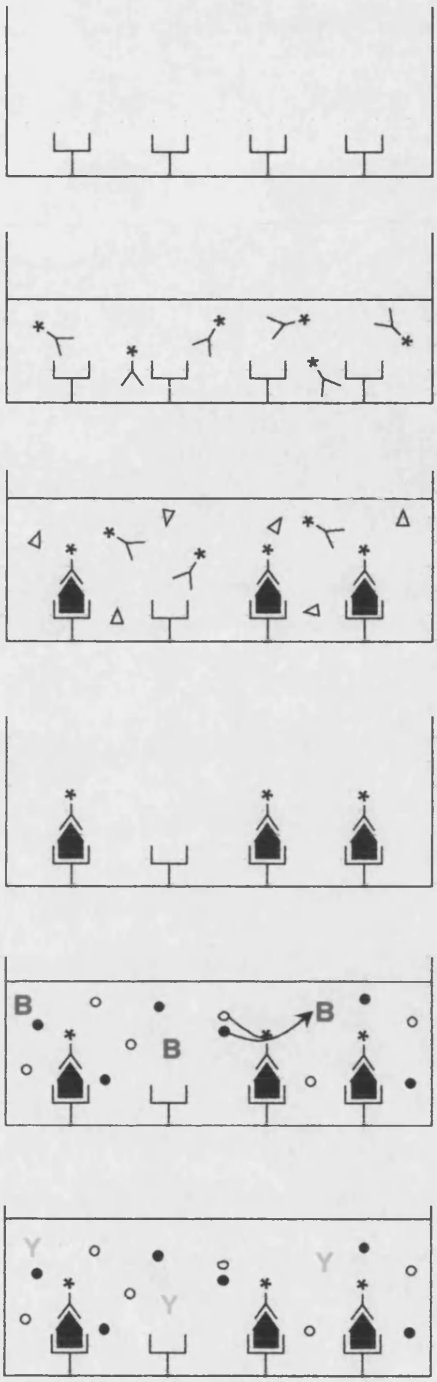

- Each well of a 96-well microplate has been pre-coated with a monoclonal antibody specific for rat/mouse cytochrome *c*. The antibody is immobile.

  Monoclonal antibody for cytochrome *c*

- A solution containing a second monoclonal antibody for cytochrome *c* is added into the well. Unlike the first, this antibody is freely mobile in the solution and is conjugated to the enzyme horseradish peroxidase (HRP).

  Monoclonal antibody for cytochrome *c* conjugated to HRP (*)

- The sample solution is added. Any cytochrome *c* present can bind to both antibodies (which are in excess). This 'sandwich' process immobilises the conjugated antibody to an extent directly proportional to the concentration of cytochrome *c*. Other proteins within the sample solution and surplus conjugated antibody remain free in the solution.

  Cytochrome *c* in sample solution

  Δ Other proteins in sample solution

- Thorough washing removes all free proteins, leaving only the cytochrome *c* and bound antibodies.

- A substrate solution is added immediately after washing. This consists of hydrogen peroxide (H_2O_2) and the chromagen tetramethylbenzidine (TMB), which are mixed immediately prior to this stage. HRP catalyses the oxidation of TMB by H_2O_2 to form a soluble blue product.

  • Hydrogen peroxide

  ○ Tetramethylbenzidine

  B Soluble blue product

- The addition of weak hydrochloric acid stops the HRP-catalysed reaction, and converts the blue product to a stable yellow product. The concentration of this product is directly proportional to the concentration of cytochrome *c* in the original sample, and can be determined by measuring the absorbance at 450nm (corrected for background signal by subtraction of absorbance at 540nm).

  Y Stable soluble yellow product

- A standard curve is created by applying the same procedure to standards of [cytochrome *c*] from 0.78 - 25ng/ml. This is then used to convert the absorbance reading to [cytochrome *c*] for the samples.

Figure 2.7

The mechanism underlying the cytochrome *c* immunoassay

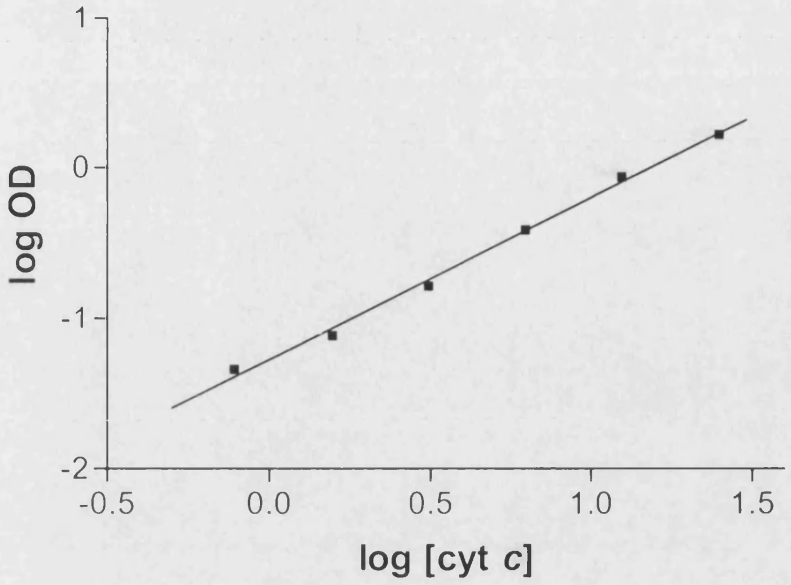

Figure 2.8

Typical standard curve from cytochrome *c* immunoassay. Log [cytochrome *c*] is plotted versus the log of the optical density measurement. The resulting best fit line can be used to calculate all experimental readings to cytochrome *c* concentrations. For example, this standard curve has the best fit equation:

$$\log OD = 1.07 \log[\text{cyt } c] - 1.27 \qquad (R^2 = 0.996)$$

This rearranges to:

$$[\text{cyt } c] = 10^{(\log OD + 1.27)/1.07}$$

2.4.2 *Citrate synthase activity*

Citrate synthase (EC 4.1.3.7) was measured using the method of Shepherd and Garland (1969). The enzyme catalyses the following reaction:

$$\text{Acetyl-CoA} + \text{oxaloacetate} + H_2O \longrightarrow \text{citrate} + \text{free CoA}$$

If 5,5'-dithiobis(2-nitrobenzoic acid) (or DTNB) is present, it can react with the free CoA product to form a *p*–nitrothiophenol anion, which absorbs at 412nm. The basis of this 'linked' assay is therefore to provide the reagents required for the citrate synthase-catalysed reaction along with DTNB and monitor the increase in absorbance at 412nm.

The assay was carried out in 96-well plate. Each well contained 250µl of 100mM Tris-HCl buffer with 0.1mM acetyl-CoA and 0.2mM DTNB at 30°C and pH 8.0. 20µl of sample was added. The plate was positioned in a plate-reading spectrophotometer (SpectraMaxPlus, Molecular Devices, Sunnyvale, CA), and the absorbance at 412nm monitored for 5 minutes to establish the background rate. After this time, 0.2mM oxaloacetate was added to initiate the reaction. The absorbance at 412nm was again monitored for 5 minutes. The background rate was subtracted from the stimulated rate of absorbance change. Using the Beer Lambert Law and a *p*–nitrothiophenol anion extinction coefficient of 13.6 x 10^3 $M^{-1}.cm^{-1}$, citrate synthase activity was expressed in $nmoles.min^{-1}.mg^{-1}$. For analysis of released citrate synthase, activity of the enzyme in the supernatant samples was shown as a percentage of the mean total mitochondrial activity.

2.4.3 *Adenylate kinase activity*

Adenylate kinase (EC 2.7.4.3) was measured using a method adapted from Kluck *et al* (1999) and Doran & Halestrap (2000). The enzyme catalyses the following reaction:

$$AMP + ATP \rightleftharpoons 2ADP$$

In this linked assay, phosphoenolpyruvate (PEP) is added with pyruvate kinase, generating pyruvate and ATP. Lactate dehydrogenase (LDH) then catalyses the conversion of pyruvate to lactate, using NADH. ATP is present in the buffer. This system therefore increases the ATP:ADP ratio. Adenylate kinase is required to restore the balance, by catalysing the reaction shown above in the forward direction. AMP is added as the substrate for the assay, allowing the reaction to proceed. The rate of adenylate kinase activity is measured by the rate of decrease in NADH levels, used at the LDH-catalysed step. The scheme for the assay is therefore:

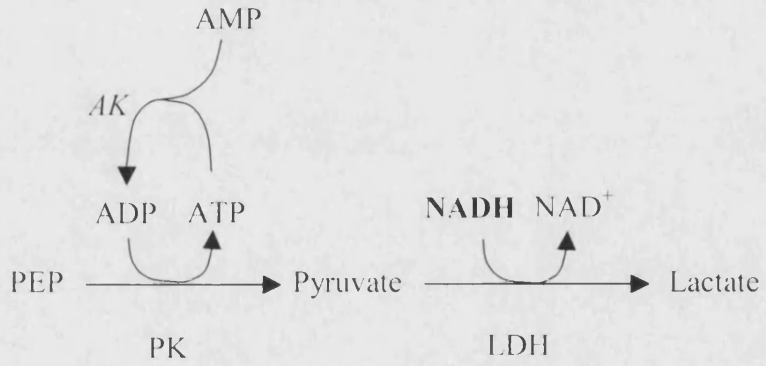

Rotenone and oligomycin are included in the buffer to prevent ETC-mediated changes in the ATP:ADP ratio. This is necessary for assaying the whole

mitochondrial adenylate kinase activity, and is retained for the measurements on supernatants for consistency.

The assay was carried out in a 96-well plate. Each well contained 250µl of 130mM KCl, 6mM $MgSO_4$, 100mM Tris, 1.5mM NADH, 0.5mM ATP, 0.5mM phosphoenolpyruvate, 5µM rotenone, 7.5µM oligomycin, 0.2U.ml^{-1} pyruvate kinase and 0.2U.ml^{-1} lactate dehydrogenase, at 30°C and pH 7.5. 20µl of the supernatant sample was added. The plate was then positioned in a plate-reading spectrophotometer (SpectraMaxPlus, Molecular Devices, Sunnyvale, CA) and allowed to equilibrate for 2 minutes. 0.6mM AMP was then added to each well, and the absorbance at 366nm monitored for 5 minutes. The normal wavelength for monitoring a loss of NADH is 340nm. However, for this assay it was found that monitoring absorbance at 340nm gave a highly unreliable signal. One or more components of the reaction mixture presumably interfere with this reading. Therefore, as in Kluck *et al* (1999), NADH was monitored at 366nm. Using a diode array spectrophotometer, it was confirmed that NADH showed significant absorbance at 366nm.

After 5 minutes incubation with AMP, 0.4mM di-adenosine pentaphosphate (specific adenylate kinase inhibitor) was added to each well, and the absorbance measured for a further 5 minutes. The inhibited rate was subtracted from the stimulated rate of change in absorbance. Adenylate kinase activity was expressed as rate of change of absorbance per mg of mitochondrial protein (Brustovetsky *et al*, 2003b). For analysis

of released enzyme, this rate was then converted to a percentage of the mean total mitochondrial activity.

2.4.4 *Mitochondrial glutathione content*

Mitochondrial GSH concentration was measured using reverse-phase HPLC, coupled to a dual-electrode electrochemical detector (Riederer *et al*, 1989).

Samples from mitochondrial incubations which had been acid extracted using orthophosphoric acid were injected (20µl) by a Kontron HPLC 360 autosampler (Watford, UK). A guard column was used to clean the sample (octadecasilyl, 3mm x 10mm). The signal was resolved using a reverse-phase Techsphere octadecasilyl column (particle size 5µm, 4.6mm x 250mm). The column was maintained at 30°C using a heater (Jones Chromatography, Glamorgan, UK). The mobile phase was 15mM orthophosphoric acid (pH 2.5), degassed using a DEG-1033 degasser (Kontron Instruments, Watford, UK). The flow rate was set at 0.5ml.min^{-1} using a Jasco PU-1580 pump (Great Dunmow, UK).

Following separation, GSH was detected using an ESA 5010 analytical cell (Aylesbury, UK). The signal was recorded as a chromatogram on a Thermoseparation Products Chromejet integrator (Anachem, Luton, UK). The chart speed was set to 25mm.min^{-1}.

5µM GSH standards were dispersed among the samples to enable calculation of GSH concentrations and to ensure continuity of signal during a run.

2.4.5 *AIF and Smac concentration*

2.4.5.1 SDS polyacrylamide gel electrophoresis

Untreated mitochondrial pellets were used as positive controls. Pellets were resuspended in lysis buffer (20mM Tris-acetate, 1mM EDTA, 1mM EGTA, 10mM sodium β-glycerophosphate, 1mM sodium orthovanadate, 5% glycerol, 1% Triton X-100, 0.27M sucrose, 1mM benzamidine, 4mg.ml^{-1} leupeptin, 0.1% β-mercaptoethanol, pH 7.4) to a concentration of 2mg.ml^{-1}. The suspension was then left on ice for 20 minutes with regular vortexing. It was centrifuged at 10000x*g* for 1 minute to pellet the non-solubilized material. The supernatant was used as the sample for electrophoresis.

Supernatant samples from rotenone- or alamethicin-treated incubations were thawed from -70°C storage and vortexed before being used for electrophoresis.

15µl of each sample was added to 8µl Laemelli sample buffer (1% SDS, 10% glycerol, 2.5% β-mercaptoethanol, 125mM Tris-HCl, 1% bromophenol blue, pH 6.8) in eppendorf tubes. A hole was punched in the top of each tube with a needle, and the sample mixtures then boiled for 5 minutes. A solution of molecular mass markers was treated in the same way.

The samples were then loaded onto a Tris-HCl 12.5% pre-cast gel (Bio-Rad, Bucks., UK) and secured in a Bio-Rad Mini-Protean II electrophoresis cell. The molecular

mass markers were run in the far left hand lane. The 30µl wells were filled to the top with running buffer (125mM Tris, 1M glycine, 0.01% SDS). The tank was also filled with running buffer and the electrodes secured. The gel was then run for 1 hour at 180V.

2.4.5.2 Electrophoretic protein transfer

The gel was then carefully removed from the supporting glass plate, and equilibrated in transfer buffer (25mM Tris, 192mM glycine, 0.01% SDS, 20% methanol) for 20 minutes. Meanwhile, a polyvinylidene fluroide (PVDF) membrane was activated in methanol at 4°C for 1 minute. The membrane was then washed in distilled water for 5 minutes, and then equilibrated in transfer buffer for 20 minutes also.

The gel was then transferred to a fibre pad on a piece of filter paper. The PVDF membrane was layered onto the gel, and bubbles removed using a glass rod. A second piece of filter paper was layered onto the membrane, and the stack assembled into the transfer cassette, using fibre pads for support. A cooling pack was placed in a Bio-Rad mini trans blot electrophoretic transfer cell along with the cassette, and the cell filled with transfer buffer. A stirrer bar was positioned in the bottom of the tank, and the electrodes fitted. The proteins were then transferred to the membrane at 80V for 2 hours.

2.4.5.3 Immunoblotting

Following transfer, the membrane was washed for 10 minutes in Tween-20 Tris buffered saline (TTBS; 10mM Tris-HCl, 150mM NaCl, 0.5% Tween-20, pH 7.4) to remove SDS and methanol. It was then immersed in blocking buffer (TTBS with 5% non-fat dried milk) at room temperature for 90 minutes with shaking. The membrane was then probed with primary antibody diluted 1 in 500 into blocking buffer, for 1 hour at room temperature. After removal of the antibody solution, the membrane was washed 3 times for 10 minutes each in TTBS. It was then incubated with a secondary antibody (donkey anti-goat) conjugated to HRP, diluted 1 in 1000 in blocking buffer, for 1 hour at room temperature. Finally, the membrane was washed 3 times more, for 10 minutes each time, in TTBS.

The membrane was then drained of excess liquid by blotting the edge against a tissue. 4ml ECL reagent (Bio-Rad, Bucks., UK) was then added to cover the membrane. It was dried quickly between two sheets of filter paper. The membrane was then fixed into an x-ray film cassette with tape and exposed to film. The exposure time was varied between 30 seconds and 10 minutes depending on the strength of the signal. The film was then soaked in developer for 1 minute, washed in acetone and finally fixed in fixer for 3 minutes.

Note that re-probing the gel to check for equal protein loading was not required in this case, since the protein content of the supernatant samples varied depending on the earlier rotenone treatment.

2.5 Assessment of mitochondrial volume

2.5.1 *Electron Microscopy*

Electron microscopy was carried out in collaboration with Professor David Landon and Mr. Brian Young (Electron Microscopy Unit, Institute of Neurology).

Samples from mitochondrial incubations were centrifuged at 17000x*g* for 5 minutes at 4°C (Sigma Laborzentrifugen 3K10, Osterode, Germany). The supernatant was then completely removed, and very carefully replaced with fixative (3% glutaraldehyde buffer, pH 7.4, with 0.1M sodium cacodylate and 5mM calcium chloride). Mitochondrial pellets treated in this way were then kept at 4°C overnight.

The pellet was then subjected to 2 brief washes with distilled water. The pellet was exposed to 1% aqueous osmium tetroxide for 2 hours, followed by a further 2 brief washes with distilled water. This treatment had further fixative properties, but also acted as an electron microscopy 'stain'.

The pellet was then dehydrated in ascending grades of alcohol (2 x 10 minute washes in 70% and 90%, 4 x 10 minute washes in 100%). Following this, the pellet received 2 x 10 minute washes in epoxy propane. This was replaced by a 1:1 mixture of epoxy propane and resin and left for 30 minutes. The resin consisted of agar 100, dodecenyl succinic anhydride (plasticiser), methyl nadic anhydride (hardener) and 2,4,6-tri(dimethyl aminomethyl) phenol (accelerator) in equal parts. This mixture was then

replaced with neat resin and left for 3 hours. The resin was then polymerised by incubating at 60°C overnight.

An RMC MT6000 ultramicrotome with Diatome diamond knife was then used to cut ultra-thin (approximately 70nm) sections from the specimen. The sections were released into a dish of distilled water and then collected on 3mm mesh copper grids. The sections were stained with 25% uranyl acetate in 50% methyl alcohol for 20 minutes, and then exposed to Reynold's lead citrate for a further 20 minutes. The grids were washed 2 x 10 minutes in distilled water, and then examined in a JOEL 1200EX electron microscope.

2.5.2 *Determination of light scattering*

A quantitative assessment of mitochondrial volume changes can be made by measuring the extent to which the mitochondria in suspension scatter light. As mitochondria swell, their refractive index decreases with the result that they scatter less light (Knight *et al*, 1981). If an incubation is carried out in a spectrophotometer, this reduced light scattering can be detected as a decrease in light intensity (Kluck *et al*, 1999; Kristiàn *et al*, 2000). The wavelength typically used as the incident beam in such an investigation is 540nm. This wavelength is almost isosbestic with respect to cytochromes *b*, *c* and c_1, and therefore minimises potential complications by changes in the redox states of these proteins.

For the purpose of these experiments, mitochondrial incubations were carried out in a 0.5ml quartz cuvette. This was placed in a Perkin Elmer Luminescence

Spectrometer, and maintained at 37°C by means of a water jacket. Using FL WinLab version 3.00 software, an incident beam of 540nm was passed through the cuvette, and the transmitted light detected at a 90° angle from the incident beam. Both slit widths were set to 2.5nm. The data was recorded as arbitrary light intensity units.

2.6 Assessment of neuronal apoptosis

2.6.1 *Assay for caspase-9 activity*

Caspase-9 activity was measured using a colorimetric assay kit purchased from R&D Systems (Abingdon, UK).

Samples were stored as cell pellets at -70°C. In order to perform the assay, pellets were thawed and then resuspended in 100µl lysis buffer (from kit). The lysing cells were kept on ice for 10 minutes, and then centrifuged at 10000x*g* for 1 minute. The supernatant was then removed and kept on ice.

The protein concentration of this pellet was measured as described in 2.7.1. A 1:50 dilution of the lysates was appropriate for the protein concentration to fall within the standard curve.

The caspase assay was carried out in a 96-well plate. 50µl reaction buffer (containing 10mM DTT) was added to each well. The same volume of cell lysate was then added. Finally 5µl caspase-9 colorimetric substrate (Leu-Glu-His-Asp or LEHD

peptide conjugated to p-nitroanilide) was added to each well. The plate was incubated in the dark at 37°C for 2 hours.

Following this incubation, the absorbance at 405nm was determined for each well using a plate-reading spectrophotometer (SpectraMaxPlus, Molecular Devices, Sunnyvale, CA). Caspase-9 activity was expressed as arbitrary absorbance units at 405nm per milligram of protein in the lysate.

2.7 Validation of preparations

2.7.1 *Assay for protein concentration*

Before any experiments could be carried out on isolated mitochondria, or enzyme activities measured in harvested cells, the exact protein concentration of the sample was required. This was determined using the DC Protein Assay from Bio-Rad (Bucks., UK). This assay is based on the Lowry method (1951), but is modified to allow for a shorter reaction time (20 minutes) and a more stable colour formation (stable for up to 2 hours).

The basis for the assay is as follows. In an alkaline medium, protein can form a complex with copper. This complex can reduce a Folin reagent, via the removal of 1, 2 or 3 oxygen atoms. The three different products from this reduction reaction are all coloured, due to the presence of the amino acids tyrosine, tryptophan, cystine,

cysteine and histidine. Furthermore, all three coloured products have a maximum absorbance at 750nm, which can be measured spectrophotometrically.

A set of protein standards are required for the assay, and these were made using fatty acid-free BSA in deionised water, at concentrations 10, 25, 50, 75 and 100μg.ml^{-1}. Deionised water served as a 0μg.ml^{-1} standard. The sample was diluted with deionised water to fit within this range of standards, according to the estimated concentration. For isolated mitochondria, a 1:200 dilution was always appropriate. For harvested neurons, the estimated concentration depended on the number of pooled wells.

40μl of standard or sample was added to a 96-well plate. To this was added 20μl Reagent A (alkaline copper tartrate solution) and then 160μl Reagent B (Folin reagent). Each standard or sample was assayed in triplicate in this way. The plate was incubated at room temperature in the dark for 20 minutes, and then the absorbance at 750nm of each well recorded using a plate-reading spectrophotometer (SpectraMaxPlus, Molecular Devices, Sunnyvale, CA). A standard curve was plotted, and the sample concentration subsequently determined.

2.7.2 *Validation of isolated brain mitochondria preparations*

2.7.2.1 Citrate synthase activity

Citrate synthase (CS) is a mitochondrial matrix enzyme which has been used routinely to indicate the extent to which the isolation procedure purifies mitochondria. It was used to validate both the non-synaptic and synaptic preparations.

Remaining whole isolated mitochondria following an experiment were stored at -70°C. Following three freeze-thaw cycles, these mitochondria were assayed for citrate synthase activity as described in 2.4.2. The same was done for whole brain homogenates, samples of which were removed following the first 8 up and down strokes in the Dounce homogeniser as described in 2.2.1.2. The protein concentration of these homogenates was determined as described in 2.7.1.

The percentage purification of citrate synthase from the whole brain homogenate to the isolated mitochondria was then used to indicate the purifity of the mitochondrial preparation. The results of this validation procedure are shown in Table 2.4.

	H	NSM	SM
CS specific activity (nmoles.min^{-1}.mg^{-1})	216.2 ± 12.6	1101 ± 80.9	440.1 ± 26.2
Purification of CS during mitochondrial isolation (Multiple of activity in whole brain homogenate)	1	5.09	2.04

Table 2.4

Citrate synthase activity of whole brain homogenate (H), isolated non-synaptic (NSM) and synaptic (SM) mitochondria. Specific activities are given ± S.E.M., n = 3. These data indicate that there is more than a 5-fold increase in citrate synthase activity during the isolation of non-synaptic mitochondria, and an approximate doubling of this activity during the isolation of synaptic mitochondria. These data represent the amount of non-mitochondrial contamination in the preparation, and suggest that there is more non-mitochondrial protein present in the synaptic preparation than the non-synaptic preparation. This should be taken into account when analysing subsequent data.

2.7.2.2 Lactate dehydrogenase activity

Lactate dehydrogenase (LDH, EC 1.1.1.27) is a cytosolic enzyme with no recognised mitochondrial isoform in brain. It can therefore be used to indicate the percentage cytosolic contamination of the mitochondrial preparations. It was used for this purpose for both non-synaptic and synaptic preparations.

The reaction catalysed by LDH is as follows:

$$\text{Lactate} + NAD^+ \rightleftharpoons \text{Pyruvate} + NADH + H^+$$

In a reaction mixture which provides the substrates for the reverse reaction, the rate of LDH activity is monitored as the rate of disappearance of NADH, as determined by the change in absorbance at 340nm.

As for citrate synthase, whole isolated mitochondria and whole brain homogenate samples were freeze-thawed three times and then assayed for lactate dehydrogenase activity. This was measured in a Uvikon 940 spectrophotometer (Kontron Instruments Ltd., Watford, UK), by the method of Vassault (1983). 8mM NADH was added into phosphate/pyruvate buffer (50mM K_2HPO_4, 8.3mM KH_2PO_4, 0.345mM sodium pyruvate, 0.5% (v/v) Triton X-100, pH 7.5) in a cuvette to a total volume of and placed in the spectrophotometer. The cuvette was maintained at 30°C by means of a water jacket. After 2 minutes of equilibration, 10μg protein was added to the cuvette. The absorbance at 340nm was monitored for 5 minutes. Using the Beer-Lambert Law and an extinction coefficient of 6.81 x 10^3 $M^{-1}.cm^{-1}$, the rate of change in absorbance was then converted to LDH enzyme activity, expressed in nmoles NADH utilised.min^{-1}.mg^{-1} protein.

Mitochondrial LDH specific activity as a percentage of that measured in whole brain homogenate was used to indicate the extent of cytosolic contamination in the preparation. The results of this validation procedure are shown in Table 2.5.

	H	NSM	SM
LDH specific activity (nmoles $NADH.min^{-1}.mg^{-1}$)	539.8 ± 18	13.7 ± 1.8	16.4 ± 2.9
Mitochondrial LDH contamination (% of whole brain homogenate)	-	2.5%	3.0%

Table 2.5

Lactate dehydrogenase activity of whole brain homogenate (H), isolated non-synaptic (NSM) and synaptic (SM) mitochondria. Specific activities are given ± S.E.M., n = 3.

The low LDH activity in the isolated mitochondrial preparations as compared to the activity in the initial homogenate indicates that there is little cytosolic contamination of the preparations. The percentage contamination is very similar for isolated non-synaptic and synaptic mitochondria.

2.7.2.3 Respiratory control ratio

The respiratory control ratio (or RCR) is a recognised parameter which describes the extent to which the isolated mitochondria in a preparation are coupled. This is done by determining the increase in oxygen consumption rate of the mitochondria in response to the addition of ADP. Traditionally (Chance & Williams, 1956), the ratio is determined in the presence of glutamate and malate as respiratory substrates. The

state 4 (in the absence of ADP) and state 3 (in the presence of ADP) oxygen consumption rates are measured potentiometrically as described in 2.3.1.1.

Mitochondria are subjected to three cycles of ADP addition, the concentration of ADP calculated such that it will be completely converted to ATP after around 30 seconds. Each state 3 oxygen consumption rate is divided by the preceding state 4 rate, and the mean of these three ratios taken as the overall RCR value. For brain mitochondria, an RCR of at least 5 is required to indicate sufficient coupling.

Following isolation from whole rat brains (2.2.1.2, 2.2.1.3) and measurement of the protein concentration (2.7.1), mitochondria were added at $0.5mg.ml^{-1}$ to respiration buffer (2.3.1.3) at 30°C (NB. This is the traditional temperature at which RCR values are measured (Chance & Williams, 1956). Although subsequent experiments are to be carried out at 37°C, this measurement is a validation process and must therefore be carried out under the traditional conditions). Fatty acid free BSA was added at $2mg.mg^{-1}$ mitochondrial protein. The suspension was incubated for 5 minutes before state 4 respiration was induced using the substrates glutamate (10mM) and malate (2.5mM). The mitochondria were then cycled three times through state 3/4 respiration by the addition of 300μM ADP for each of the three additions. The respiratory control ratio (RCR) was calculated as the average ratio of state 3: state 4 respiration rates.

A typical RCR trace is shown in Figure 2.9. It can clearly be seen that the oxygen consumption rate increases very rapidly in response to ADP addition, and that there is

a marked gradient change between state 3 and state 4 respiration. In the trace shown, the RCR was calculated as >8. Mitochondria consistently demonstrated RCR>5.

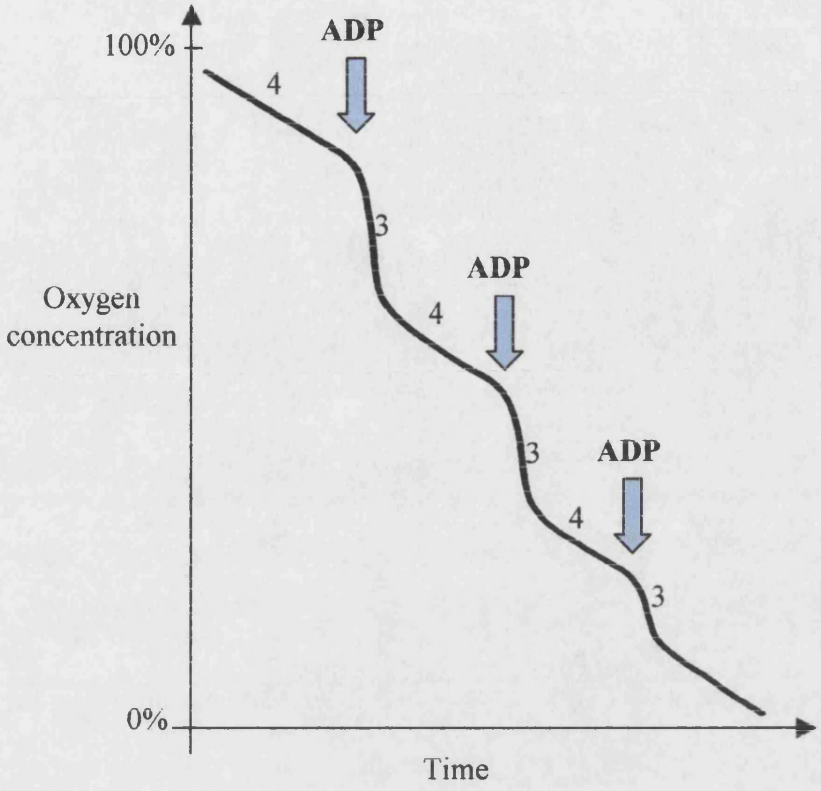

Figure 2.9

Typical Respiratory Control Ratio trace for isolated non-synaptic mitochondria. Similar traces were observed for isolated synaptic mitochondria. The RCR in this trace was calculated as >8.

2.7.3 *Validation of neuron-rich primary culture*

2.7.3.1 Immunochemical assessment of purity

By staining a culture of primary neurons, the purity of the culture can be determined. A dye which causes all nuclei to fluoresce (DAPI) is used alongside an antibody for neuron-specific beta III tubulin. The percentage of the total number of cells which are neurons can then be estimated by observation through a confocal microscope.

In order to observe stained cell through the confocal microscope, the cells were required to be grown on glass coverslips. The culture procedure was very similar to that described for plastic wells (2.2.2.1). However, prior to the preparation, glass coverslips were immersed in 20% HNO_3 overnight at room temperature, washed 3 times in distilled water, dried in acetone and then incubated at 180°C for 2 hours. Following cooling, the coverslips were placed one per well in a sterile 6-well culture plate. 1ml poly-D-lysine was added per well, and the plate incubated at 37°C for 1 hour. The wells were then washed 3 times with sterile distilled water and dried under UV light. 100µl coating solution (neurobasal with 5% horse serum, 5% FBS, 2mM L-glutamine, 62.5mM glutamate, 2% B27 with antioxidants) was added to each coverslip, and the plate then incubated at 37°C until the preparation was complete.

Following the preparation of the cells, they were resuspended to a concentration of 2 x $10^6.ml^{-1}$ (double the concentration described in 2.2.2.1). 100µl of cell suspension was added to into the coating solution on each coverslip. This was incubated for 1

hour in the 37°C incubator described above (2.2.2.1). 2ml neurobasal medium was then added into each well, and the cells cultured for 6 days as described in 2.2.2.1.

At day 6 of culture, the neuronal medium was removed from cells and replaced with 2ml.well^{-1} Tris-buffered saline (TBS; 10mM Tris-HCl, 150mM NaCl, pH 7.4). The TBS was removed after 5 minutes, and 2ml.well^{-1} ice cold methanol added in its place. The cells were fixed in this way for 10 minutes on ice. The cells were then rinsed twice with TBS as before, for 5 minutes each time. The cells were then permeabilised by the addition of 4mM sodium deoxycholate for 10 minutes at room temperature. Following permeation, the cells were rinsed twice for 5 minutes each, this time with TBS containing 0.025% Triton X-100. The cells were then blocked using TBS containing 1% BSA and 10% goat serum for 2 hours at room temperature. After this time, the blocking solution was removed. Mouse anti-tubulin (1:500) was then added in TBS with 1% BSA. The cells were incubated with this primary antibody at 4°C overnight.

Following removal of the primary antibody, the cells were washed twice at room temperature with TBS for 5 minutes each. They were then incubated for 1 hour at room temperature with a FITC-conjugated secondary antibody, diluted 1:500 in TBS with 1% BSA. They were then washed twice with TBS for 5 minutes each, followed by incubation with 0.01% DAPI for 10 minutes at room temperature. Finally, the cells were washed once more with TBS for 5 minutes.

The coverslips were then removed from the TBS with forceps, and mounted face-down on glass microscope slides using 10µl citifluor as a mounting solution.

Three combinations of treatments were used on the coverslips: DAPI stain alone, DAPI with FITC-conjugated secondary antibody and finally DAPI, secondary antibody and the primary antibody anti-tubulin. The coverslips mounted on slides were observed under a Zeiss 510 laser scanning confocal microscope at x20 objective with numerical aperture 0.75. A 364nm line of argon UV laser was used to excite DAPI, and 488nm used to excite FITC. The emitted light was detected using a photomultiplier tube. The data was analysed using Zeiss LSM image browser software.

The DAPI stain alone and the DAPI stain with secondary antibody both showed the same result, with only nuclei visible. This demonstrated that the secondary antibody contributed no artefactual background signal. The cells which were treated with DAPI and both antibodies however clearly showed nuclei with surrounding tubulin stain. A typical field of view is shown in Figure 2.10. The apparently complete co-localisation of nuclei with tubulin stain demonstrates the purity of the culture.

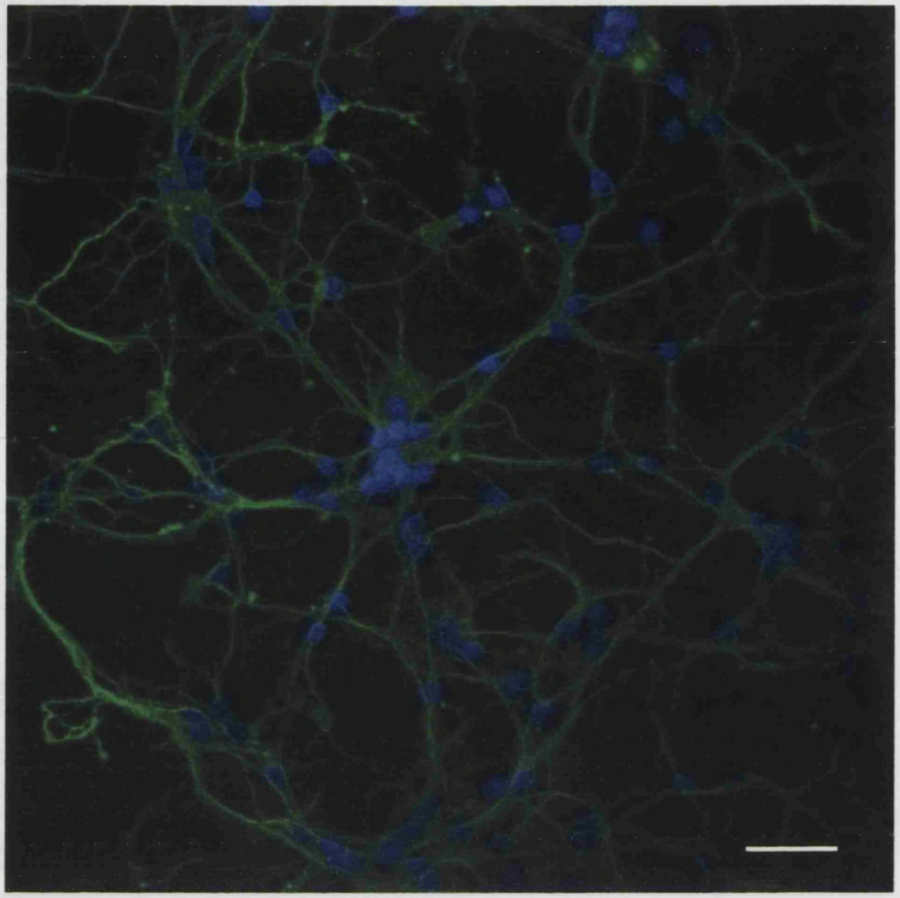

Figure 2.10

Confocal micrograph of neuron-rich primary culture for foetal rat cortex, x20 objective. The cells were treated with DAPI, primary anti-tubulin antibody and FITC-conjugated secondary antibody. Blue areas represent DAPI-stained nuclei, green regions represent neuron-specific tubulin, visualised with FITC. There are no nuclei which are isolated from the neuron-specific tubulin, demonstrating an extremely pure neuronal preparation. Scale bar represents 40μm.

2.8 Statistical analysis

Statistics were calculated using GraphPad Prism ™ Version 3.00 software (GraphPad Software Inc., CA, USA).

Data are presented as mean ± standard error of the mean (S.E.M.). Linear regression analysis and the Student's t test were used for statistical comparisons. A p-value of < 0.05 was considered significant.

CHAPTER 3

Quantifying the release of cytochrome *c* from brain mitochondria

3.1 Introduction

3.1.1 *The mechanism of release*

The release of cytochrome *c* is often taken as an indication of commitment to apoptosis. As such, it has tended to be thought of as a discrete event, with little consideration for any potential sophistication of the signal itself.

If postulated swelling-dependent mechanisms of release are to be believed, it is quite understandable that the event should be of the all-or-none nature described in Goldstein *et al* (2000). Even taking into account mitochondrial heterogeneity, if a small number of more susceptible mitochondria were to lose integrity to the extent that the IM was ruptured, calcium homeostasis would be lost. An increased cytosolic calcium concentration would be likely to trigger MPT in further mitochondria, thus triggering a chain reaction.

However, the majority of recent investigations into mechanisms of CCR describe features more consistent with the OM channel hypothesis. Release has been reported in the absence of mitochondrial swelling, prior to dissipation of $\Delta\psi_m$ and independently of release of any other soluble intermembrane proteins (SIMPs) (Andreyev *et al*, 1998; Bossy-Wetzel *et al*, 1998; Brustovetsky *et al*, 2003b; Doran & Halestrap, 2000; Eskes *et al*, 1998; Jürgensmeier *et al*, 1998; Kluck *et al*, 1999; Von Ahsen *et al*, 2000; Więckowski *et al*, 2001;). Furthermore, increasing awareness of the importance of quantitatively assessing CCR has led to demonstration of

incomplete release (Brustovetsky *et al*, 2002). All of these features are more consistent with the theory of release via an OM channel.

Bearing in mind the requirement for ATP in the apoptotic program, it is important for IM integrity to be maintained to a certain extent (especially in neurons, 1.3.5.3). For this reason, MPT is becoming increasingly regarded as an event downstream of CCR, possibly with the role of amplifying the signal for death (Marzo *et al*, 1998). A role for MPT is recognised in the necrotic death program, for which ATP is not required (Crompton *et al*, 2002; Kim *et al*, 2003).

3.1.2 *The extent of release*

There is growing interest in post-mitochondrial regulation of apoptosis. The IAP proteins (1.3.6.1) inhibit activated caspases, and it is suggested that this may serve to prevent 'inappropriate' apoptosis (Hengartner, 2000). There is now widespread recognition that such 'inappropriate' apoptosis contributes significantly to neurodegenerative cell loss (reviewed by Thompson, 1995). This regulatory system is therefore of particular interest in the brain.

The fact that this system exists implies that a certain amount of CCR can occur without apoptosis proceeding. This calls into question the claim of Goldstein *et al* (2000) that release is an all-or-none event. It makes little biological sense that such a crucial signal, which leads to an amplifying cascade of lethal protease activity, should be as strong in response to a mild insult as it is to a highly toxic one.

The question of *to what extent* cytochrome *c* is released from mitochondria has been inadequately addressed. Studies tend to use strong and/or artificial stimuli (eg. Staurosporine, Bertrand *et al*, 1994) and measure release using methods with little quantitative value (Western Blotting, fluorescence labelling). Furthermore, the majority of studies involve whole cells. Increasing awareness of post-mitochondrial mechanisms for regulation of cytochrome *c*-induced apoptosis (1.3.6) highlight the uncertainty surrounding the fate of cytochrome *c* in the cytosol. Sequestration or degradation of the protein may hinder the detection of subtle changes in cytosolic cytochrome *c* concentration.

3.1.3 *The model*

In this initial section of the study, isolated mitochondria were used as the experimental subject, in order to eliminate the issues described above concerning the fate of cytochrome *c* in cytosol. The mitochondria were isolated from brain because of the particular interest in 'inappropriate' apoptosis and its regulation in this organ with respect to neurodegeneration. Both non-synaptic and synaptic mitochondrial populations were studied (see 1.1.4.2).

The study aimed to titrate the severity of an insult to the mitochondria, to observe whether CCR was induced and whether it was an all-or-none phenomenon or sensitive to the severity of insult. It was central to this investigation that the treatment applied to the mitochondria modelled an effect which occurs naturally *in vivo*. The insult chosen was depletion of Complex I activity, since this is a recognised feature of several neurodegenerative disorders, particularly Parkinson's

disease (Schapira *et al*, 1990). Inhibition of this enzyme complex was achieved using the specific inhibitor rotenone (1.1.2.1).

The rate of oxygen consumption and $\Delta\psi_m$ (1.1.2) were measured as respiratory parameters, and related to the amount of cytochrome *c* released by the mitochondria. This was measured using a quantitative and sensitive immunoassay method.

3.2 Aims

The aim of this initial study was to determine whether a mild respiratory insult, which models an early neurodegenerative disease state, induces isolated rat brain mitochondria to release cytochrome *c*. The use of a quantitative assay for measuring CCR made it possible to determine whether any release was sensitive to the severity of the insult.

3.3 Results

3.3.1 *Titration of mitochondrial respiratory function using rotenone*

Non-synaptic or synaptic mitochondria were isolated from whole rat brains (2.2.1.2, 2.2.1.3). The protein concentrations were measured (2.7.1) and the mitochondria then incubated at 37°C in the electrode chamber according to Incubation Scheme 1 (2.3.1.3). Typically, a non-synaptic mitochondrial preparation provided sufficient

protein for 7 incubations, whereas a synaptic preparation allowed 3 or 4. One incubation served as a control (ie. ethanol vehicle alone) for each preparation. The remainder were treated with a range of concentrations of rotenone. Thorough washing of the chamber with ethanol and water was carried out between each incubation. However, since rotenone is understood to have resilient binding properties (Ramsay & Singer, 1992), incubations were always performed in order of increasing rotenone concentration.

Once a suitable range of rotenone concentrations had been established (based on Davey & Clark, 1996; Davey *et al*, 1998) for either population of mitochondria, sufficient preparations were performed to provide $n \geq 3$ for each rotenone concentration.

Oxygen consumption rate and $\Delta\psi_m$ were recorded (2.3.1.1, 2.3.1.2) between t = 7 minutes and t = 10 minutes. At t = 10 minutes, a 100µl was removed from the chamber and frozen immediately in liquid nitrogen, then stored at -70°C until being assayed for Complex I activity as described in 2.3.2.1. A 400µl aliquot was also removed and centrifuged at 17000x*g* for 5 minutes at 4°C and then the supernatant frozen immediately in liquid nitrogen. This sample was also stored at -70°C until used for assay of cytochrome *c* concentration (these data are discussed in 3.3.2).

Non-synaptic mitochondria were treated with rotenone in the range 0 – 0.45 nmoles.mg^{-1} mitochondrial protein. This produced a titration of Complex I activity between (mean value of $n \geq 3$) 280.9 ± 25.0 nmoles.min^{-1}.mg^{-1} protein and 66.8 ± 15.4 nmoles.min^{-1}.mg^{-1} protein (100% to 23.8%), as shown in Figure 3.1. The

corresponding oxygen consumption rates were found to be inhibited from 84.2 ± 3.7 nmoles.min^{-1}.mg^{-1} protein to 6.6 ± 1.3 nmoles.min^{-1}.mg^{-1} protein (100% to 7.8%), as shown in Figure 3.2. $\Delta\psi_m$ was inhibited from 170.9 ± 5.2 mV down to 91.8 ± 8.1 mV (100% to 53.7%), as shown in Figure 3.3.

Synaptic mitochondria were treated with rotenone in the range 0 – 0.25 nmoles.mg^{-1} mitochondrial protein. This produced a titration of Complex I activity between (mean value of n ≥ 3) 103.3 ± 5.9 nmoles.min^{-1}.mg^{-1} protein and 17.3 ± 4.3 nmoles.min^{-1}.mg^{-1} protein (100% to 16.7%), as shown in Figure 3.4. The corresponding oxygen consumption rates were found to be inhibited from 51.7 ± 2.8 nmoles.min^{-1}.mg^{-1} protein down to 9.6 ± 2.6 nmoles.min^{-1}.mg^{-1} protein (100% to 18.6%), as shown in Figure 3.5. Measurement of $\Delta\psi_m$ using synaptic mitochondria was found to be problematic. Only a very weak and unreliable TPP^+ signal was obtained, unfortunately making the data unusable (discussed in 3.4.1.2).

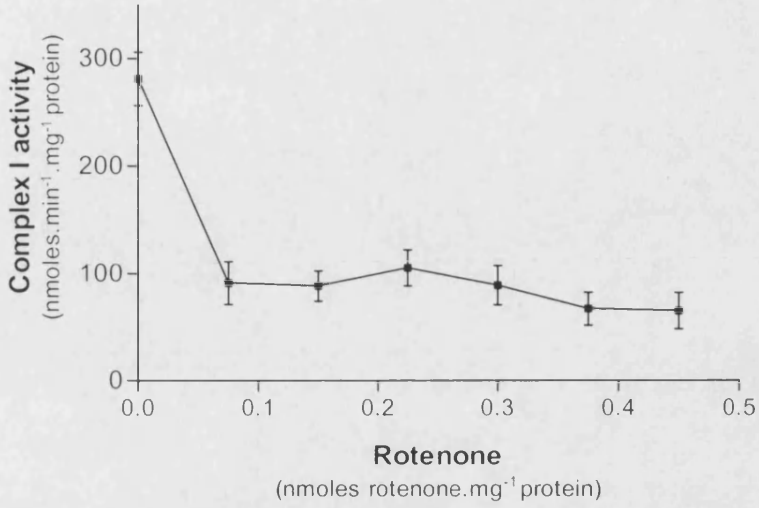

Figure 3.1

Concentration-dependent inhibition of non-synaptic mitochondrial Complex I activity by rotenone. n 3 for each rotenone concentration. Data shown ± S.E.M. The assay was carried out on mitochondria which had undergone three freeze-thaw cycles.

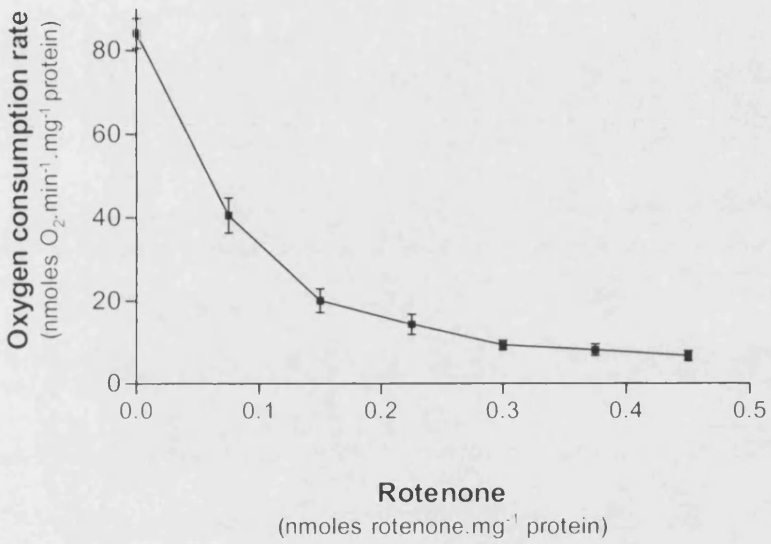

Figure 3.2

Concentration-dependent inhibition of non-synaptic mitochondrial state 3 oxygen consumption rate by rotenone. n 3 for each rotenone concentration. Data shown ± S.E.M. Measurements were made *in situ* in the electrode chamber, in the presence of glutamate, malate and pyruvate as substrates.

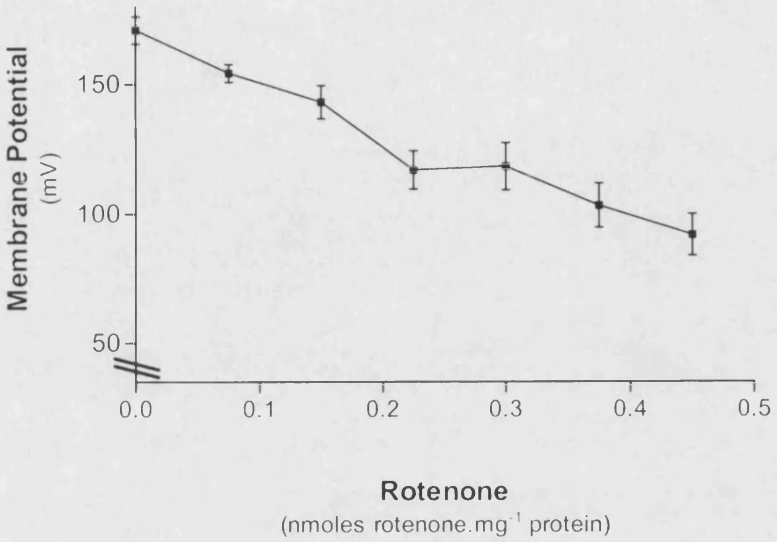

Figure 3.3

Concentration-dependent inhibition of non-synaptic mitochondrial state 3 $\Delta\psi_m$ by rotenone. n 3 for each rotenone concentration. Data shown ± S.E.M. Measurements were made *in situ* in the electrode chamber, in the presence of glutamate, malate and pyruvate as substrates.

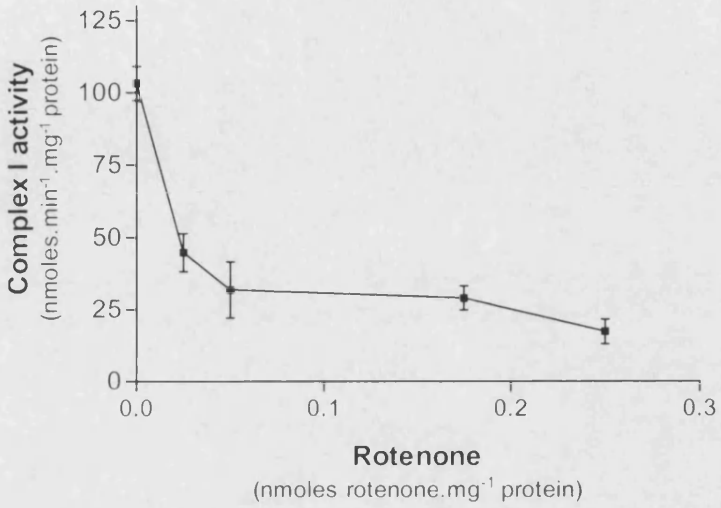

Figure 3.4

Concentration-dependent inhibition of synaptic mitochondrial Complex I activity by rotenone. n 3 for each rotenone concentration. Data shown ± S.E.M. The assay was carried out on mitochondria which had undergone three freeze-thaw cycles.

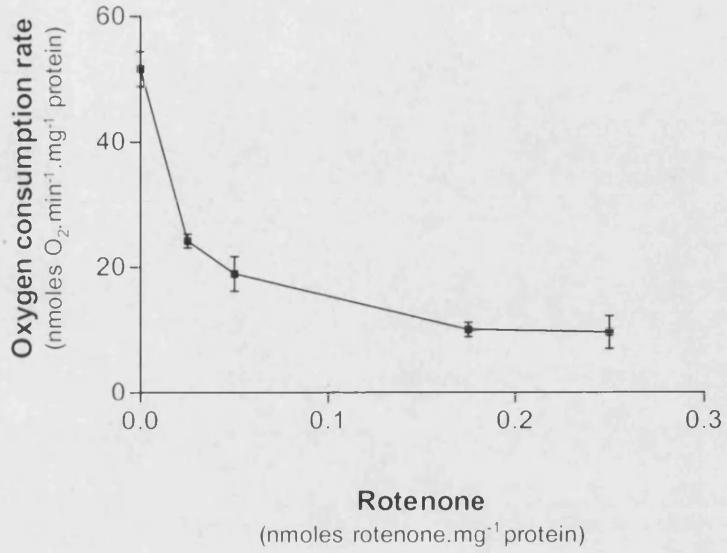

Figure 3.5

Concentration-dependent inhibition of synaptic mitochondrial state 3 oxygen consumption rate by rotenone. n 3 for each rotenone concentration. Data shown ± S.E.M. Measurements were made *in situ* in the electrode chamber, in the presence of glutamate, malate and pyruvate as substrates.

3.3.2 *Relationship between respiratory function and cytochrome c release*

The 400µl supernatants from the incubations described in 3.3.1 were assayed for cytochrome *c* concentration (2.4.1). The assay was also performed on untreated isolated mitochondria which had been subjected to three freeze-thaw cycles, in order to determine total mitochondrial cytochrome *c* concentration. Released cytochrome *c* was then expressed as a percentage of total mitochondrial content.

It was found that in the case of both non-synaptic and synaptic mitochondria, as their respiratory function was inhibited, they released small amounts of cytochrome *c* to the surrounding buffer. The amount of cytochrome *c* released was proportional to the extent of the respiratory inhibition. This was determined by plotting the measured respiratory parameters (oxygen consumption rate and $\Delta\psi_m$) versus the percentage cytochrome *c* released. The results are as follows:

Non-synaptic mitochondria had a mean cytochrome *c* concentration of 0.38 ± 0.015 nmoles.mg^{-1} protein (n = 4). Oxygen consumption rate was plotted versus percentage released cytochrome *c*, as shown in Figure 3.6. The linear regression line for this scatter graph showed a significant deviation from zero slope ($p < 0.0001$), and had the equation $y = -0.105x + 26.4$. Similarly, $\Delta\psi_m$ was plotted versus percentage released cytochrome *c*, as shown in Figure 3.7. The linear regression line for this scatter graph also showed a significant deviation from zero slope ($p < 0.0001$), and had the equation $y = -0.101x + 36.1$.

Synaptic mitochondria had a mean cytochrome *c* concentration of 0.14 ± 0.002 nmoles.mg^{-1} protein (n = 4). Oxygen consumption rate was plotted versus percentage

released cytochrome *c*, as shown in Figure 3.8. The linear regression line for this scatter graph showed a significant deviation from zero slope ($p < 0.005$), and had the equation $y = -0.127x + 26.3$.

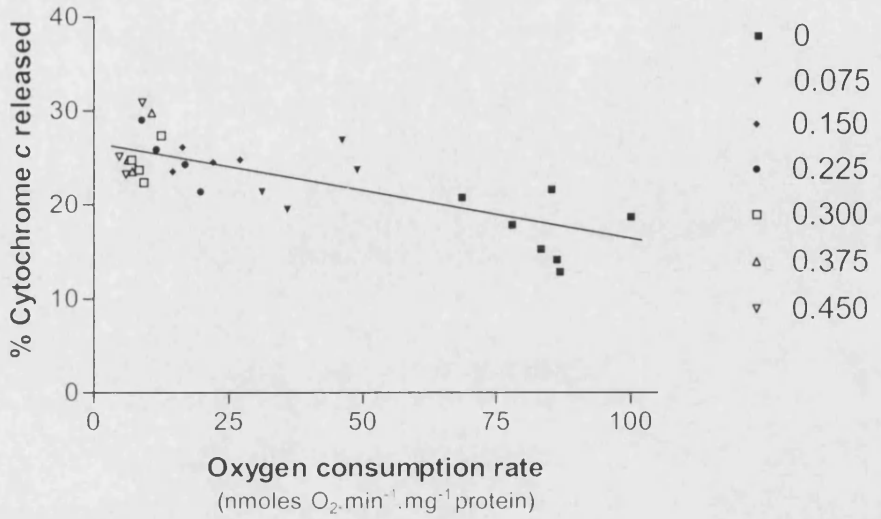

Figure 3.6

Relationship between oxygen consumption rate and percentage release of cytochrome *c* in non-synaptic mitochondria. Linear regression line has equation y = -0.105x + 26.4 and is of significant deviation from zero slope ($p < 0.0001$). Key indicates rotenone concentration (nmoles.mg^{-1} protein) used to achieve inhibition.

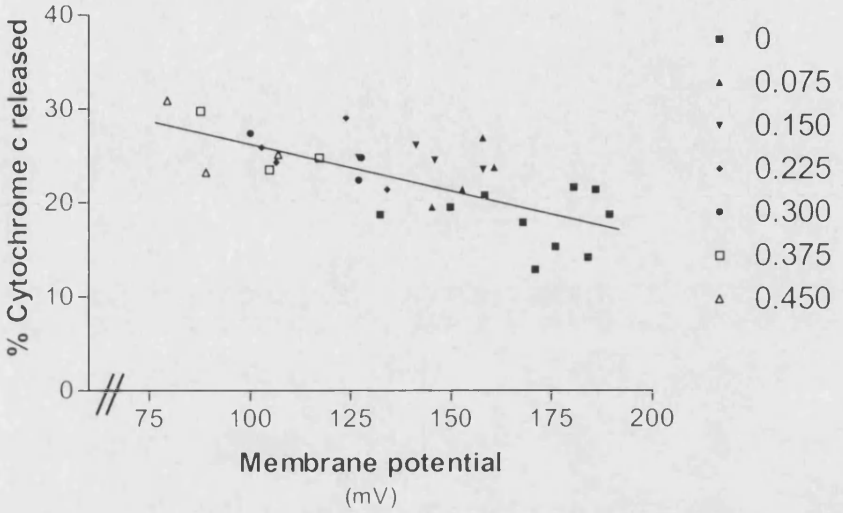

Figure 3.7

Relationship between $\Delta\psi_m$ and percentage release of cytochrome *c* in non-synaptic mitochondria. Linear regression line has equation y = -0.101x + 36.1 and is of significant deviation from zero slope ($p < 0.0001$). Key indicates rotenone concentration (nmoles.mg^{-1} protein) used to achieve inhibition.

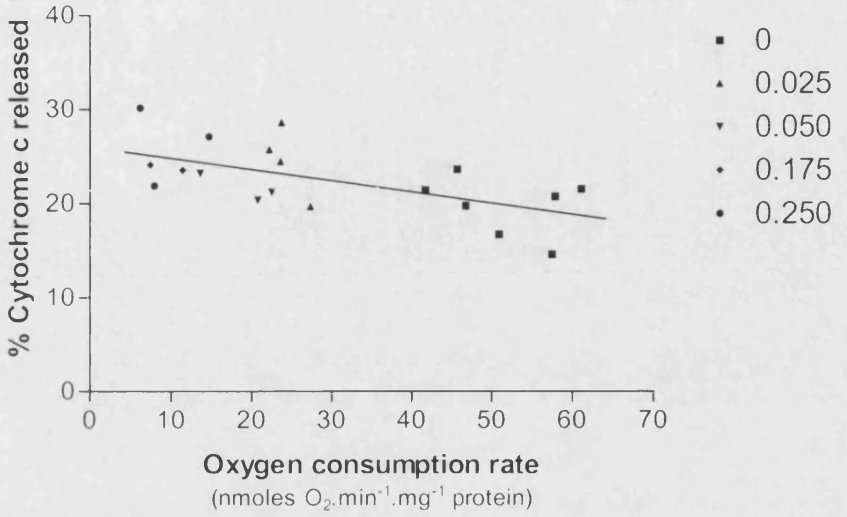

Figure 3.8

Relationship between oxygen consumption rate and percentage release of cytochrome *c* in synaptic mitochondria. Linear regression line has equation $y = -0.127x + 26.3$ and is of significant deviation from zero slope ($p < 0.005$). Key indicates rotenone concentration (nmoles.mg^{-1} protein) used to achieve inhibition.

3.3.3 *'Background' release in the absence of rotenone*

As can be seen in Figures 3.6, 3.7 and 3.8, approximately 15-20% total mitochondrial cytochrome *c* is released by the isolated mitochondria under control conditions, ie. where respiratory parameters are not subject to rotenone treatment and are therefore at their highest. In order to determine the trigger for this background level of release, mitochondria ($0.5mg.ml^{-1}$) were incubated according to Incubation Scheme 3 (2.3.1.3). At t = 10 minutes, a 400µl aliquot was removed and centrifuged at 17000x*g* for 5 minutes at 4°C. The supernatant was frozen immediately in liquid nitrogen and then stored at -70°C until being used for assay of cytochrome *c* concentration (2.4.1).

In the case of both non-synaptic and synaptic mitochondria, there was no significant difference (unpaired t-test) between the percentage cytochrome *c* released after treatment with vehicle alone under Incubation Scheme 1 (see 3.3.2) and that released when mitochondria are simply added into buffer at 37°C with fatty acid-free BSA and incubated for 10 minutes (ie. Incubation Scheme 3). The data from these experiments are shown in Table 3.1.

	% CCR (experimental control)	% CCR (incubation control)
Non-synaptic mitochondria	15.3 ± 0.51	18.5 ± 1.11
Synaptic mitochondria	25.7 ± 2.98	19.6 ± 1.38

Table 3.1

Percentage CCR under experimental control conditions (treatment with vehicle alone under Incubation Scheme 1) and incubation control conditions (Incubation Scheme 3). Data shown is mean of $n \geq 4$, ± S.E.M. There was no significant difference (unpaired t-test, $p > 0.05$) between the two controls in either non-synaptic or synaptic mitochondria.

3.3.4 *'Background' release in the presence of rotenone*

As described earlier, titration of respiratory function on each separate preparation of isolated mitochondria was carried out in order of increasing rotenone concentration. For this reason, a control experiment was required to demonstrate that the increasing CCR detected with increasing rotenone concentration was not purely an artefact of deterioration of mitochondrial integrity over time.

The maximum time between completion of the isolation procedure and completion of the final incubation in a titration run was under 2 hours for non-synaptic mitochondria and under 90 minutes for synaptic mitochondria. Mitochondria therefore underwent a control incubation (vehicle alone, according to Incubation Scheme 1) at t = 0 and 120 minutes (non-synaptic mitochondria) or t = 0 and 90 minutes (synaptic mitochondria). Both were then treated with rotenone (0.375 nmoles.mg^{-1} protein for non-synaptic mitochondria, 0.25 nmoles.mg^{-1} protein for synaptic mitochondria), according to Incubation Scheme 1, at the appropriate upper time point. A 400µl aliquot was removed and centrifuged at 17000x*g* for 5 minutes at 4°C. The supernatant was frozen at -70°C and assayed for cytochrome *c* concentration as described in 2.4.1.

In the case of both non-synaptic and synaptic mitochondria, it was found that the 120/90 minute delay (respectively) did not cause a significant increase in the percentage cytochrome *c* released. Rotenone treatment however caused a significantly greater amount of release than either of the control incubations. The data were analysed using a paired t-test and are shown in Tables 3.2 and 3.3.

	t = 0, [rotenone] = 0	t = 120 mins, [rotenone] = 0	t = 120 mins, [rotenone] = 0.375nmoles.mg^{-1}
% Cytochrome *c* released	16.2 ± 2.7	19.3 ± 1.1	**26.0 ± 1.9** *

Table 3.2

Percentage cytochrome *c* released from non-synaptic mitochondria under Incubation Scheme 1 after treatment with vehicle alone at t = 0 and t = 120 minutes and with rotenone (0.375 nmoles.mg^{-1} protein) at t = 120 minutes. Only the final treatment shows an increase in released cytochrome *c* (* indicates $p > 0.05$, assessed by paired t-test). Data shown is mean of $n \geq 3$, ± S.E.M.

	t = 0, [rotenone] = 0	t = 90 mins, [rotenone] = 0	t = 90 mins, [rotenone] = 0.25nmoles.mg^{-1}
% Cytochrome *c* released	17.1 ± 2.66	19.5 ± 2.01	**26.1 ± 1.74** *

Table 3.3

Percentage cytochrome *c* released from synaptic mitochondria under Incubation Scheme 1 after treatment with vehicle alone at t = 0 and t = 90 minutes and with rotenone (0.25 nmoles.mg^{-1} protein) at t = 90 minutes. Only the final treatment shows an increase in released cytochrome *c* (* indicates $p < 0.05$, assessed by paired t-test). Data shown is mean of $n = 4$, ± S.E.M.

3.4 Discussion

3.4.1 *Titration of respiratory function by rotenone*

3.4.1.1 Non-synaptic and synaptic mitochondria

This study was carried out first on non-synaptic mitochondria, and subsequently on synaptic mitochondria. It was considered vital to the interpretation of the data that both populations be observed. Non-synaptic mitochondria originate from both astrocytes and neurons (excepting neuronal synaptic terminals). Although neurodegeneration is primarily concerned with a reduction in synaptic transmission (itself sufficient to justify the use of synaptic mitochondria in the investigation), the viability of the remainder of the neuron is of course equally crucial. Furthermore, the supporting role of glia, and astrocytes in particular, in the maintenance of synaptic transmission has recently been highlighted (reviewed by Aschner, 2000). For example, it is thought that *in vivo* astrocytes provide precursors for neuronal glutathione synthesis (Dringen *et al*, 1999). These considerations support the use of non-synaptic mitochondria in this study.

From a more practical point of view, most clinical reports of reduced respiratory complex activity in cases of neurodegenerative disease rely on tissue homogenates or isolated non-synaptic mitochondrial populations (Schapira *et al*, 1990; Mutisya *et al*, 1994). By far the majority of mitochondria in a tissue homogenate sample would be classified as 'non-synaptic'. Furthermore, the yield of non-synaptic mitochondria is significantly greater than that of synaptic mitochondria, relative to the original mass of brain tissue.

Finally, although the range of rotenone concentrations used was based on Davey & Clark (1996), the incubation conditions in this study were not identical to those used in the 1996 report. (The incubations were carried out at 37°C and pyruvate was included as an additional substrate. Both changes created a more physiologically relevant environment). The treatments therefore needed to be re-defined for the altered incubation conditions. Although further 'fine tuning' was likely to be needed for the synaptic titrations, the initial 'broad tuning' was carried out in non-synaptic mitochondria, thus reducing the number of animals used for this preparatory stage.

It was determined that the range of rotenone concentrations required to suitably titrate non-synaptic respiratory activity was greater than that required to create a similar percentage change in synaptic mitochondria. In Davey and Clark (1996) and Davey *et al* (1998) the IC_{50}s for the effect of rotenone on oxygen consumption rates were comparable. This may be explained by the discrepancy in control Complex I activities measured: in this study the mean Complex I activity in non-synaptic mitochondria was 137% of that reported in Davey & Clark (1996), whereas in synaptic mitochondria, this study obtained a value only 76% of that in Davey *et al* (1998). The latter difference may be contributed to by a suspected contamination of the synaptic preparation by synaptosomal membranes (discussed later in this section). It is however recognised that control levels of non-synaptic Complex I activity are higher than those in synaptic mitochondria. Therefore the trend is as expected, even if the amplitude of the difference appears large.

Mention should be made of the difficulty experienced in obtaining a reliable $\Delta\psi_m$ measurement during incubations of synaptic mitochondria. The mV reading resulting from TPP^+ distribution was extremely small, and highly unreliable. It should be noted that the volume used for these incubations (800µl) is lower than generally used for TPP^+ measurements (Brand, 2002). However, the system did prove to be highly reliable for measuring $\Delta\psi_m$ in non-synaptic mitochondria. It is thought that the problem may have been due to contamination of the synaptic preparations by synaptosomal membranes. The second Ficoll gradient (see 2.2.1.3) is designed to remove such contamination, therefore further optimisation of this gradient may be required.

The presence of such membranes would contribute to the protein measurement. The assumption of synaptosomal membrane contamination is therefore supported by the observations of lower than expected measurements per mg of protein of citrate synathase (2.7.2.1), Complex I activity (3.3.1) and cytochrome *c* content (3.3.2). However, the titrations of oxygen consumption rate and Complex I activity were found to be highly reproducible for synaptic populations (see Figures 3.4 and 3.5). Any contamination is therefore either minimal or extremely consistent in terms of percentage contamination. It is possible that these low measurements per unit protein are due to an increased overall protein concentration per mitochondrion, as a result of the synaptic machinery.

Since measurements of CCR are to be relative to respiratory parameters and not protein content, this possible contamination does not affect the conclusions of this study.

3.4.1.2 Profiles of inhibition of respiratory parameters

When the profiles of inhibition of non-synaptic mitochondrial complex I and respiratory parameters are compared (Figures 3.1, 3.2 and 3.3), there appears to be some inconsistency in the data. The profile of complex I inhibition appears almost flat at rotenone concentrations of 0.075 nmoles.mg^{-1} mitochondrial protein and above, although the inhibition is not complete. However, the oxygen consumption rate and $\Delta\psi_m$ continue to decrease throughout the range of rotenone concentrations used. It is recognised that complex inhibition and the resulting inhibition of respiration rate do not follow the same profiles. Indeed the curves for inhibition of respiratory complexes and respiration rate were observed to cross by Davey & Clark (1996) and Davey *et al*, (1998). However, the apparent insensitivity of complex I activity to rotenone above 0.075 nmoles.mg^{-1} mitochondrial protein is inconsistent with the observed effects on oxygen consumption rate and $\Delta\psi_m$. This suggests a problem with the assay for complex I activity. The three freeze-thaw cycles could perhaps be responsible for an artefactually high background rate of rotenone-sensitive NADH oxidation. This might be resolved if complex I activity could be measured *in situ* with the other respiratory parameters.

Interestingly, this inconsistency was not observed with the isolated synaptic mitochondria. Here, complex I activity decreased across the range of rotenone concentrations used. This was consistent with the resulting profile of inhibition of oxygen consumption rate.

Nonetheless, despite this anomaly and aside from the differences described concerning thresholds for inhibition (3.4.1.1), the two populations of brain mitochondria displayed overall the same effect. Their respiration was titrated by increasing the concentration of the rotenone treatment. This concentration-dependent inhibition of respiratory function by rotenone was simply a tool for observing a downstream effect.

There is one more observation, however, which is worthy of discussion. As described, the non-synaptic mitochondrial incubations yielded measurements of both oxygen consumption rate and $\Delta\psi_m$. The relationship between rotenone concentration and oxygen consumption rate was clearly non-linear, instead displaying a pseudo-exponential form (see Figures 3.2 and 3.5). Rotenone concentration versus $\Delta\psi_m$ was however a near linear relationship (see Figure 3.3). It is not immediately clear why the profiles of the two parameters should differ.

One possible explanation involves the 'proton leak' across the IM. As described (1.1.2), protons are pumped from the matrix into the IMS across the IM by Complexes I, III and IV, creating a $\Delta\psi_m$. This gradient is sacrificed in order to power the ATP synthase. However, a certain amount of protons 'leak' back into the matrix by other means. This means that some of the electron transport process, and so the oxygen consumption rate, is 'wasted', in counteracting the leaking protons. The dynamics of this proton leak are unclear, but it is quite possible that it may act in a regulatory manner, such that when the $\Delta\psi_m$ is large (ie. very depolarised), the proton leak is great, but that if the $\Delta\psi_m$ is dissipated, proton leak decreases accordingly. This would serve to 'buffer' the $\Delta\psi_m$ against extreme change. If this were the case, at

the more inhibited end of the curves, less oxygen consumption would be required to support the same $\Delta\psi_m$. This hypothesis is consistent with the recognised non-ohmic relationship between $\Delta\psi_m$ and proton influx, and is demonstrated in Figure 3.9.

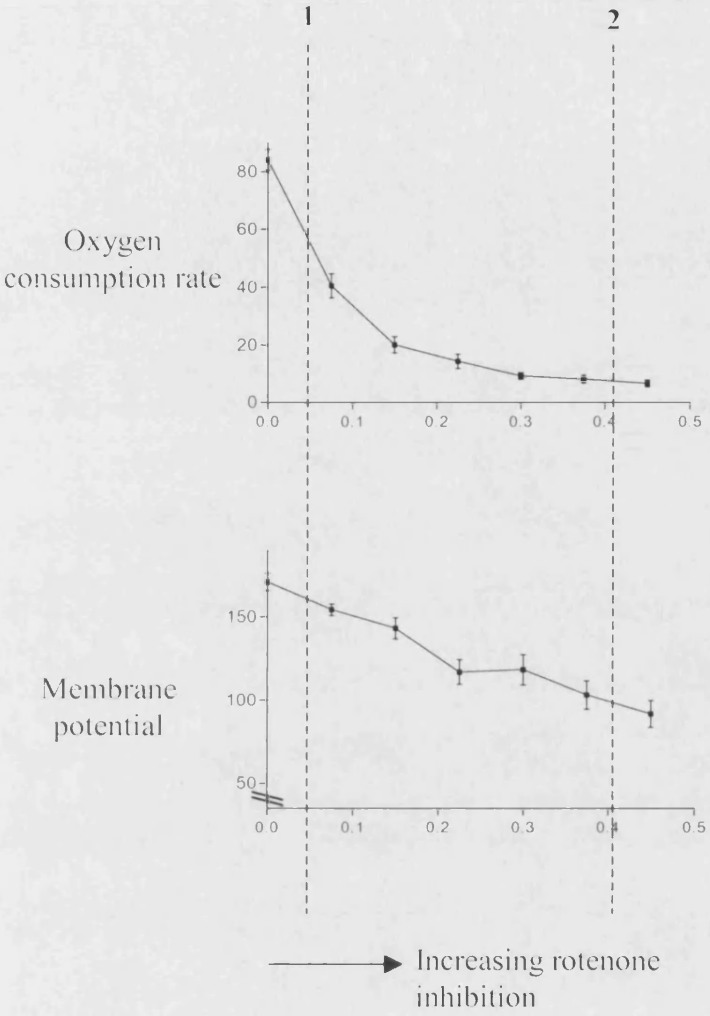

Figure 3.9

Hypothesised explanation for profiles of oxygen consumption rate and $\Delta\psi_m$ with rotenone treatment. (Data shown is rotenone titration of non-synaptic mitochondrial respiration; original figures 3.2 and 3.3). **1** $\Delta\psi_m$ is high, therefore proton leak is high. A relatively high oxygen consumption rate is required to maintain $\Delta\psi_m$ at this point. **2** $\Delta\psi_m$ is low, therefore proton leak is low. A relatively low oxygen consumption rate required to maintain $\Delta\psi_m$ at this point.

3.4.2 *Effect of respiratory inhibition on cytochrome c release*

3.4.2.1 Release proportional to severity of respiratory deficiency

In both populations of isolated brain mitochondria, there was a clear effect of rotenone-induced respiratory inhibition on the distribution of cytochrome *c*. It was found that as respiratory function was reduced, cytochrome *c* was released from the mitochondria in a manner proportional to the extent of inhibition. A near linear inversely proportional relationship was found between the percentage CCR and both oxygen consumption (both populations of mitochondria) and $\Delta\psi_m$ (only non-synaptic data available), despite these two parameters not showing a linear relationship themselves. There was no apparent threshold effect – the relationship was linear from the control point. The possibility that the increased CCR detected was an artefact of mitochondrial deterioration over time (note that titrations were performed in order of increasing rotenone concentration - see 3.3.1) was eliminated by control experiments.

Since cytochrome *c* measurements were being made in a respiration medium of known composition and not in the cytosolic compartment of cells, the measurements can be taken as a direct indication of the extent of release. The maximum level of CCR detected was approximately 25-30% of the total mitochondrial content. This was true of both non-synaptic and synaptic mitochondria, despite the total mitochondrial content of the former being over double that of the latter (0.38 nmoles.mg^{-1} protein versus 0.14 nmoles.mg^{-1} protein).

There was a certain level (approximately 15-20%) of CCR to the surrounding medium even under control conditions (ie. treatment with ethanol vehicle alone). Further investigation determined that this control level of release could be induced by simply adding the isolated mitochondria into the warmed buffer and incubating for the full ten minutes. In the absence of substrates and ADP, these mitochondria are in a quiescent state, and therefore this basal release is a result of incubation artefacts, rather than being related to any respiratory changes. Such artefacts may include temperature shock (the isolated mitochondria are stored on ice until used for experimentation at 37°C) and physical damage through centrifugation (performed after the incubation in order to separate the supernatant from the mitochondrial pellet).

The basal level of release essentially shifts the relationship down the y-axis by 10-15%, such that in both populations, rotenone treatment in the range selected induced a maximum release of approximately 10-15% total mitochondrial cytochrome *c*.

3.4.2.2 Implications of respiratory inhibition-induced release

The data from this study demonstrate that if Complex I activity is lowered using the specific inhibitor rotenone in isolated brain mitochondria, cytochrome *c* is released. Only small percentages of the total mitochondrial content are released, the extent of release being directly proportional to the extent of respiratory inhibition.

These findings are a clear contradiction to the claim of Goldstein *et al* (2000) that CCR is an 'all-or-none' event. The authors categorically state that the extent and time course of release is unaffected by the intensity of the pro-apoptotic stimulus. In direct

challenge to that statement, it is concluded here that if CCR is measured using a sensitive, quantitative assay and a physiologically relevant stimulus is used, then the release is indeed sensitive to the strength of the insult.

This 'physiologically relevant stimulus' models a recognised pathology in Parkinson's disease (Perier *et al*, 2003; Schapira *et al*, 1990). By titrating the activity of Complex I, this study has modelled a physiological to pathological transition, rather than simply selecting a stimulus known to induce apoptosis. The observation that CCR was directly proportional to respiratory inhibiton, rather than showing a threshold effect, implies that low levels of CCR can occur before any symptoms of disease are apparent. If CCR can be induced by such mild insults, it appears likely that low levels of release would be insufficient to induce apoptosis.

This hypothesis is consistent with the growing understanding of post-mitochondrial regulation of apoptosis. Concannon *et al* (2001) claim that the molecular chaperone Hsp27 can sequester cytochrome *c* (in addition to pro-caspase 3) in the cytosol, preventing correct formation of the apoptosome complex. Hsp90 is thought to be associated with Apaf-1 in the cytosol with the same effect (Pandey et al, 2000). More widely recognised is the role of IAP proteins in inhibiting the action of activated caspases (Deveraux *et al*, 1997). These mechanisms of control have been suggested to prevent 'inappropriate' initiation of apoptosis in neurodegenerative disease (Hengartner, 2000; Kugler *et al*, 2000). These defensive mechanisms would only be in place if it were possible for cytochrome *c* to be released in small enough quantities for its pro-apoptotic action to be overcome. If CCR were an 'all-or-none' process, these levels of control would be redundant. Notably, physiological concentrations of

potassium appear to set a threshold of cytosolic cytochrome *c* required to induce apoptosis (Cain *et al*, 2001).

It is likely that a certain amount of cytochrome *c* is being released into the cytosol under normal physiological conditions. The 'trigger' for release is discussed in more detail in Chapter 5, but fluctuations in the activity of the ETC are inevitable and these data imply that as a result, so are fluctuations in CCR. Furthermore, cytochrome *c* may need to be translocated to the cytosol for degradation, as part of the normal turnover cycle (1.2.2.3). Reports have identified a basal cytosolic cytochrome *c* concentration under physiological conditions (Kluck *et al*, 1997; Adachi *et al*, 1998). (It is interesting to note the confirmation that the sensitivity of the quantitative ELISA technique for measuring cytochrome *c* concentrations allows detection of low levels of the protein which cannot be picked up using Western blotting (Brustovetsky *et al*, 2003b)). It is possible to regulate a system more tightly if there is a control level of signal which can be up- or down-regulated along a continuous scale. A system where the signal is simply on or off allows much less control. Bearing in mind the potentially lethal effect of releasing too much cytochrome *c*, such a strict level of control is vital. This is especially true of neurons, where the implications of 'inappropriate' apoptosis have been discussed (3.1.2).

Although it will be shown later (5.3.2) that the effect on CCR is not common to all respiratory inhibition, the data from this investigation indicate that the extent of CCR subtly reflects the extent of respiratory stress influencing the mitochondria. It is therefore possible that the presence of cytochrome *c* in the cytosol could have some signalling role more subtle than the initiation of apoptosis, perhaps indicating an

imminent fall of ATP levels, and therefore the requirement for increased synthesis of respiratory proteins (the majority of whose subunits are encoded by nuclear and not mitochondrial DNA) or even increased mitochondrial turnover. It is interesting to note the claim of Ramasarma *et al* (1992) that cytochrome *c* has a molecular chaperone role. This could also be a feature of a cytochrome *c*-mediated stress response.

As described (1.2.3.3), low levels of cytochrome *c* external to the mitochondria appear capable of ameliorating ETC-mediated ROS generation. Bearing in mind the suggested importance of electron leak at the site of complex I in ROS generation (1.1.3), the CCR detected here could be a defensive anti-oxidant mechanism.

These speculations are secondary, however, to the more strongly implied hypothesis that low levels of CCR do not necessarily lead to apoptosis. The post-mitochondrial mechanisms for preventing apoptosis could contribute to a threshold of cytochrome *c* required for activation of caspases (Waterhouse *et al*, 2002).

3.5 Conclusions

When the respiration of isolated brain mitochondria is inhibited at the level of Complex I by rotenone, the mitochondria release cytochrome *c* to the surrounding medium. The release is partial, and occurs to an extent directly proportional to the severity of respiratory deficiency.

The data imply that CCR is a more common event than previously thought, but that it is also more subtle and tightly regulated than has been suggested (Goldstein *et al*, 2000). It would seem likely that small amounts of CCR are a normal physiological occurrence, or at least occur upstream in the progression of neurodegenerative disease to the stage where symptoms become apparent.

The hypothesis which has arisen from this study is that small amounts of CCR can occur in brain cells without apoptosis proceeding.

CHAPTER 4

Establishing the mechanism of release of cytochrome *c* from brain mitochondria

4.1 Introduction

4.1.1 *The two categories of release mechanism*

All of the current postulated CCR mechanisms fall into one of two categories. These are described in detail in 1.3.5. Briefly, release is thought to occur due to either physical rupture of the OM or formation of channels in the OM. The former category includes release via MPT, where OM rupture occurs due to loss of osmotic balance, matrix swelling and outward force by the convoluted IM (Petit *et al*, 1998; Scarlett & Murphy, 1997). Also, it is suggested that hyperpolarisation of the membrane potential resulting from failure of the ATP/ADP exchange system leads to osmotic swelling with the same effect (Vander Heiden *et al*, 1999). In contrast, postulated swelling-independent release mechanisms involve formation of OM channels, usually involving combinations of Bcl-2 family members and the VDAC (Andreyev *et al*, 1998; Doran & Halestrap, 2000; Eskes *et al*, 1998; Jürgensmeier *et al*, 1998; Kluck *et al*, 1999).

As described in 3.4.2.2, the data obtained thus far imply that a certain amount of CCR may be a normal physiological occurrence, or at least occur prior to onset of disease symptoms, and therefore be unlikely to lead to apoptosis. If this conclusion is to be drawn, it is crucial to determine the release mechanism. For low levels of release to be 'safe', not only must they be insufficient to induce apoptosis, but the release mechanism must leave the host cell energetically viable.

Release via swelling-dependent mechanisms, particularly MPT, have debilitating effects on mitochondrial integrity. ATP synthesis by oxidative phosphorylation is prevented, and there is non-specific release of SIMPs (many of which have pro-apoptotic properties (Du *et al*, 2000; Suzuki *et al*, 2001; Verhagen *et al*, 2000; Yu *et al*, 2002) to the cytosol. Such a dramatic loss of homeostasis in the cell is unlikely to be a normal physiological occurrence (Crompton, 2000). Formation of channels in the OM, however, would be expected to allow controlled and specific release of cytochrome *c*. There is evidence to suggest that if released in this manner, sufficient cytochrome *c* can remain associated with the IM for electron transport to continue (Cortese *et al*, 1995; Ott *et al*, 2002). The capacity to synthesise ATP is therefore retained in this case and changes in levels of other SIMPs (note that the SIMP adenylate kinase, for example, is required for respiratory function) are not a consideration. These features may simply enable enough ATP synthesis for the apoptotic program to be completed (see 1.3.3.1). However, they may also allow retention of a cell's energetic viability if the cytochrome *c* released was not to induce death of the cell.

Therefore if low levels of CCR are indeed a normal physiological occurrence, the release mechanism would be expected to fall into the swelling-independent category.

4.1.2 *Mitochondrial enzymes*

The distribution of mitochondrial enzymes can be a useful experimental tool for determining effects on the integrity of mitochondrial membranes.

Adenylate kinase (EC 2.7.4.3, AK2 isoform, 23.6kDa) is found, like cytochrome *c*, in the IMS. Measurement of AK activity external to the mitochondria has been used as a method for establishing whether a release mechanism has been specific for cytochrome *c* or a general OM permeabilisation (Doran & Halestrap, 2000; Siskind *et al*, 2002; Crouser *et al*, 2003).

Citrate synthase (CS, EC 4.1.3.7) is a matrix enzyme of 280kDa. It will only be released from mitochondria if both the IM and OM have been ruptured.

4.2 Aims

This investigation aimed to determine whether the CCR induced by respiratory inhibition, as described in 3.4.2, was associated with mitochondrial swelling. The distributions of AK and CS were then used to determine how IM and OM integrity were affected by the release mechanism. Inhibitors of the primary candidates for release mechanisms were also used to provide additional information on the specificity of the release process.

4.3 Results

4.3.1 *Effect of rotenone on mitochondrial volume*

Two methods were used for determining changes in mitochondrial volume during the release process. Electron microscopy was used to qualitatively demonstrate the

effects, whereas changes in light scattering properties provided a quantitative measurement.

4.3.1.1 Electron microscopy

Non-synaptic or synaptic mitochondria were isolated from whole rat brains (2.2.1.2, 2.2.1.3). The protein concentrations were measured (2.7.1) and the mitochondria then incubated at 37°C in the electrode chamber according to Incubation Scheme 1 (2.3.1.3). Three incubations were carried out for each population of mitochondria. Non-synaptic mitochondria were subjected to a control incubation (ethanol vehicle alone), treatment with rotenone (0.375 nmoles.mg^{-1} protein) and finally treatment with alamethicin (75μg.mg^{-1} protein). Alamethicin is an antibiotic peptide, which non-specifically permeabilises membranes (Woolley & Wallace, 1992) and has been used to induce mitochondrial swelling as a positive control in volume studies (Kluck *et al*, 1999; Kristiàn *et al*, 2000). Synaptic mitochondria received the same three treatments, except that the rotenone used in the second incubation was of concentration 0.25 nmoles.mg^{-1} protein.

After each incubation, a 700μl aliquot was removed from the chamber, and immediately centrifuged at 17000x*g* for 5 minutes at 4°C (Sigma Laborzentrifugen 3K10, Osterode, Germany). The supernatant was discarded, and the pellet was treated as described in 2.5.1. Electron microscopy images were generated and compared by observation.

Typical examples of mitochondria as seen by electron microscopy are shown in Figures 4.1 (A-C) and 4.2 (A-C). The rotenone treatment induced no observable

change in the typical morphology of the non-synaptic or synaptic mitochondria. The rotenone concentrations selected had caused a significant amount of CCR as compared to control conditions in each population (see Figures 3.6, 3.7 and 3.8). However, alamethicin treatment caused a marked change in morphology. All mitochondria now appeared swollen or burst. Again, this was the case for both non-synaptic and synaptic populations.

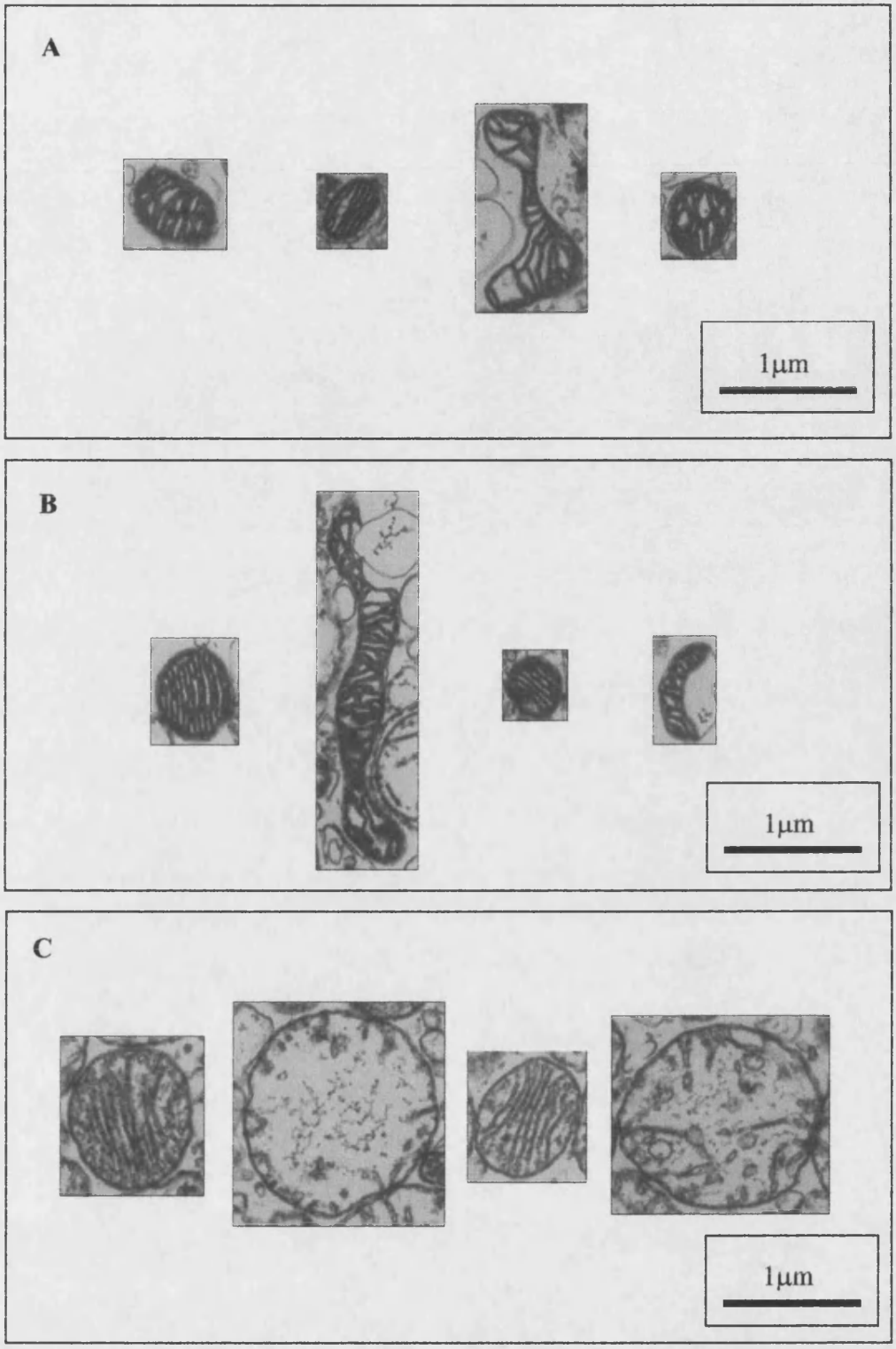

Figure 4.1

Representative electron microscope images of isolated non-synaptic rat brain mitochondria after control incubation (A), treatment with rotenone (0.375nmoles.mg^{-1} protein) (B) and treatment with alamethicin (75μg.mg^{-1} protein) (C).

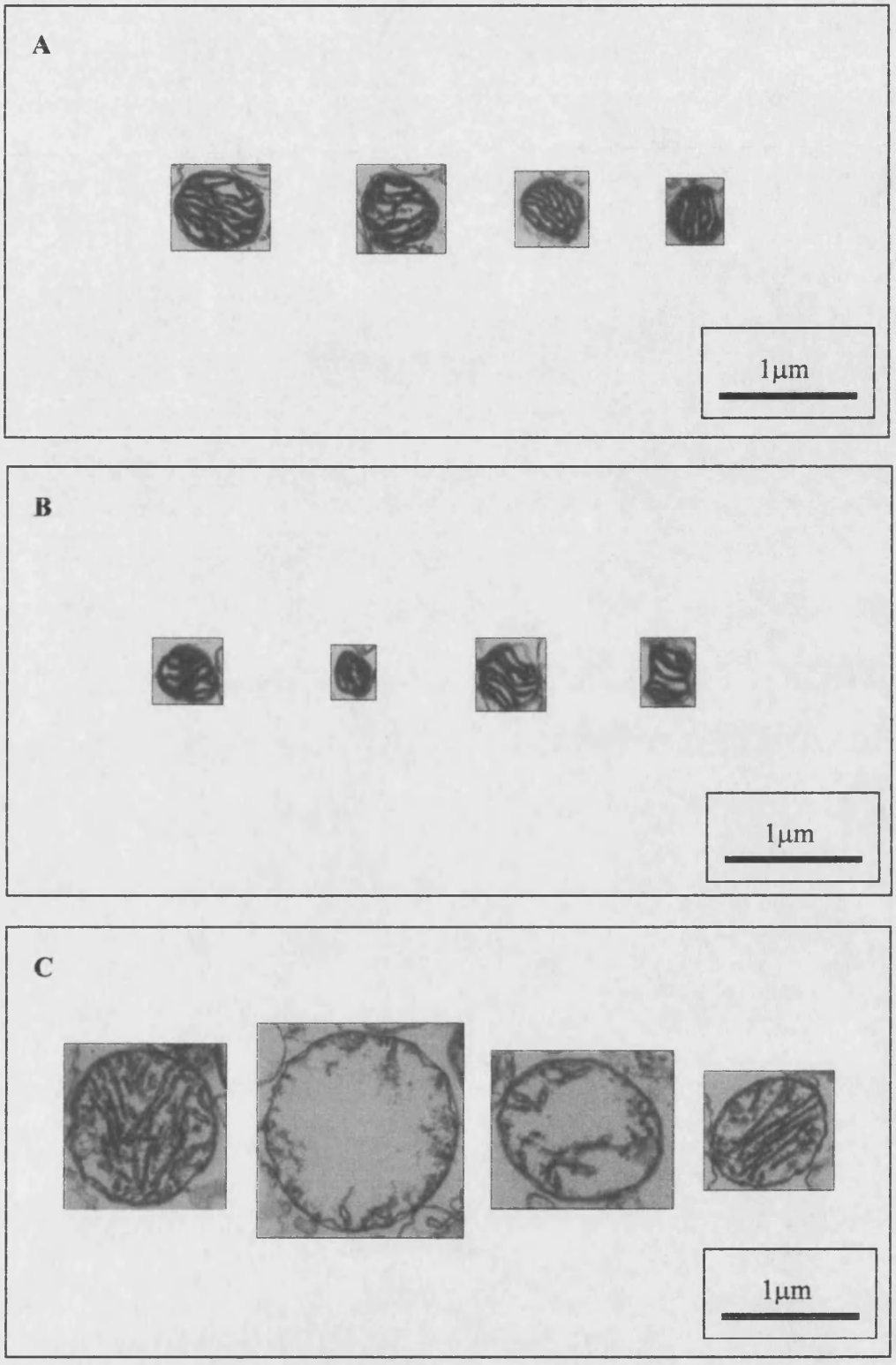

Figure 4.2

Representative electron microscope images of isolated synaptic rat brain mitochondria after control incubation (A), treatment with rotenone (0.25nmoles.mg^{-1} protein) (B) and treatment with alamethicin (75μg.mg^{-1} protein) (C).

4.3.1.2 Light scattering

Non-synaptic or synaptic mitochondria were isolated from whole rat brains (2.2.1.2, 2.2.1.3). The protein concentrations were measured (2.7.1) and the mitochondria then incubated at 37°C in a 0.5ml quartz cuvette according to Incubation Scheme 1 (2.3.1.3). Between t = 7 and t = 10 minutes, the light intensity (540nm) at 90° was recorded as described in 2.5.2. Three incubations were carried out for each population, the treatments exactly as described in 4.3.1.1. Each set of three incubations was repeated three times, and the mean light intensity calculated for each treatment. This value was proportional to the extent of scattering, and therefore a reduction in light intensity represents an increased mean volume. These values are shown in Tables 4.1 and 4.2.

Light intensity values were unchanged between controls and rotenone treatment for both non-synaptic and synaptic mitochondria. Alamethicin however caused a significant reduction in intensity in both cases. This was determined using a paired t-test between treated and control mitochondria.

	Control	Rotenone	Alamethicin
Light intensity (arbitrary units)	90.1 ± 3.5	94.4 ± 4.1	**55.2 ± 5.1** **

Table 4.1

Effect of rotenone (0.375nmoles.mg^{-1} protein) and alamethicin (75µg.mg^{-1} protein) on the detected light intensity (540nm) of isolated non-synaptic brain mitochondria. Values are mean ± S.E.M, n = 3. ** Indicates $p < 0.01$.

	Control	Rotenone	Alamethicin
Light intensity (arbitrary units)	152.2 ± 2.6	145.3 ± 0.7	**116.1 ± 1.3** **

Table 4.2

Effect of rotenone (0.25nmoles.mg^{-1} protein) and alamethicin (75µg.mg^{-1} protein) on the detected light intensity (540nm) of isolated synaptic brain mitochondria. Values are mean ± S.E.M, n = 3. ** Indicates $p < 0.01$

4.3.2 *Enzyme distribution*

Non-synaptic or synaptic mitochondria were isolated from whole rat brains (2.2.1.2, 2.2.1.3). The protein concentrations were measured (2.7.1) and the mitochondria then incubated at 37°C in the electrode chamber according to Incubation Scheme 1 (2.3.1.3). Titrations were performed using rotenone concentration exactly as in 3.3.1 for both non-synaptic and synaptic mitochondria. $n \geq 3$ was obtained for each rotenone concentration. A 400µl aliquot was removed at t = 10 minutes, and centrifuged at 17000x*g* for 5 minutes. The supernatant was assayed for AK (see 2.4.3) and CS (see 2.4.2) activity.

The AK and CS activity of whole untreated non-synaptic and synaptic mitochondria was assayed after three freeze-thaw cycles. The mean values for these activities were calculated for n = 4. In non-synaptic mitochondria, AK activity was determined to be 2088 ± 103.2 units.mg^{-1} protein and CS to be 1101 ± 80.9 nmoles.min^{-1}.mg^{-1} protein. In synaptic mitochondria, AK activity was determined to be 238.4 ± 39.6 units.mg^{-1} protein and CS to be 440.1 ± 26.2 nmoles.min^{-1}.mg^{-1} protein. Released enzyme was then expressed as a percentage of total mitochondrial content in all cases. The effect of rotenone treatment on the release of AK and CS is shown in Figures 4.3 - 4.6. A range of rotenone concentrations seen earlier (3.3.2) to induce a significant change in CCR was found to have no significant effect on the distribution of AK or CS. This was true of both non-synaptic and synaptic mitochondria. There was a significant basal level of both enzymes in the supernatants (approximately 15-20% AK and 5-7% CS).

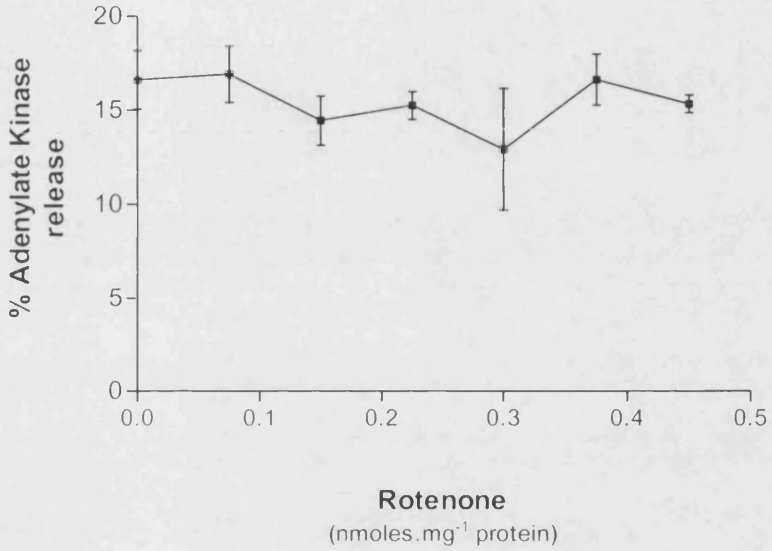

Figure 4.3

Effect of rotenone concentration on adenylate kinase release from non-synaptic brain mitochondria. Data is expressed as AK activity in supernatant as a percentage of total mitochondrial activity. Analysis of the regression shows that the slope is not significantly deviant from zero ($p > 0.05$).

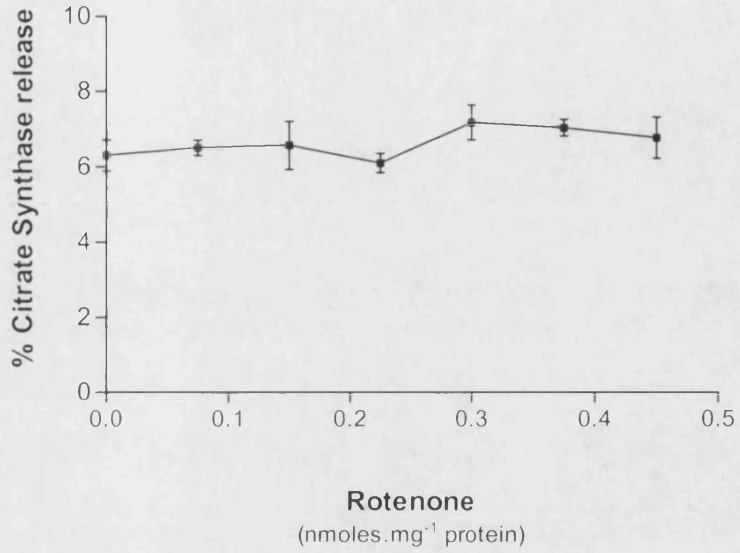

Figure 4.4

Effect of rotenone concentration on citrate synthase release from non-synaptic brain mitochondria. Data is expressed as CS activity in supernatant as a percentage of total mitochondrial activity. Analysis of the regression shows that the slope is not significantly deviant from zero ($p > 0.05$).

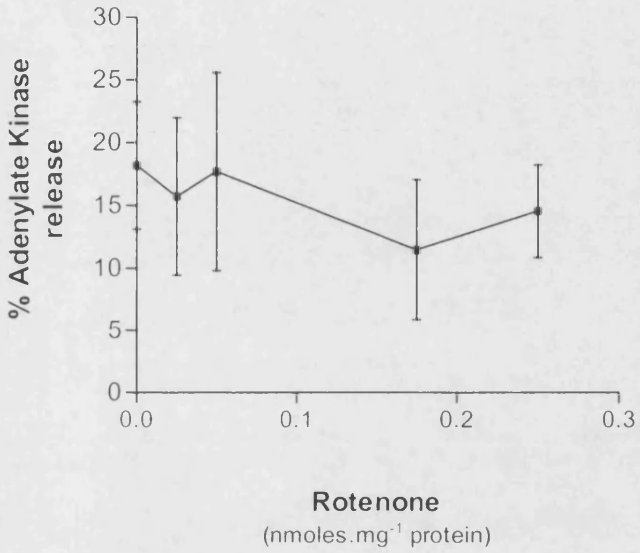

Figure 4.5

Effect of rotenone concentration on adenylate kinase release from synaptic brain mitochondria. Data is expressed as AK activity in supernatant as a percentage of total mitochondrial activity. Analysis of the regression shows that the slope is not significantly deviant from zero ($p > 0.05$).

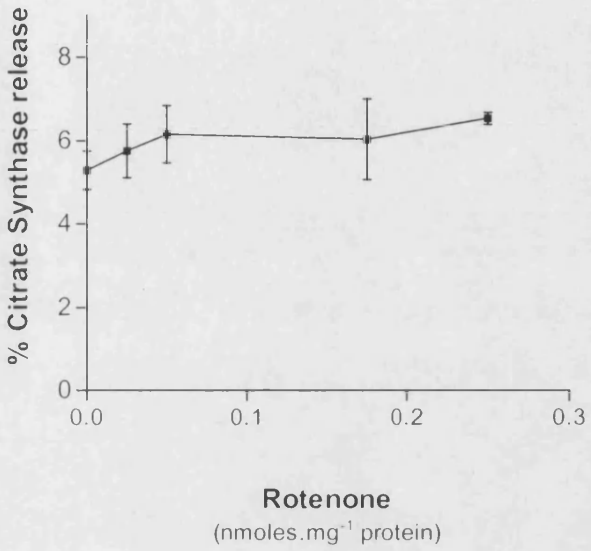

Figure 4.6

Effect of rotenone concentration on citrate synthase release from synaptic brain mitochondria. Data is expressed as CS activity in supernatant as a percentage of total mitochondrial activity. Analysis of the regression shows that the slope is not significantly deviant from zero ($p > 0.05$).

4.3.3 *The use of synaptic mitochondria*

At this point in the study, the findings on non-synaptic mitochondria versus synaptic mitochondria were compared. Aside from a difference in sensitivity to rotenone, the effects observed had not differed between the two populations. Due to the particularly poor yield of synaptic mitochondria considering the number of animals used (3.4.1.1), it was decided that from this point onwards, non-synaptic mitochondria only would be used for investigations.

4.3.4 *Inhibition of candidates for release mechanism*

Three different inhibitors were used in this investigation. The format of the experiment was however the same in each case. Four incubations were carried out on each preparation of mitochondria. They were as follows:

Incubation	Rotenone?	Inhibitor?
1	X	X
2	X	✓
3	✓	X
4	✓	✓

The incubation procedure is described in Incubation Scheme 2 (2.3.1.3). Mitochondria were allowed to incubate with the inhibitor for 10 minutes before treatment with rotenone.

Where either or both rotenone and inhibitor were not being added, the appropriate vehicle was added in their place.

Results were expressed as rotenone-induced CCR in the absence and presence of the particular inhibitor. Rotenone-induced CCR in the absence of inhibitor was calculated as measurement 3 minus measurement 1 above. Rotenone-induced CCR in the presence of inhibitor was measurement 4 minus measurement 2. Expressing the data in this way eliminated any effect of the particular inhibitor on the basal level of release seen without rotenone. The two calculated values were then compared using a paired t-test.

4.3.4.1 Cyclosporin A

Earlier it was observed that the respiratory inhibition-induced CCR was not accompanied by any mitochondrial volume changes. However, it has been suggested that MPT may cause CCR in a manner independent of volume changes (De Giorgi *et al*, 2002). Therefore it was desirable to further investigate whether MPT played a role by using the MPT inhibitor Cyclosporin A (CsA).

Non-synaptic mitochondria were isolated from whole rat brains (2.2.1.2). The protein concentrations were measured (2.7.1) and the mitochondria then incubated at 37°C in the electrode chamber according to Incubation Scheme 2 (2.3.1.3). The procedure described in 4.3.4 was carried out, using rotenone at 0.375 nmoles.mg^{-1} protein and CsA at 1μM. Ethanol vehicles were used in place of both rotenone and CsA where appropriate.

As can be seen in Figure 4.7, rotenone-induced CCR appears to be attenuated in the presence of 1μM CsA. However, the effect is not significant, as assessed by a paired t-test. This is likely to be due in part to the variability of the data. Hence no effect of CsA can be claimed.

Since MPT causes an inevitable dissipation of $\Delta\psi_m$, this parameter was also recorded during the CsA incubations. The TPP^+ electrode was used (2.3.1.2) between t = 15 and t = 18 minutes to record $\Delta\psi_m$ during all four incubations as defined in 4.3.4. The data are expressed in Table 4.3 as rotenone-induced dissipation of $\Delta\psi_m$ in the absence and presence of CsA (rotenone at 0.375 nmoles.mg^{-1} protein). The lack of significant difference indicates that the dissipation of $\Delta\psi_m$ induced by rotenone is not contributed to by any CsA-sensitive mechanism.

	[CsA] = 0	**[CsA] = 1μM**
Rotenone-induced $\Delta\psi_m$ (mV)	71.2 ± 12.9	74.7 ± 4.6

Table 4.3

Dissipation of $\Delta\psi_m$ (mV) induced by rotenone (0.375 nmoles.mg^{-1} protein) in the absence and presence of 1μM CsA. Where CsA was absent, ethanol vehicle was substituted. There was no significant difference between the values ($p > 0.05$, paired t-test). Values are mean ± S.E.M., n = 4.

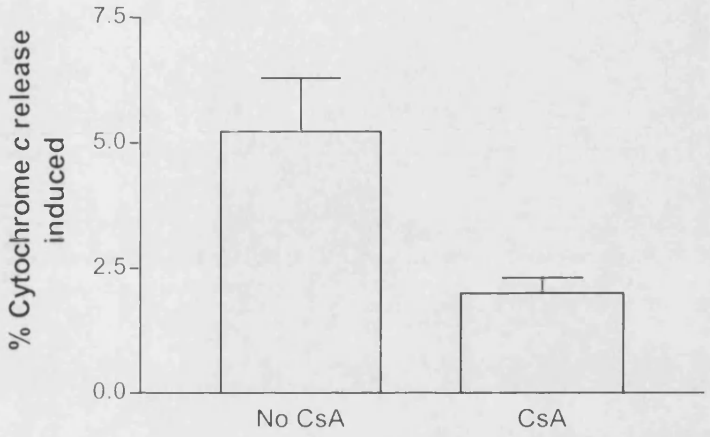

Figure 4.7

Effect of 1μM cyclosporin A on rotenone-induced CCR. Although CsA appears to attenuate the release, the effect is not significant as assessed by a paired t-test ($p > 0.05$). Data is mean ± S.E.M., n = 4.

4.3.4.2 Konig's Polyanion

As discussed in 4.1.1, the hypothesis that low levels of CCR need not induce apoptosis would be supported by demonstration of release via an OM channel. The VDAC is thought to be a major OM component of the PTP, but has also been strongly implicated in allowing swelling-independent release of cytochrome *c* (see 1.3.5.2). If the release described in 3.3.2 was indeed occurring via an OM channel or pore, it was likely that the VDAC could be involved. For this reason, the experimental procedure described in 4.3.4 was repeated using Konig's Polyanion (KPa). KPa is a 10kDa, 1:2:3 copolymer of methacrylate, maleate and styrene. By increasing the voltage dependence of VDAC more than five-fold, KPa blocks the channel (Colombini *et al*, 1987), and has been used previously to determine the role played by VDAC in CCR from isolated mitochondria (Brustovetsky *et al*, 2003b). The chemical is from an original and finite stock, synthesised by Tamas Konig (University of Maryland, USA). For the purpose of this study, it was generously donated by Professor Marco Colombini (University of Maryland, USA). KPa was used at $40\mu g.ml^{-1}$. A distilled water vehicle was used in place of KPa where appropriate.

The data are shown in Figure 4.8. Rotenone-induced CCR is significantly ($p < 0.05$) attenuated in the presence of KPa.

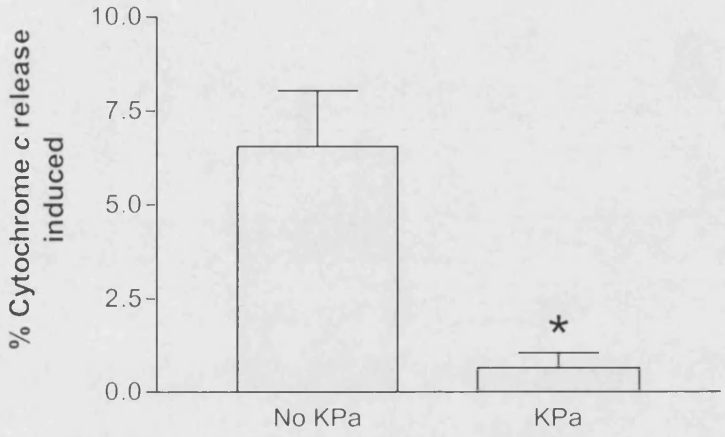

Figure 4.8

Effect of 40μg.ml^{-1} Konig's Polyanion on rotenone-induced CCR. Release is significantly attenuated in the presence of KPa (* represents $p < 0.05$). Data is mean ± S.E.M., n = 4.

4.3.4.3 Anti-Bak

As described (1.3.5.2), postulated OM channels which allow CCR nearly always incorporate pro-apoptotic Bcl-2 family members. In general, it is considered that anti-apoptotic members are localised to mitochondria and other membranes eg. endoplasmic reticulum and nuclear envelope (de Jong *et al*, 1994; Krajewski *et al*, 1993; Monaghan *et al*, 1992). The pro-apoptotic counterparts, in contrast, are thought to constitutively reside in the cytosol, and translocate to the mitochondria in response to a pro-apoptotic stimulus (Wolter *et al*, 1997). However, there are reports of a loose association of Bax with the OM, and detectable levels of Bax have been demonstrated in isolated rat liver mitochondria (Doran & Halestrap, 2000). Data obtained since this report has been contradictory (Polster *et al*, 2001; Brustovetsky *et al*, 2003b). In contrast, and inconsistent with the generalisation described above, Bak is considered to have constitutive localisation to the mitochondrial OM (Eskes *et al*, 2000). Demonstration of the presence of Bak in isolated rat brain mitochondria appears to be a repeatable result (Polster *et al*, 2001; Brustovetsky *et al*, 2003b).

Since this study demonstrated CCR from isolated brain mitochondria, the considerations above presented Bak as a possible candidate for the release mechanism.

Bearing these findings in mind, the inhibitor experiments described above (4.3.4) were carried out using polyclonal anti-Bak (G23, Santa Cruz Biotechnology Inc., CA, USA). The antibody was used at $20\mu g.mg^{-1}$ protein. A distilled water vehicle was used in place of anti-Bak where appropriate.

The data are shown in Figure 4.9. Rotenone-induced CCR was significantly attenuated in the presence of anti-Bak (20μg.mg^{-1} protein). This was assessed using a paired t-test ($p < 0.05$).

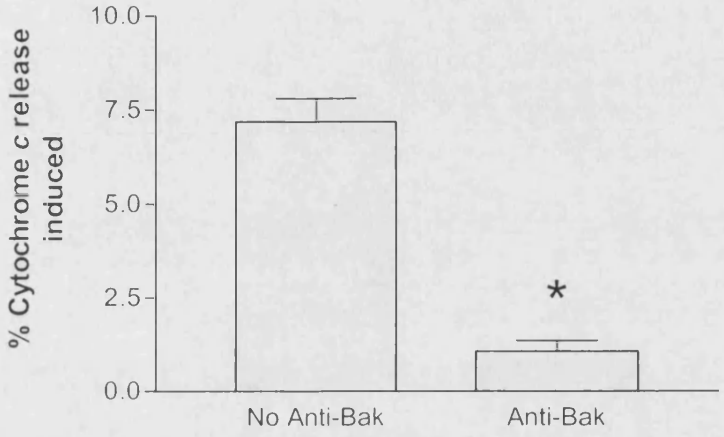

Figure 4.9

Effect of anti-Bak (20μg.mg^{-1} protein) on rotenone-induced CCR. Release is significantly attenuated in the presence of the antibody (* represents $p < 0.05$). Data is mean ± S.E.M., n = 4.

4.4 Discussion

4.4.1 *Release via a swelling-independent mechanism*

It has been demonstrated both quantitatively and qualitatively that the CCR induced by rotenone treatment is not associated with any significant change in mitochondrial volume. This was true of both non-synaptic and synaptic mitochondrial populations. This immediately rules out the 'swelling-dependent mechanisms' described in 1.3.5.1 as being responsible for CCR in this case. It could be claimed that, given the data from 3.3.2, the release was proportional to the extent of the insult because the heterogeneous population of mitochondria were undergoing MPT at different times, due to their varying susceptibility (Gogvadze *et al*, 2001). However, if this were the case, it would be apparent both on the electron microscope images (where the proportion of swollen mitochondria would increase with rotenone treatment) and in the light scattering measurements (where the average mitochondrial volume would increase with rotenone treatment).

Release of cytochrome *c* by means of MPT is generally considered to occur following non-specific OM rupture caused by matrix swelling. It can be argued that further downstream of this, the IM would also lose integrity by the same process, causing complete breakdown of the mitochondrion as a discrete organelle. If 'weaker' mitochondria in a heterogeneous population were to undergo this process, the loss in mitochondrial number would mask the swelling of less susceptible mitochondria during light scattering measurements.

Given the mild nature of the stimulus, and other data contradicting involvement of the MPT (4.3.1, 4.3.4.1), this would be an extremely unlikely explanation for the lack of swelling observed in this study. The possibility has been conclusively eliminated, however, by the CS data. CS is a matrix enzyme of 280kDa. It is therefore far too large to permeate via the PTP. However, if mitochondrial number were to decrease through complete IM breakdown, the CS concentration in the surrounding medium would increase. This was not the case, therefore the swelling data can be taken to truly indicate a lack of increased mitochondrial volume.

The fact that the rotenone-induced dissipation of $\Delta\psi_m$ had no CsA-sensitive component further supports the conclusion that MPT was not responsible for the observed CCR. If rotenone was inducing MPT, even in only a fraction of the mitochondria, then the rotenone-induced drop in $\Delta\psi_m$ would exhibit a certain extent of CsA-sensitivity.

In conclusion therefore, the results of this investigation are inconsistent with the release having occurred via non-specific rupture of the OM due to matrix swelling. Instead, it can be hypothesised that release is occurring via an OM channel.

4.4.2 *The nature of the OM release channel*

Assaying for AK is a particularly useful tool because the enzyme is localised to the IMS like cytochrome *c*. The fact that the distribution of AK was found, like that of CS, to be unaffected by rotenone treatment indicates that although CCR appears, by

default, to be released through an OM channel, this channel does not allow non-specific release of SIMPs. Either there is a size cut-off point between the two proteins in question, or the release channel is specific for cytochrome *c*. The size of AK has significance when compared to that of Smac, another IMS protein known to have pro-apoptotic properties (see 1.3.6.2). Smac is of almost identical size (23.7kDa) to AK (23.6kDa), and the AK data would imply that Smac might not be released along with cytochrome *c* in response to this rotenone treatment. This suggestion is to be strongly supported later by Western blotting (see Chapter 6). Bearing in mind the important (and possibly essential – Deshmukh *et al*, 2002) role of Smac in the induction of apoptosis in neurons, this finding is consistent with the hypothesis (3.5) that low levels of CCR, induced by respiratory deficiency, may be insufficient to induce apoptosis.

It should be noted that although respiratory inhibition did not induce release of CS or AK, there were basal levels of both enzymes present in the supernatant samples. This could be interpreted as an artefact of the incubations, as discussed for the control level of CCR (see 3.4.2.1). However, there is a notably higher level of AK (15-20% total mitochondrial content) than CS (5-7%) present. There is a cytosolic isoform of AK (Ruan *et al*, 2002), and this high basal activity in the supernatant could be due to cytosolic contamination of the mitochondrial preparation. However, validation of the preparations by means of LDH assay (2.7.2.2) suggested that this contamination was very low.

There is an alternative explanation which also has implications for the basal level of cytochrome *c* detected after control incubations. The variation in control rate of

release of different proteins may lie in their constitutive rates of turnover. It is suggested (Bachmair *et al*, 1986) that the N-terminal amino acid of a protein can give an indication of its physiological half-life. Using this theory, cytochrome *c* (methionine at N-terminal) is suggested to have an approximate $t_{½}$ of 30 hours, whereas AK (N-terminal alanine) is closer to 4 hours. These data are purely theoretical, but suggest that a relatively fast turnover rate for AK may help to explain the high background release.

The release mechanism therefore appeared to be specific for cytochrome *c*, or at least have a size cut-off which was smaller than other SIMPs which may contribute to a pro-apoptotic signal. Thus far, the findings are consistent with the hypothesis that low levels of CCR may not lead to apoptosis. The release mechanism was then further characterised in order to gain as much information as possible about whether the CCR was an isolated event in response to rotenone treatment.

Although CsA looks to impact CCR, the effect was not statistically significant. CsA is known to have numerous targets other than cyclophilin d (Capano *et al,* 2002; Kim *et al*, 2003; Sanchez *et al*, 2003; among others). However, the major alternative inhibitor is bonkrekic acid (which blocks MPT via the ANT), which was until recently difficult to obtain commercially. By far the majority of studies into MPT use CsA as an inhibitor, and it is notable that there appears to be very little concordance between studies on whether or not otherwise similar release mechanisms are CsA-sensitive. The lack of statistically significant effect of CsA on the CCR observed in this study support the conclusion that MPT is not the mechanism responsible.

However, a recent report claims to reconcile much of the discordance over the role of MPT in CCR (de Giorgi *et al*, 2002). The authors argue that if reversible openings of the PTP are triggered, the consequent dissipation of $\Delta\psi_m$ signals for Bax translocation to the mitochondria, and subsequent release of cytochrome *c* via Bax-mediated OM channels. Whilst this provides possible resolution to claims of CCR which is independent of swelling, but appears to be sensitive to CsA, it is inconsistent with the data from this study on two counts. Firstly, the presence of CsA had no effect on the amplitude of the $\Delta\psi_m$ after rotenone treatment (Table 4.3). If the mechanism proposed by De Giorgi and colleagues was responsible for release here, then rotenone would be inducing a dissipation of the $\Delta\psi_m$ via reversible openings of the PTP, which would be prevented by the addition of CsA. Secondly, if a reduction in $\Delta\psi_m$ was sufficient to trigger Bax translocation and channel formation, then CCR would have been observed in response to cyanide-induced respiratory inhibition (see chapter 5).

It seems most appropriate to conclude, therefore, that the release mechanism is not dependent on MPT. It is possible that a certain amount of sensitivity to CsA was conferred by other PTP components which may be involved in the release mechanism here, in a role independently of the rest of the PTP.

Such components were indeed confirmed to be involved by the use of KPa and anti-Bak. These inhibitors implicated the VDAC and Bak, since inhibition of the former and sequestration of the latter both significantly attenuated rotenone-induced CCR.

The study by Brustovetsky *et al* (2003b) promoted Bak to a primary role in regulating CCR from isolated brain mitochondria. Our data clearly demonstrated that inhibition

of Bak attenuated respiratory deficiency-induced CCR. Bak and Bax are very closely related proteins, sharing sequence homology of the BH1, BH2 and BH3 regions. The postulated role of Bax in associating with the VDAC to form a channel which is permeable to cytochrome *c* has been described (1.3.5.2). It is reported that Bak can induce the same effect (Shimizu *et al*, 1999). Combining the observed effect of anti-Bak with that of KPa in this study, an OM channel formed by the association of Bak and VDAC is strongly implicated.

These two channel-forming proteins are both postulated components of the PTP complex (see 1.3.5.1). However, arguments have been made against the involvement of MPT in the observed CCR. It can be hypothesised therefore that the channel is of the VDAC-Bax/Bak formation which is being increasingly accepted. Previous work on this channel complex may therefore be used to aid in the understanding of the effect which its opening might have on mitochondrial viability.

VDAC-Bax channels have been reconstituted in liposomes (Shimizu *et al* 2000). This intriguing study demonstrated that a VDAC-Bax channel is nearly continuously in an open state, in contrast to VDAC alone, which rapidly fluctuates between open and closed formations. The pore diameter of the combined channel also appears to be four times larger than that of VDAC alone, thus overcoming suggestions that VDAC in isolation has too narrow a pore diameter to permit passage of cytochrome *c* (Manella, 1998). The VDAC-Bax channel was seen to have a size limit for permeation of less than 50kDa. Without further clarification of the size cut-off point, this information is of limited use, since other pro-apoptotic proteins (Smac, 23.7kDa; Omi, 38kDa) are smaller than this limit (although AIF, at 67kDa, is larger).

However, studies which conclude CCR by means of a VDAC-Bax/Bak channel have claimed a lack of associated AK and Smac release (Brustovetsky *et al*, 2003b; Doran & Halestrap, 2000). This implies that the VDAC-Bax/Bak channel is either specific for cytochrome *c* or at least has a pore diameter too small to allow the release of other recognised pro-apoptotic SIMPs.

Although there are significant benefits in the use of isolated mitochondria for this study (see 3.1.3), the data concerning the role of Bak highlight the importance of considering whole cells. As discussed (4.3.4.3), Bak is thought to be constitutively localised to the mitochondrial OM, but the majority of other pro-apoptotic Bcl-2 proteins are considered cytosolic under control conditions. The discrepancy between two major studies (Brustovetsky *et al*, 2003b; Doran & Halestrap, 2000) in their findings on the presence of Bax in isolated mitochondria would be partly due to tissue heterogeneity, but may also be contributed to by a higher percentage cytosolic contamination of the preparation in the former study. Neither study provides LDH data to allow for accurate comparison of cytosolic contamination.

The LDH data used for validation of the isolated mitochondria preparations (2.7.2.2) demonstrated very low cytosolic contamination. It is likely, therefore, that in this case there was little contribution of cytosolic Bcl-2 proteins to the CCR mechanism. This demonstrates the only significant drawback of using isolated mitochondria for these experiments. The amplitude of the CCR event might be significantly altered if the experiment was carried out using whole cells, due to the added capacity for involvement of Bax, etc. There is no reason to suspect that CCR would no longer be proportional to complex I inhibition, but the gradient of the near-linear relationship

might be altered. This limitation of the isolated mitochondria model therefore necessitates further investigation in whole cells. This is to be carried out in Chapter 6.

4.5 Conclusion

Previously, the demonstration of a subtle, controlled release of cytochrome *c* in proportion to respiratory inhibition presented the hypothesis that a certain amount of CCR may be tolerated by the host cell. For this hypothesis to be upheld, it was essential that the release mechanism did not impose any insurmountable damage to the mitochondria.

This study has now demonstrated that the release mechanism does not involve the swelling and non-specific rupture of the OM that has been described to be associated with CCR in some situations (Brustovetsky *et al*, 2002; Petit *et al*, 1998; Scarlett & Murphy, 1997). Rather, the mechanism appears to be dependent on two OM channel forming proteins, VDAC and Bak. Whether the channel is a complex composing both proteins, or whether Bak induces a conformational change in VDAC which allows cytochrome *c* to permeate (Tsujimoto & Shimizu, 2000) is irresolvable at this stage. However, previous studies on the channel formed by the coordinate action of these two proteins would suggest that it may be specific for cytochrome *c* (Doran & Halestrap, 2000; Brustovetsky *et al*, 2003b). This eliminates a number of important pro-apoptotic signals, in the form of other SIMPs.

This investigation has supported the conclusion that, at the mitochondrial level, the cell will remain viable during partial CCR induced by respiratory inhibition. Concluding that this release is 'safe' however is subject to post-mitochondrial mechanisms 'buffering' low levels of CCR. This conclusion may only be drawn entirely if demonstrated in whole cells, since there is insufficient understanding of these control mechanisms to be able to model them in an isolated mitochondrial system.

CHAPTER 5

Determining the trigger for cytochrome *c* release from brain mitochondria

5.1 Introduction

5.1.1 *The 'bottom up' approach*

It is common for studies on CCR to utilise stimuli selected for their recognised ability to induce apoptosis, eg. Staurosporine (Bertrand *et al*, 1994) or microinjection of cytochrome *c* (Deshmukh *et al*, 2002; Li *et al*, 1997; Zhivotovsky *et al*, 1998), rather than their capacity to model an underlying pathology. By diminishing Complex I activity, this study has, in contrast, modelled the pathology to determine whether there is an effect on apoptotic signals. This 'bottom-up' approach is a more interesting strategy with respect to elucidating molecular mechanisms of disease pathology.

The data obtained by using this strategy have suggested that low levels of CCR occur in response to changes in flux through the ETC. It has been hypothesised, considering this result, that small amounts of CCR may be harmless to the host cell. This is because fluctuations in electron flux are a physiological occurrence and there is no basis for expecting them to induce apoptosis.

The respiratory inhibition induced CCR showed a good correlation ($p < 0.001$) with $\Delta\psi_m$ (see 3.8). Reduced amplitude of the $\Delta\psi_m$ is a plausible candidate for the physical manifestation of respiratory inhibition which regulates CCR. If $\Delta\psi_m$ were to directly regulate CCR in this model, this would support the hypothesis that low levels of CCR are a normal physiological occurrence, since fluctuations in $\Delta\psi_m$ are inevitable (Buckman & Reynolds, 2001).

5.1.2 *Dissipation of mitochondrial membrane potential.*

It has been suggested on many occasions that a reduction in the $\Delta\psi_m$ is an obligatory event in the apoptotic pathway, occurring upstream of CCR (Barbu *et al*, 2002; Zamzami *et al*, 1995; among others). This was consistent with the theory that MPT was the underlying release mechanism, since MPT is both triggered by, and inevitably causes, a dissipation of $\Delta\psi_m$.

However, the issue has since become hotly debated, with numerous reports concluding that a reduced $\Delta\psi_m$ is a consequence, rather than a cause, of the CCR event. Dissipation of $\Delta\psi_m$ which occurs secondary to CCR is suggested to be associated with opening of the PTP downstream of the initial caspase activation (Bossy-Wetzel *et al*, 1998), an event which may be involved in amplification of the initial pro-apoptotic signal (Marzo *et al*, 1998). Late dissipation of $\Delta\psi_m$ is also suggested by some to be the simple result of reduced flux through the ETC due to limiting cytochrome *c* concentrations after CCR (Madesh *et al*, 2002; Mootha *et al*, 2001).

It is therefore unclear as to whether the reduced $\Delta\psi_m$ induced by complex I inhibition (see Figure 3.3) would act as a trigger for CCR. Although dissipation of $\Delta\psi_m$ does not appear to be a prerequisite in all situations where cytochrome *c* is released, it may nonetheless be sufficient to induce it. Studies using uncouplers have attempted to resolve this issue, with mixed results (de Giorgi *et al*, 2003; Finucane *et al*, 1999; Niemenen *et al*, 1995).

The debate may be reconciled when considering the claim of Marzo *et al* (1998) that an initial partial drop in $\Delta\psi_m$ is sufficient to induce CCR and caspase activation. This protease activity then induces a secondary large amplitude dissipation of $\Delta\psi_m$. Bearing in mind the limited quantitative value of the fluorescent dye methods used by the majority of investigators, it is quite possible that a large proportion do not detect the initial partial change in potential. Considering this hypothesis, and the highly quantitative method used in this study for monitoring $\Delta\psi_m$, it appears possible that this parameter could be the link between Complex I inhibition and CCR.

5.1.3 *Inhibition of Complex IV*

In order to determine whether dissipation of $\Delta\psi_m$ is indeed sufficient to trigger CCR, a second series of titrations was carried out on isolated non-synaptic mitochondria. By titrating Complex IV activity using potassium cyanide (KCN), $\Delta\psi_m$ would be reduced, and the effect on the extent of CCR could be determined. By comparing the relationship between $\Delta\psi_m$ and CCR in the two titrations (complex I and IV), the role of $\Delta\psi_m$ in triggering CCR could be assessed.

Cyanide is a recognised potent inhibitor of Complex IV. As described in 1.1.2.4, the final step in the function of complex IV is the donation of an electron from the heme a_3/Cu_B complex to molecular oxygen to form water. Cyanide is thought to act by bridging the heme a_3-Cu_B bimetallic centre, with the result that electron transfer is arrested just prior to completion of the pathway (Gardner *et al*, 1996).

5.2 Aims

By repeating the titration of mitochondrial respiratory function by targeting complex IV rather than complex I, it was intended to investigate whether dissipation of $\Delta\psi_m$ provides the link between respiratory inhibition and CCR. This link would be supported if the correlation between $\Delta\psi_m$ and CCR was consistent between the two titrations.

This would either provide support or suggest modification of the hypothesis that CCR is a normal, physiological occurrence.

5.3 Results

5.3.1 *Titration of mitochondrial respiratory function using potassium cyanide*

Non-synaptic mitochondria were isolated from whole rat brains as described (2.2.1.2). The protein concentrations were measured (2.7.1) and the mitochondria then incubated at 37°C in the electrode chamber according to Incubation Scheme 1 (2.3.1.3). One incubation from each preparation served as a control (distilled water vehicle alone) and the remainder were subjected to a range of concentrations of KCN. Each titration was carried out in order of increasing KCN concentration.

It was established (based on Davey & Clark, 1996) that treatment with KCN in the range 0 – 400 nmoles.mg^{-1} protein caused inhibition of respiration in the order seen

by the rotenone treatment (3.3.1). Sufficient preparations were then performed to provide n = 4 for each KCN concentration.

As before, oxygen consumption rate and mitochondrial $\Delta\psi_m$ were recorded (2.3.1.1, 2.3.1.2) between t = 7 minutes and t = 10 minutes. At 10 minutes, an aliquot of 100µl was removed and frozen immediately in liquid nitrogen. A second aliquot of 400µl was removed and centrifuged at 17000x*g* for 5 minutes at 4°C. The supernatant was removed and frozen immediately in liquid nitrogen. Both were stored at -70°C until assays were performed. The former aliquot was assayed for Complex IV activity as described in 2.3.2.2. The latter was to be used for assay of cytochrome *c* concentration (see 5.3.2).

Complex IV activity was found to be reduced from 27.6 ± 1.2 $kmin^{-1}.mg^{-1}$ protein (mean of n = 4) to 9.7 ± 1.5 $kmin^{-1}.mg^{-1}$ protein (100% to 35.1%) by the range of KCN concentrations tested, as shown in Figure 5.1.

The corresponding oxygen consumption rates were inhibited from 97.5 ± 4.3 nmoles $O_2.min^{-1}.mg^{-1}$ to 10.3 ± 0.62 nmoles $O_2.min^{-1}.mg^{-1}$ (100% to 10.6%) as shown in Figure 5.2. $\Delta\psi_m$ was reduced from 175.1 ± 2.5 mV to 99.7 ± 3.5 mV (100% to 57.0%) as shown in Figure 5.3.

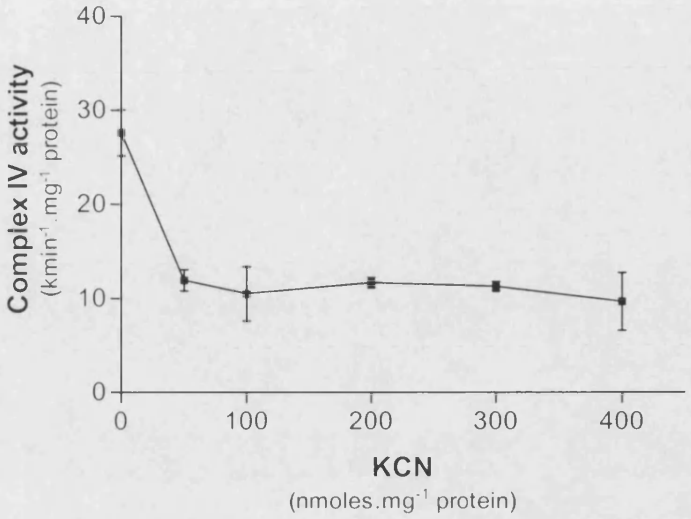

Figure 5.1

Concentration-dependent inhibition of non-synaptic mitochondrial Complex IV activity by potassium cyanide. n = 4 for each KCN concentration. Data shown ± S.E.M. The assay was carried out on mitochondria which had undergone three freeze-thaw cycles.

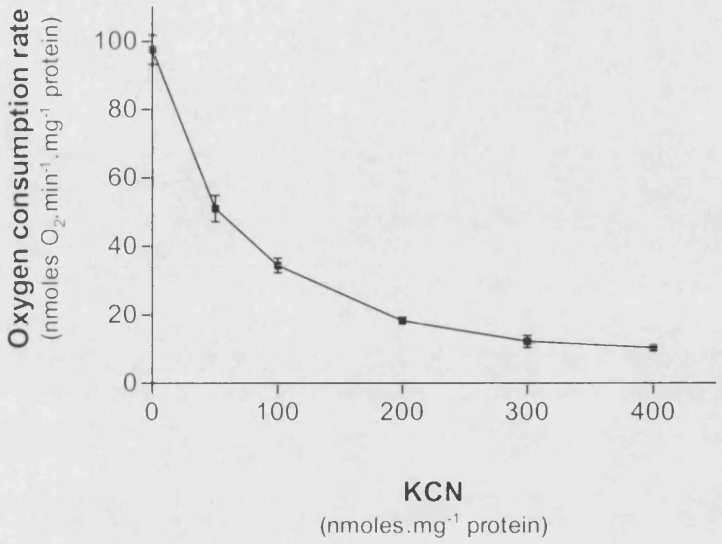

Figure 5.2

Concentration-dependent inhibition of non-synaptic mitochondrial state 3 oxygen consumption rate by potassium cyanide. n = 4 for each KCN concentration. Data shown ± S.E.M. Measurements were made *in situ* in the electrode chamber, in the presence of glutamate, malate and pyruvate as substrates.

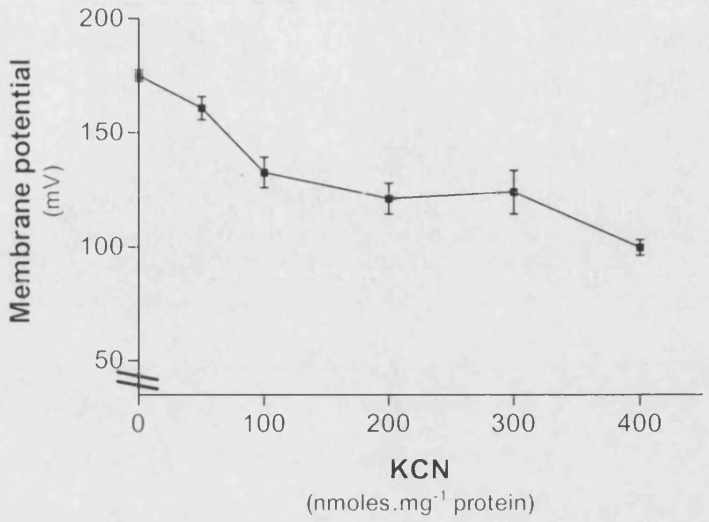

Figure 5.3

Concentration-dependent inhibition of non-synaptic mitochondrial state 3 $\Delta\psi_m$ by potassium cyanide. n = 4 for each KCN concentration. Data shown ± S.E.M. Measurements were made *in situ* in the electrode chamber, in the presence of glutamate, malate and pyruvate as substrates.

5.3.2 *Relationship between respiratory function and cytochrome c release*

Supernatants derived from the incubations described in 5.3.1 were assayed for cytochrome *c* concentration (2.4.1). The total mean cytochrome *c* content of isolated non-synaptic rat brain mitochondria had been determined as described earlier (3.3.2). Released cytochrome *c* was then expressed as a percentage of the total mitochondrial content.

Oxygen consumption rate and $\Delta\psi_m$ of the KCN-treated mitochondria were plotted against percentage CCR (see Figures 5.4 and 5.5). In both cases, respiratory inhibition did not appear to induce CCR. The regression did not show a significant deviation from zero slope in either case ($p > 0.05$). This is despite the extent of inhibition of these parameters being similar to that induced by rotenone (see figure 5.6).

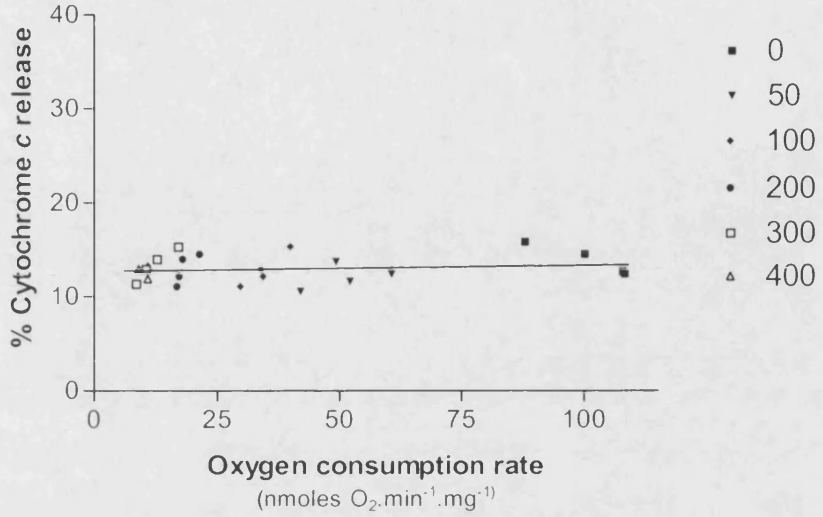

Figure 5.4

Relationship between oxygen consumption rate and percentage release of cytochrome *c* in non-synaptic mitochondria inihibited using potassium cyanide. Linear regression line has equation $y = 0.007x + 12.7$ and is not of significant deviation from zero slope ($p > 0.05$). Key indicates cyanide concentration (nmoles.mg^{-1} protein) used to achieve inhibition.

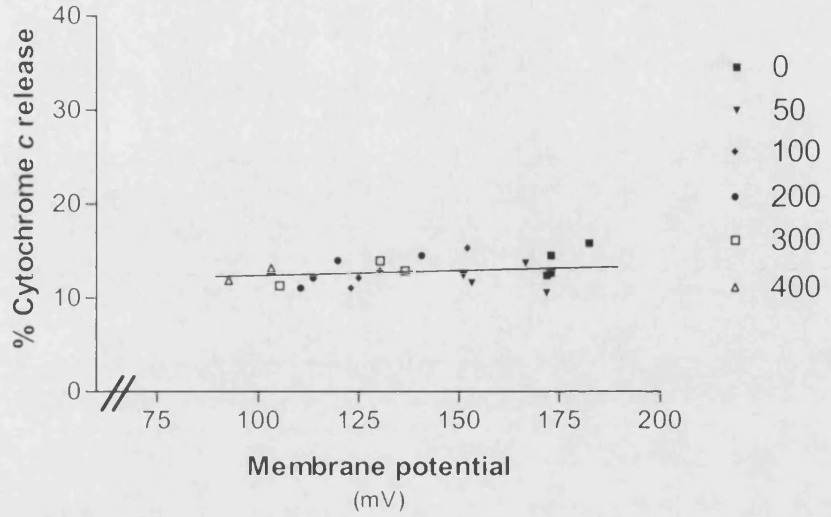

Figure 5.5

Relationship between $\Delta\psi_m$ and percentage release of cytochrome *c* in non-synaptic mitochondria inihibited using potassium cyanide. Linear regression line has equation $y = 0.02x + 10.4$. Although the regression line suggests a reverse relationship ($\Delta\psi_m$ and percentage CCR directly proportional), it does not have a significant deviation from zero slope ($p > 0.05$). Key indicates cyanide concentration (nmoles.mg^{-1} protein) used to achieve inhibition.

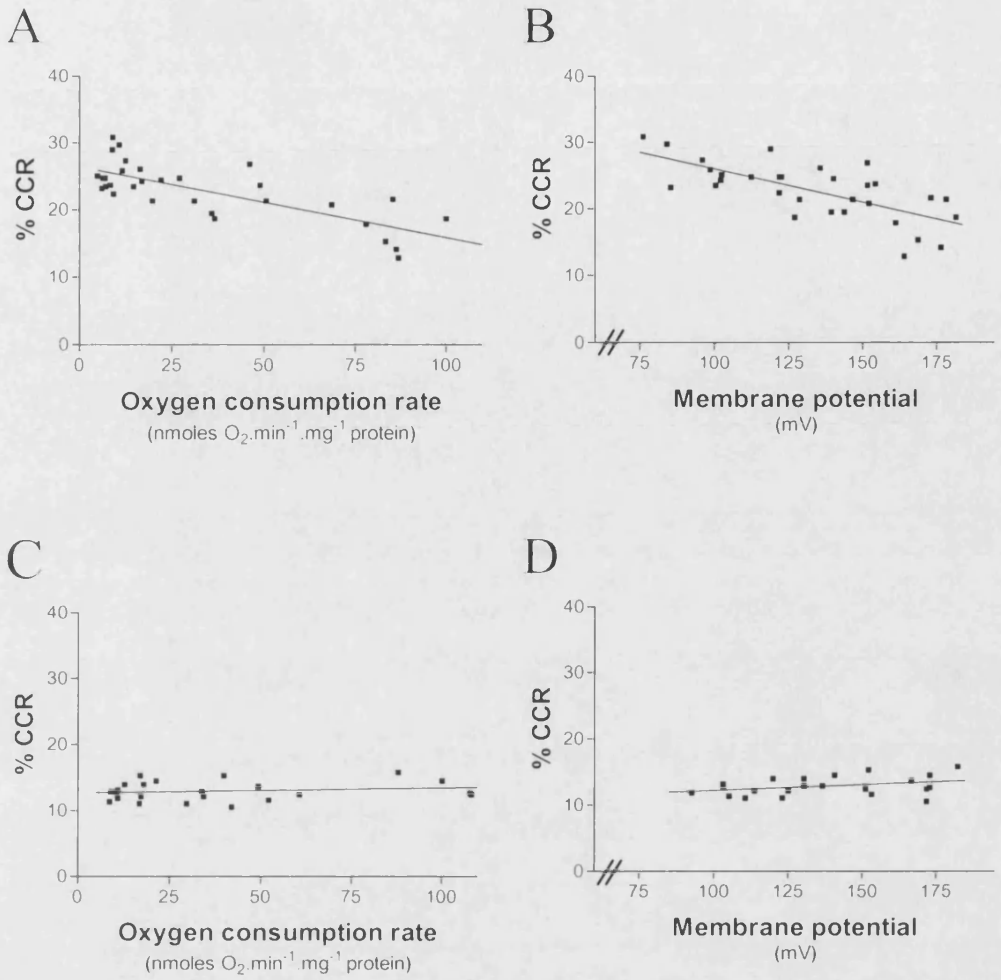

Figure 5.6

Collated data for rotenone and potassium cyanide-induced CCR. Ranges of oxygen consumption rate and $\Delta\psi_m$ are the same for both inhibitors. However, both oxygen consumption rate and $\Delta\psi_m$ display a significant inverse correlation with percentage CCR after rotenone treatment (**A** and **B** respectively), whereas inhibition of oxygen consumption rate and $\Delta\psi_m$ using KCN has no effect on CCR (**C** and **D** respectively).

5.3.3 *Rotenone-induced oxidative stress*

Reducing $\Delta\psi_m$ did not appear sufficient to induce CCR. It was hypothesised that the discrepancy between the effect of rotenone and cyanide on CCR could instead be explained by the synthesis of ROS. If superoxide was generated by the inhibition of Complex I, it would be rapidly converted to hydrogen peroxide by superoxide dismutase. H_2O_2 is then reduced by glutathione peroxidase, using reduced glutathione (γ-glutamylcysteinylglycine, GSH) as an electron donor. As a result, GSH is oxidised to GSSG (glutathione disulphide) (see 1.1.3). If this system were at work, the mitochondrial glutathione would be increasingly present in the oxidised rather than the reduced form. This would be detectable as a reduction in the GSH level, which can be measured by HPLC.

Non-synaptic mitochondria were isolated from whole rat brains as described (2.2.1.2). The protein concentrations were measured (2.7.1) and the mitochondria then incubated at 37°C in the electrode chamber according to Incubation Scheme 1 (2.3.1.3). The titration of Complex I activity described in 3.3.1 was repeated. A 100µl aliquot was taken at t = 10 minutes, and immediately acid extracted by adding to 0.5ml 15mM orthophosphoric acid. The mixture was vortexed and frozen immediately in liquid nitrogen. The samples were then stored at -70°C until GSH measurement.

GSH levels in the samples were measured by reverse-phase HPLC using electrochemical detection as described in 2.4.4.

The data are shown in Figure 5.7. Increasing the concentration of the rotenone treatment had no effect on the GSH content of isolated non-synaptic brain mitochondria, as assessed by linear regression across the whole range of rotenone concentrations used (insignificant deviation from zero slope, $p > 0.05$). However, observation of the data shown in Figure 5.7 suggested that the GSH levels measured following milder rotenone concentrations (notably 0.150 nmoles.mg^{-1} protein) might be higher than those following stronger treatment (0.225 nmoles.mg^{-1} protein). This was confirmed using an unpaired t-test ($p < 0.05$). There is therefore some indication that GSH levels are reduced by concentrations of rotenone which cause CCR. Rather than demonstrating a linear trend across the range, GSH levels appear to show a form of threshold effect.

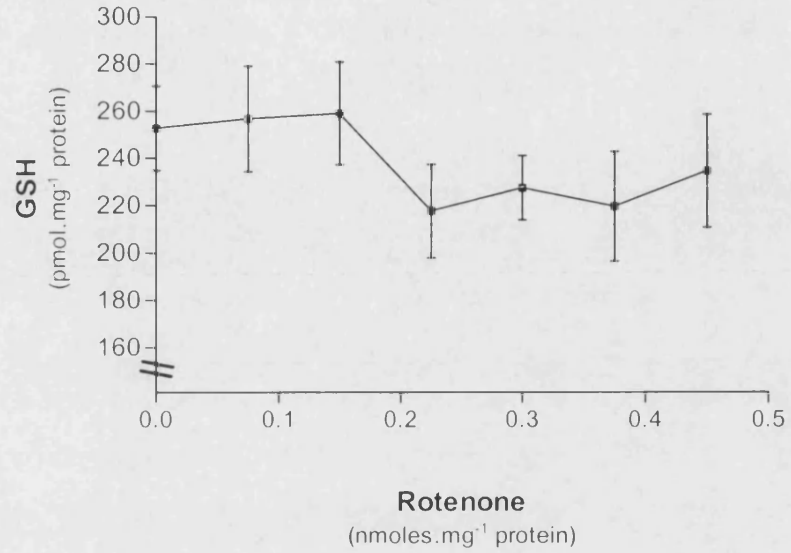

Figure 5.7

Effect of rotenone treatment on GSH content of isolated non-synaptic rat brain mitochondria. There is no linear trend across the range of rotenone concentrations tested, as assessed by linear regression. However, there is a significant difference between the GSH content of mitochondria treated with rotenone at 0.150 nmoles.mg^{-1} protein and that of mitochondria treated with rotenone at 0.225 nmoles.mg^{-1} protein ($p < 0.05$, unpaired t-test).

5.4 Discussion

5.4.1 *Titration of respiratory function by cyanide*

This part of the study was carried out using isolated non-synaptic rat brain mitochondria only, for the reasons discussed in 4.3.3. Basing the treatment conditions on Davey and Clark (1996), the mitochondria were treated with cyanide in the range 0 - 400 nmoles.mg^{-1}.

Increasing the concentration of the cyanide treatment resulted in a titration of mitochondrial oxygen consumption and $\Delta\psi_m$ as expected. However, the same anomaly identified following the rotenone titration (3.4.1.2) was observed in this case also. Complex IV activity appeared insensitive to cyanide concentration above 50 nmoles.mg^{-1} mitochondrial protein, although the inhibition was not complete. The flat profile of this region of the curve is inconsistent with the cyanide concentration-dependent inhibition of oxygen consumption rate and $\Delta\psi_m$ across the entire range. If this problem is an experimental error which results from freeze-thawing of the samples, as suggested in 3.4.1.2, the issue could be resolved in this case by *in situ* measurement of complex IV activity. This can be done by isolating complex IV from the rest of the ETC, using ascorbate and TMPD (N,N,N',N'-tetramethyl-*p*-phenylenediamine) as substrates and monitoring oxygen consumption rate.

5.4.2 *Lack of effect of cyanide on cytochrome c release*

Bearing in mind the marked effect of rotenone treatment on CCR from isolated non-synaptic brain mitochondria, it was surprising to observe that cyanide-induced respiratory inhibition caused no such effect. The relationship actually appeared very slightly reversed, ie. respiratory inhibition reduced CCR to below control levels. However, statistically, the regression line shows no significant deviation from zero, therefore it is concluded that there is no effect of cyanide treatment in this range on CCR.

The extent of release under control conditions was slightly lower (13.8 ± 0.8 % total mitochondrial cytochrome *c*) in this study than was observed during the rotenone titrations (17.3 ± 1.3 % total mitochondrial cytochrome *c*). This may indicate an effect of the presence of small amounts of ethanol in the rotenone titrations. If the ethanol was indeed responsible for some of the basal CCR, this highlights the importance of adding the appropriate vehicle in the control incubations.

5.4.3 *Rotenone versus cyanide treatment*

This observation clearly demonstrates that dissipation of $\Delta\psi_m$ caused by reduced flux through the ETC is not sufficient to induce CCR from isolated non-synaptic brain mitochondria.

Also affected by respiratory inhibition are the ATP levels. ATP is thought to induce a conformational change in cytochrome *c*, which alters its association with

cardiolipin, the IM 'anchor' (see 1.2.2.2) (Tuominen *et al*, 2001). Although ATP levels were not measured in this study, Davey and Clark (1996, 1998) demonstrated that ATP levels follow an almost identical pattern to oxygen consumption rate during inhibitor titrations of isolated brain mitochondria. It can therefore be concluded by inference that lower levels of ATP were not the trigger in this case for the release of cytochrome *c*.

Rather than such parameters which are affected in the same way by rotenone and cyanide, the CCR must be induced by some factor/factors which are affected differently by the two inhibitors. There are two main candidates:

5.4.3.1 Oxidative stress

The ETC is recognised as a major generator of ROS. Electrons which are leaked from the chain can associate with molecular oxygen to form superoxide. The presence of mitochondrial superoxide dismutase allows the superoxide to be quickly converted to hydrogen peroxide, which is then subject to reduction to water by the glutathione peroxidase system (see 1.1.3). Due to the rapid dismutation of superoxide, increased superoxide production is not likely to be detectable (Forman & Azzi, 1997). However, changes in the oxidation state of glutathione can be detected as described (5.3.3), indicating an upstream alteration in superoxide levels.

Measurement of GSH levels by reverse phase HPLC initially suggested that there was no significant effect of rotenone treatement on the GSH concentration in isolated non-synaptic rat brain mitochondria. This was due to analysis of the regression line, which displayed no significant deviation from zero slope. However, observation of

the data suggested a reduction in GSH levels when the rotenone concentration is raised to 0.225 nmoles.mg^{-1} protein. Indeed, when assessed using an unpaired t-test, mitochondria treated with rotenone of 0.150 nmoles.mg^{-1} protein contained significantly more ($p < 0.05$) GSH than those treated with rotenone of 0.225 nmoles.mg^{-1} protein. The reason for this apparent threshold effect is unclear, and there is no correlating jump in the cytochrome *c* data at this point.

Therefore, despite the lack of linear trend between the concentration of rotenone used for treatment and GSH content of the mitochondria, there is some indication that rotenone can cause a reduction in GSH levels. This is consistent with the hypothesis that Complex I inhibition via rotenone is causing increased superoxide production, and that this may be the factor causing the increased CCR.

There has been considerable investigation into the generation of ROS by the ETC, particularly with respect to which complexes are primarily responsible. A number of studies have highlighted complexes I and III as the most important sites of superoxide production (Turrens *et al*, 1985; Turrens & Boveris, 1980), but it is complex I which is emerging as the most physiologically and pathologically relevant site (Liu *et al*, 2002; among others). This theory is consistent with the hypothesis that a discrepancy in ROS generation in response to rotenone versus cyanide treatment may underlie the differing effects on CCR.

A recent report on ETC-mediated ROS generation has particularly interesting implications for the interpretation of these data. Sipos and colleagues (2003) titrated the activities of complexes I, III and IV in a manner similar to that used in this study,

although using synaptosomes rather than isolated mitochondria. The authors determined by monitoring superoxide and hydrogen peroxide levels that complexes III and IV demonstrated a threshold effect for ROS production. This effect was similar to that described in Davey and Clark (1996) and Davey *et al* (1998) with respect to changes in respiration rate and ATP synthesis. Notably, cyanide treatment was found not to induce ROS generation until complex IV was inhibited by more than 70%. In this study, the maximum cyanide treatment used only inhibited complex IV activity to approximately 35% of the control level. Although the study by Sipos *et al* (2003) was carried out using synaptosomes, and the differences between mitochondria from synaptic and non-synaptic origin are recognised, it might be expected that the extent of inhibition afforded by cyanide in this study was sub-threshold with respect to ROS generation.

The findings of Sipos *et al* (2003) with respect to complex I inhibition by rotenone are even more interesting. Unlike complexes III and IV, complex I did not exhibit a threshold effect for ROS generation. Rotenone treatment caused proportional amounts of superoxide and hydrogen peroxide production from very low levels of inhibition. The extent of ROS generation was however very small when compared to that measured after super-threshold inhibition of complexes III or IV. This effect is remarkably similar to the profile of rotenone-induced CCR demonstrated in this study.

It would appear likely, therefore, that the CCR induced by mild rotenone treatment is mediated at least in part by a corresponding dose-dependent increase in superoxide generation. The inability of cyanide to induce CCR might be explained by the

threshold effect described by Sipos *et al* (2003). The extent of inhibition of complex IV was probably insufficient to induce ROS generation. However, if the inhibition were to be increased to exceed the threshold, the large amplitude ROS generation described by Sipos *et al* (2003) would be predicted to induce a sudden and extensive cytochrome *c* translocation.

It is possible that generation of ROS proportional to the extent of Complex I inhibition may explain the effect of rotenone on GSH levels, as observed in 5.3.3 Small amounts of superoxide could be 'dealt with' by the GSH system. However, if superoxide was increasingly generated as the concentration of the rotenone treatment increased, at a certain threshold level, the GSH system would be overwhelmed and GSH levels would start to decline without being replenished by glutathione reductase. This would explain the 'lag' effect observed in Figure 5.7, as low levels of oxidative stress can be effectively buffered by anti-oxidant mechanisms (reminiscent of the hypothesis concerning cytochrome *c*). Only once the limited capacity of the GSH regeneration system is exceeded do the GSH levels begin to decline. This is in contrast to the near-linear profile of induced CCR with rotenone treatment, and therefore implies that the release may not be induced purely by increased oxidative stress, but perhaps by a number of coordinate signals.

Despite claims that the transient nature of superoxide makes it less amenable to measurement than downstream indicators of oxidative stress (eg. hydrogen peroxide, change in GSH levels), the study by Sipos *et al*, among others (Liu *et al*, 2002) have demonstrated that it is possible to reliably measure superoxide. Interpretation of the GSH data relies on certain assumptions, eg. mitochondrial SOD present in excess. A

more direct measurement of ROS production eg. assay for aconitase activity (Hausladen & Fridovich, 1996), might provide more informative data in this study.

Oxidative stress is recognised as a trigger for activation of the MPT (reviewed by Kowaltowski *et al*, 2001). However, superoxide has also been linked with CCR by means of the VDAC (Madesh & Hajnóczky, 2001). This study used a human cell line rather than primary tissue, and demonstrated a number of difference results from this study (namely lack of involvement of Bax (see 4.3.4.3) and the concurrent release of Smac (see 6.3.1)). However, the report highlights the potential for an MPT-independent, VDAC-mediated release mechanism to be affected by an increased superoxide concentration.

As described (1.1.3), it has been suggested that if generated at complex I, superoxide is released on the matrix side of the IM (St-Pierre *et al*, 2002). Therefore if it is true that superoxide has a role in mediating CCR, there must be a mechanism for its translocation from the matrix across the IM to reach the OM release apparatus. An 'inner membrane anion channel' (IMAC) has been described (Beavis, 1992) and appears to be capable of allowing such translocation of superoxide (Aon *et al*, 2003).

It is interesting to consider the claim of Korshunov *et al* (1999) that low levels of cytochrome *c* external to the mitochondria are capable of inhibiting hydrogen peroxide generation by complex I. As discussed (3.4.2.2), low amplitude CCR could serve as a defensive anti-oxidant system. This role of cytochrome *c* therefore supports ETC-mediated ROS generation as a trigger for CCR.

It is believed that 1-3% of the total oxygen consumed at the ETC is converted to ROS due to electron leak (Boveris *et al*, 1972). If CCR is induced in proportion to mitochondrial ROS generation, this lends further support to the hypothesis that low levels of CCR can be tolerated and do not in all cases lead to apoptosis.

5.4.3.2 Redox status of cytochrome c

As described, there is a good case for the involvement of ROS in rotenone-induced CCR. However, there is also a more fundamental difference between rotenone and cyanide treated mitochondria which is implied by the basic features of the ETC. Rotenone prevents electron transfer at the stage of reduction of free ubiquinone. Therefore in the course of the rotenone titration, the redox components of the ETC which are downstream of the rotenone-sensitive site, including cytochrome *c* will be increasingly in the oxidised state. In contrast, cyanide halts electron transfer at the final stage of the ETC, where electrons are donated to molecular oxygen. In this case, redox components of the ETC which are upstream of the cyanide-sensitive site, including cytochrome *c* will be increasingly reduced during the course of the cyanide titration.

Is there a case for an increase in the ferri:ferrocytochrome *c* ratio causing an increase in the amount of cytochrome *c* which is released? The cytochrome *c* immunoassay kit manufacturers (R&D Systems, Abingdon, UK) are unaware of any reason that the assay should differ in its sensitivity for ferri and ferrocytochrome *c* (personal communication). Therefore the data described in 5.3.2 would be consistent with a CCR mechanism which only permitted release of ferricytochrome *c*.

It is understood that cytochrome *c* undergoes a conformational change on transition between redox states (Bret *et al*, 2002; Calvert *et al*, 1997). It is conceivable that such a change could alter the extent to which cytochrome *c* is associated with the IM via cardiolipin (see 1.2.2.2). There has been suggestion that electrostatic associations of cytochrome *c* with the IM could be important in regulating its release (Ott *et al*, 2002). It has also been reported that ferricytochrome *c* is generally more mobile than ferrocytochrome *c* (Bartalesi *et al*, 2003). Ferricytochrome *c* is also thought to be subject to larger volume fluctuations than ferrocytochrome *c* (Eden *et al*, 1982). Effects on the redox state of cytochrome *c* could therefore influence the potential for CCR. In addition, from a functional point of view, an increasing ferri:ferrocytochrome *c* ratio would be indicative of reduced work load on the ETC. It is possible that more cytochrome *c* would be released to the cytosol for degradation as an adaptive mechanism if a particular mitochondrion was less metabolically active.

It would be extremely interesting to investigate the relative apoptosis-inducing properties of ferri and ferrocytochrome *c*, perhaps using an *in vitro* caspase activation assay. However, similar approaches have so far yielded contrasting results (Hampton *et al*, 1998; Pan *et al*, 1999).

5.4.4 *Implications of the lack of effect of cyanide on cytochrome c release*

This study has demonstrated that although a controlled, dose-dependent increase in CCR is induced by rotenone, no such effect is observed in reponse to cyanide treatment. From the report by Sipos *et al* (2003), it can be hypothesised that a sudden increase in CCR may be induced by cyanide once the threshold for ROS generation is

reached. This possibility has important implications for the physiological regulation of mitochondrial respiration.

It has been put forward that the inhibition of complex IV by nitric oxide may serve as a physiological mechanism for regulating the rate of respiration. Nanomolar concentrations of NO reversibly inhibit complex IV (Brown & Cooper, 1994; Stewart *et al*, 2000). Since the inhibition is of a competitive nature with oxygen, it has been suggested that NO may act as a physiological regulator of the sensitivity of the respiratory chain to oxygen (Brown, 1995).

The data from this study would suggest that such a form of regulation would be unlikely to lead to any CCR from the mitochondria. This is consistent with the concept of complex IV inhibition as a physiological mechanism. In contrast, physiological concentrations of NO do not appear to affect complex I activity (Bolanos *et al*, 1994). The data from this study, describing CCR proportional to complex I inhibition, are consistent with mild complex I depletion as an early pathological rather than physiological event.

5.5 Conclusions

In this investigation, it was determined that CCR is not induced purely by reduced flux through the ETC and therefore reduced $\Delta\psi_m$. The release has been dissociated from these measurable parameters via a cyanide-induced titration of respiratory function.

The literature and, to a certain extent, data obtained in this study concerning mitochondrial GSH status, suggest that this discrepancy is mediated by the extent of oxidative stress imposed by the two inhibitors. It is likely that rotenone induces superoxide generation in a dose-dependent manner, which would then be expected to cause CCR. Cyanide is unlikely to be causing the same increase in ROS synthesis, indeed perhaps none at all, as suggested by Sipos *et al* (2003).

It is also possible that the release process may be affected by the redox state of the mitochondrial cytochrome *c*, although this study has not provided evidence for this hypothesis.

The discrepancy between the effects of complex I and complex IV inhibition with respect to CCR are consistent with the theory that modulation of complex IV activity (by NO) is a physiological process. No such role for complex I has yet been described. This consideration leads to a slight modification of the hypothesis arising from this study. Rather than suggesting that low levels of CCR are a normal, physiological event arising from any fluctuation in respiratory activity, it may be preferable to conclude that the event is indeed a pathological pro-apoptotic signal. It most likely results from increased levels of ROS generation. However, in very mild disease states where the CCR is at a low level, the signal is subject to buffering in the cytosol by IAPs, HSPs, GSH etc. Only once these other protective mechanisms are compromised (for example by increasing oxidative stress) or if the CCR rises to a level above that which can be overcome by these systems, will apoptosis begin to implement the neurodegenerative process.

CHAPTER 6

Does cytochrome *c* release necessarily induce apoptosis?

6.1 Introduction

6.1.1 *Progression from isolated brain mitochondria to cultured neurons*

It has been shown that very mild inhibition of complex I can induce a proportional amount of CCR from isolated brain mitochondria. This effect is not seen following complex IV inhibition, and it is suggested that the release induced by complex I inhibition is primarily mediated by ROS generation at this site. The release appears to occur via an OM channel and therefore the mitochondria probably remain energetically viable. The data imply that CCR induced in this manner is a pro-apoptotic signal which, instead of being of an all-or-none nature, is subtly representative of the level of stress (perhaps oxidative stress). It is hypothesised that low amplitude CCR need not lead to apoptosis.

All of the data thus far originate from studies on isolated brain mitochondria. The reasons for using these organelles in isolation were explained in (3.1.3). This choice has yielded observations which may have simply been undetectable in whole cells. However, if the hypothesis that low levels of CCR can occur in response to respiratory inhibition without apoptosis proceeding is to be proven fully, it is necessary to demonstrate that it is the case in whole cells. Uncertainty regarding the fate of released cytochrome *c* in the cytosol is a hindrance in detecting changes experimentally. Nonetheless the cytosolic effects on cytochrome *c* are crucially important in the interpretation of the results. The post-mitochondrial regulation events which occur in the cytosol determine whether or not apoptosis is allowed.

6.1.2 *Post-mitochondrial control mechanisms*

As has been alluded to several times, there are a number of reasons that released cytochrome *c* may not induce apoptosis:

6.1.2.1 Insufficient release

The cytosolic IAPs (Crook *et al*, 1993; Holcik *et al*, 2001), the chaperone Hsps (Pandey *et al*, 2000; Saleh *et al*, 2000), physiological concentrations of K^+ (Cain *et al*, 2001) and perhaps other, as yet unrecognised mechanisms, act to prevent 'inappropriate' apoptosis. This implies that purely the amplitude of the cytochrome *c* signal determines whether or not it overcomes the regulatory mechanisms. Murphy *et al* (2003) have provided an interesting demonstration of the importance of the amplitude of the cytochrome *c* signal. It appears that in human neutrophils, which contain significantly less cytochrome *c* than other cells (and are largely incapable of mitochondrial respiration), the apoptotic pathway is adapted to exhibit dramatically reduced requirements for the protein in the formation of the apoptosome.

6.1.2.2 Solitary release

It has been reported on numerous occasions that microinjection of cytochrome *c* into cell cytosol is sufficient to induce apoptosis (Li *et al*, 1997; Zhivotovsky *et al*, 1998; among others). However, it was noted that NGF-maintained sympathetic neurons are remarkably resistant to this insult (Neame *et al*, 1998). This observation has been taken further by Deshmukh *et al* (2002), who claim that in primary neurons, CCR is insufficient as an isolated event to induce apoptosis. The authors state that the cell only develops 'competence to die' when the pro-apoptotic protein Smac is present in

the cytosol along with cytochrome *c*. It is implied that if CCR occurs by a mechanism which does not also cause Smac release, the cell is safe from apoptosis. Since these conclusions were drawn from a study involving microinjection of the pro-apoptotic proteins, it is unlikely that an explanation of insufficient cytochrome *c* to overcome the IAP defence is valid.

6.1.2.3 Redox state of cytochrome c

As mentioned previously (1.3.6.5, 5.4.3.2), it has been suggested that the redox state of cytochrome *c* determines whether or not it will cause apoptosis to proceed. Hancock *et al* (2001) suggest that cytochrome *c* acts in a pro-apoptotic manner only when in the ferri (Fe^{3+}) form. Unless the GSH status is compromised, for example by increased ROS generation, GSH will serve to keep cytochrome *c* in a reduced, and therefore 'safe' state.

6.2 Aims

Due to particular interest in the claim of Deshmukh *et al* (2002) regarding the requirement for Smac release for apoptosis in cultured neurons, further experiments were carried out on isolated non-synaptic rat brain mitochondria to determine whether rotenone treatment caused Smac release in addition to CCR.

Crucial experiments were then carried out on primary cortical neurons to determine whether rotenone treatment could induce detectable CCR which was insufficient to induce apoptosis.

6.3 Results

6.3.1 *The effect of rotenone treatment on Smac and AIF release*

It was decided to investigate the release of AIF (1.3.3) alongside Smac, since release of the former would induce death via a caspase-independent pathway, and so dramatically change the interpretation of the data thus far.

Non-synaptic mitochondria were isolated from whole rat brains (2.2.1.2). The protein concentrations were measured (2.7.1) and the mitochondria then incubated at 37°C in the electrode chamber according to Incubation Scheme 1 (2.3.1.3). Titrations were carried out as in 3.3.1, using the same range of rotenone concentrations. However, two additional incubations were made for the purpose of this experiment. Prior to the rotenone titration, mitochondria ($0.5mg.ml^{-1}$) were incubated according to Incubation Scheme 3 (2.3.1.3). The second additional incubation was made after the final rotenone titration was complete. This was carried out according to Incubation Scheme 1 (2.3.1.3), using alamethicin ($75\mu g.mg^{-1}$ protein) in place of rotenone, as a positive control for membrane rupture, as described in 4.3.1.1.

No recordings of oxygen consumption rate or $\Delta\psi_m$ were made, but a 400µl aliquot was removed after each incubation and centrifuged at 17000x*g* for 5 minutes at 4°C. The supernatant was frozen immediately in liquid nitrogen and then stored at -70°C. Preparations were repeated to obtain n = 3 for each rotenone concentration. Any remaining untreated mitochondria after each titration were centrifuged at 17000x*g* for 5 minutes at 4°C, and the supernatants removed. The mitochondrial pellet was then

also stored at -70°C, to be used as a positive control when blotting for the released proteins.

The supernatant samples were thawed and loaded onto a Tris-HCl pre-cast 12.5% gel (Bio-Rad, Bucks., UK) as described (2.4.5.1). The mitochondrial pellet sample was resuspended in lysis buffer, and stored on ice for 10 minutes with regular shaking. The sample was then centrifuged at 17000x*g* for 1 minute at 4°C, and the supernatant loaded onto the gel also.

Once the gels had been run and transferred (2.4.5.1, 2.4.5.2), the membranes were probed for Smac and AIF (using V-17 anti-smac and D-20 anti-AIF, Santa Cruz Biotenhnology Inc., respectively) (2.4.5.3). Typical blots (from n = 3) for each of the two proteins can be seen in Figure 6.1a and 6.1b. Figure 6.1a. demonstrates the effect of rotenone treatment on AIF release. There is a very strong signal (somewhat difficult to resolve) resulting from the whole mitochondrial pellet and a clear band from the supernatant of alamethicin treated mitochondria. There is a very faint band arising from the control incubation (mitochondria in 37°C buffer with BSA) and this is unchanged throughout the rotenone titration.

Figure 6.1b demonstrates the effect of rotenone treatment on Smac release. The positive control (whole mitochondrial pellet) yielded a faint band, but no other treatments caused any detectable Smac signal. The background from the Smac blots was more variable than for the AIF blots, due to the longer exposure time required to visualise the positive controls.

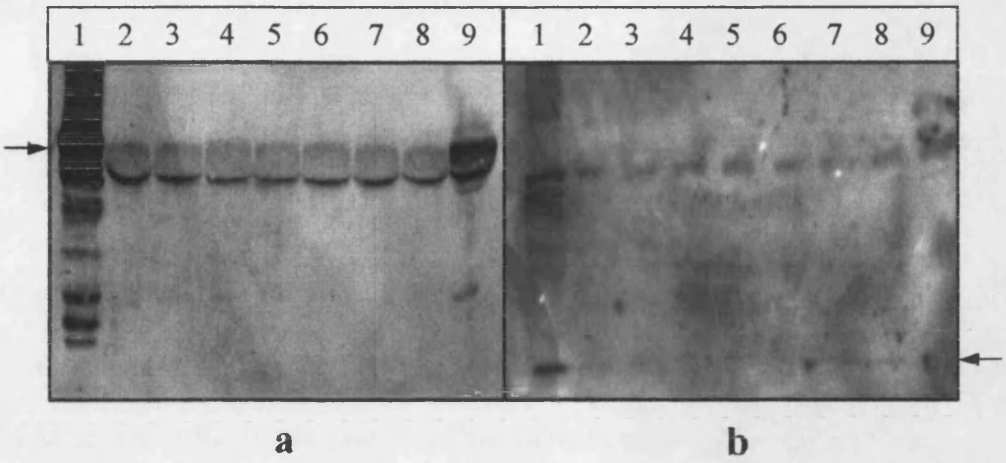

Figures 6.1a and b

Western blots demonstrating the release of AIF (**a**) and Smac (**b**) from isolated non-synaptic rat brain mitochondria. In **a**, arrow marks 67kDa, in **b**, arrow marks 24kDa. Lane numbers indicate the following treatments:

Lane	Sample type	Incubation Scheme	Rotenone (nmoles.mg^{-1} protein)	Alamethicin (µg.mg^{-1} protein)
1	Lysed mitochondria (30µg)	N/A	N/A	N/A
2	Supernatant (15µl)	3	0	0
3	Supernatant (15µl)	1	0	0
4	Supernatant (15µl)	1	0.075	0
5	Supernatant (15µl)	1	0.150	0
6	Supernatant (15µl)	1	0.225	0
7	Supernatant (15µl)	1	0.300	0
8	Supernatant (15µl)	1	0.375	0
9	Supernatant (15µl)	1	0	75

6.3.2 *Treatment of primary cortical neurons with rotenone*

Primary cortical neurons were grown in culture as described in 2.2.2.1. At day 6, they were treated using neuronal medium containing ethanol vehicle or sterile rotenone. Experiments were carried out to determine the range of rotenone concentrations required for titration. A maximum concentration was sought which would be just sufficient to cause an observable deterioration of viability (as assessed by phase contrast light microscopy). Each preparation yielded approximately 20-30 million neurons, and 8 million cells were to be required for each rotenone concentration in the experiments to follow (see 6.3.2.1 and 6.3.2.2). Therefore, the 'titration' would consist only of one control and two rotenone treatments. The treatment conditions selected from the preliminary experiments were 0nM (ie. control, ethanol vehicle alone), 10nM and 20nM rotenone. The treatment was applied for 24 hours.

Phase contrast light microscope images of neurons following these treatments are shown in Figures 6.2a, 6.2b and 6.2c. There is no observable difference between the morphology of control treated neurons and those subjected to 10nM rotenone. However, the cells treated with 20nM rotenone are beginning to show marked deterioration of their connections and the density of viable cell bodies is reduced.

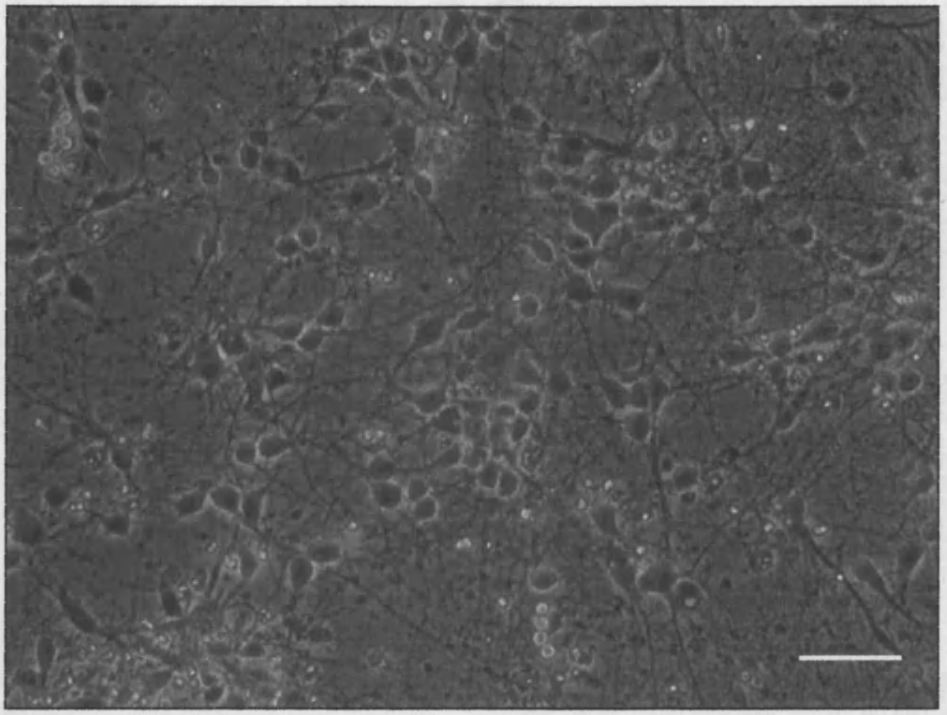

Figure 6.2a

Primary cortical neurons following 24 hours treatment with ethanol vehicle alone. Phase contrast light microscope image at X20 objective, scale bar represents 40μm.

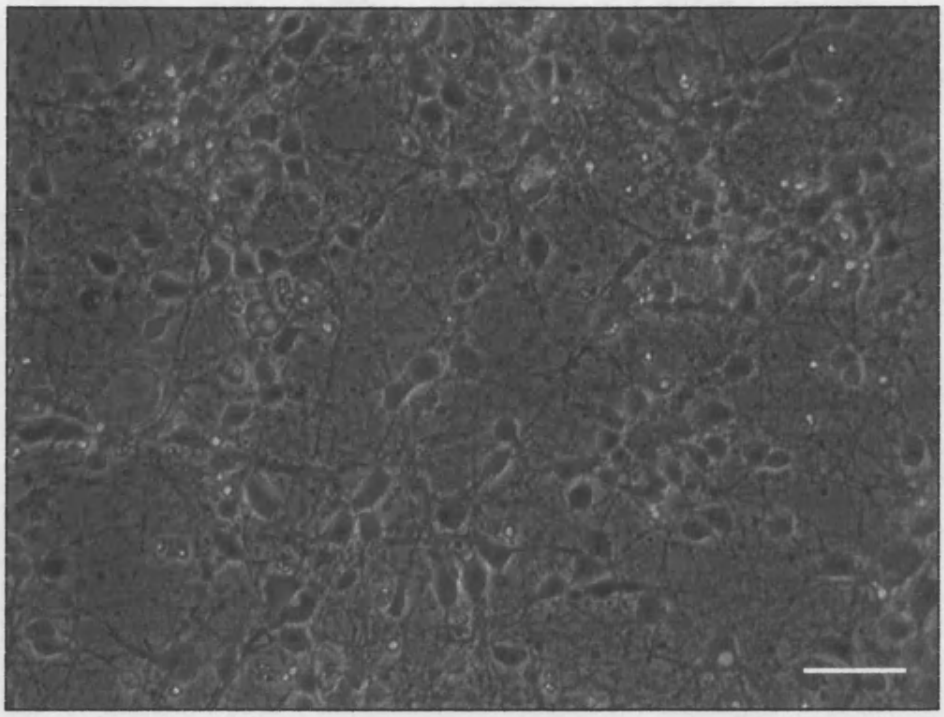

Figure 6.2b

Primary cortical neurons following 24 hours of treatment with 10nM rotenone. The cells demonstrate no observable difference in morphology from control neurons (See Figure 6.2a). Phase contrast light microscope image taken at X20 objective, scale bar represents 40μm.

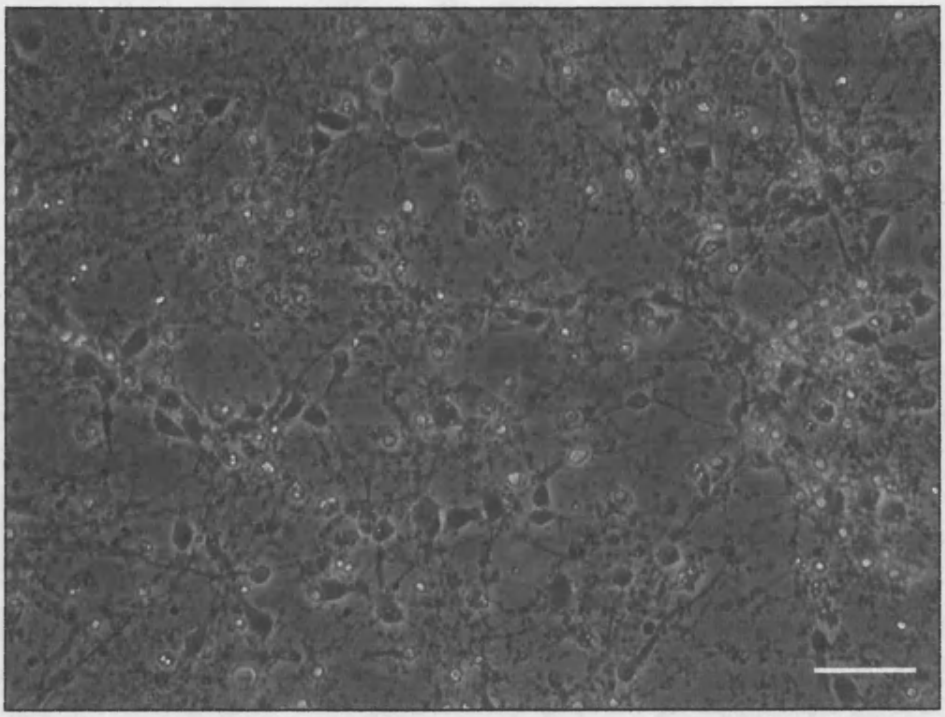

Figure 6.2c

Primary cortical neurons following 24 hours of treatment with 20nM rotenone. The connections between the cells have visibly deteriorated, and there are less cell bodies apparent than control neurons (see Figure 6.2a) or those which have been treated with 10nM rotenone (see Figure 6.2b). Phase contrast light microscope image taken at X20 objective, scale bar represents 40μm.

6.3.2.1 Induction of caspase-9 activity by rotenone

Having established 0, 10 and 20nM rotenone as the treatment conditions (6.3.2), an experiment was carried out to determine the effect of rotenone treatment on caspase-9 activity. Primary cortical neurons were cultured as described. On day 6, each of the three treatments was applied to 8 million cells (ie. each treatment used on 4 wells of neurons). After 24 hours, 4 million cells from each treatment condition were harvested by scraping in HBSS (at 37°C). The cells were centrifuged at 500x*g* for 5 minutes at 4°C, and the supernatant removed. The pelleted cells were then frozen immediately in liquid nitrogen and stored at -70°C. (The other 4 million cells for each treatment condition were to be used as described in 6.3.2.2).

The pellets were thawed and lysed by incubating with lysis buffer (from colorimetric caspase-9 activity kit, R&D Systems, Abingdon, UK) for 10 minutes on ice with gentle shaking. The lysed suspension was then centrifuged at 10000x*g* for 1 minute. 50µl of the resulting supernatant was used to assay for caspase-9 activity as described in 2.6.1.

The results are shown in Figure 6.3. There was no significant change in caspase-9 activity from control levels following 24 hours treatment with 10nM rotenone ($p > 0.05$, paired t-test). However, following 24 hours of treatment with 20nM rotenone, there was a significant increase in caspase-9 activity as compared to control levels ($p < 0.05$, paired t-test).

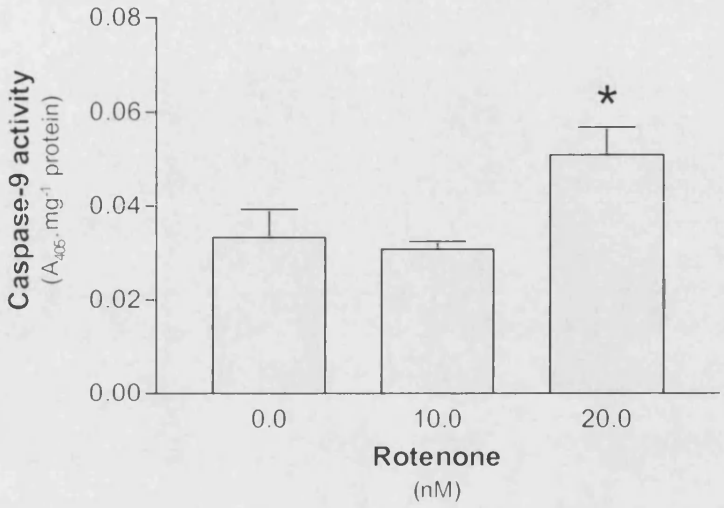

Figure 6.3

Effect of rotenone treatment on caspase-9 activity, expressed in arbitrary units of absorbance (at 405nm) per milligram protein. 10nM rotenone does not affect the level of caspase-9 activity, but 20nM rotenone significantly increases it ($p < 0.05$, paired t-test). Data shown ± S.E.M., n = 4.

6.3.2.2 Induction of cytochrome c release by rotenone

The primary cortical neurons treated as described above (6.3.2.1) were also used to assay for CCR into the cytosol. The second 4 million cells from each treatment were harvested by scraping into HBSS (at 37°C), and then centrifuged at 500x*g* for 5 minutes at 4°C. A cytosolic extract was then obtained by resuspending the cell pellet in lysis buffer (from colorimetric caspase-9 activity kit, R&D Systems, Abingdon, UK) for 10 minutes on ice with gentle shaking. This lysis buffer ruptures the cell membrane but leaves intracellular organelles eg. mitochondria, intact. After 10 minutes, the suspension was centrifuged at 17000x*g* for 10 minutes at 4°C. The supernatant was removed and frozen immediately in liquid nitrogen. The sample was stored at -70°C.

The samples were collected and then thawed together and assayed for protein content (2.7.1). The cytochrome *c* content was then measured (2.4.1). The cytochrome *c* concentration expressed per milligram of protein is plotted against rotenone concentration in Figure 6.4.

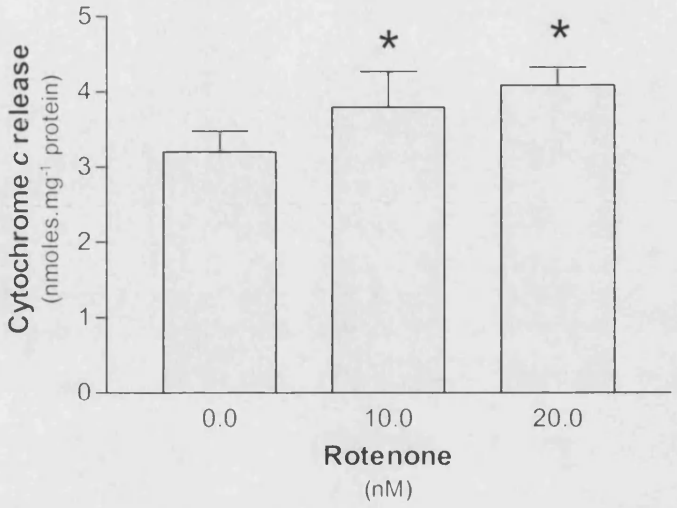

Figure 6.4

Effect of rotenone treatment on the release of cytochrome *c* in primary cortical neurons. Cells treated with 10nM rotenone had a significantly ($p < 0.05$, paired t-test) greater cytochrome *c* concentration in the cytosolic fraction than control cells. Cytosolic fractions of cells treated with 20nM rotenone also contained significantly more cytochrome *c* than controls ($p < 0.05$, t-test), but not significantly ($p > 0.05$, paired t-test) more than the 10nM treated cells. Data shown ± S.E.M., n = 4.

6.4 Discussion

6.4.1 *Specificity of rotenone-induced cytochrome c release*

A recent study by Desmukh *et al* (2002) claimed that the presence of cytochrome *c* in the cytosol of neurons is insufficient to induce apoptosis. The authors state that in order to develop 'competence to die', a neuron must also overcome regulation of active caspases by the IAP system. This occurs when Smac is released from the mitochondrial IMS. It would have been interesting for the study to have investigated further into the effect of varying the amplitude of the microinjected cytochrome c signal, since it would be expected that if the concentration of cytochrome *c* were to be made high enough, the IAP system would be overwhelmed. Perhaps the coordinate release of Smac is only required if the cytochrome *c* signal is especially weak. The threshold concentration of cytochrome *c* required may be higher in neurons due to the presence of extra IAP capacity, in the form of NAIP (1.3.6.1). Whether or not their hypothesis requires further validation, the authors of this intriguing study highlighted the important role of Smac in determining the fate of the host cell.

It was therefore considered important to investigate whether the rotenone-induced CCR detected in 3.3.2 was accompanied by Smac release. In contrast to cytochrome *c*, there is no commercially available immunoassay kit for Smac. Therefore the release of Smac was analysed by Western blotting. A positive Smac signal could only be detected in the lysed mitochondria. None of the supernatants, including that from the mitochondria treated with alamethicin, showed any detectable signal. Although alamethicin is known to be capable of causing CCR (Kluck *et al*, 1999), it

has never been shown to induce Smac release. It is thought that Smac and cytochrome *c* are released by different mechanisms (Kandasamy *et al*, 2003; Rehm *et al*, 2003), and so it is possible that additional events other than OM rupture are required for Smac release. Alternatively, the lack of evidence for Smac in the supernatant from alamethicin-treated mitochondria may simply indicate that the method has insufficient sensitivity for detection of the protein in these supernatant samples. Therefore, the conclusion that rotenone in the experimental range does not induce Smac release can only be drawn tentatively. This uncertainty highlights the considerable benefits of the quantitative immunoassay technique for assaying CCR.

In contrast, blotting for AIF proved more conclusive. AIF is another IMS protein which may be released to induce apoptosis (1.3.3). Western blotting demonstrated clearly that AIF was present in the mitochondrial control and in the supernatant from alamethicin-treated mitochondria. A much lower level was present in the supernatant from the mitochondria which were simply incubated in buffer at 37°C containing BSA. This level was consistent across the rotenone treatments, implying that rotenone in this range does not induce AIF release.

AIF is a much larger protein than cytochrome *c* (67kDa as opposed to 12.1kDa). It is therefore not very surprising that the CCR mechanism does not extend to AIF, bearing in mind the data obtained with respect to AK release (4.3.2). More interesting from this aspect is the tentative claim that Smac is not released with cytochrome *c*. As discussed (4.4.2), AK and Smac are almost identical sizes, both approximately double the size of cytochrome *c*. When it was determined that AK was not released with cytochrome *c*, it was hypothesised that the same might be true

of Smac. The blotting data is supportive of the suggestion that the release mechanism is either specific for cytochrome *c*, or carries a size 'cut-off' between 12.1 and 24kDa.

The fact that neither of these pro-apoptotic proteins appear to be released with cytochrome *c* is consistent with the hypothesis that low levels of CCR induced by rotenone may be 'safe'. The lack of AIF release suggests that caspase-independent death will not be induced. The apparent lack of Smac release leaves the cytosolic IAP system with its full capacity for buffering low levels of CCR.

6.4.2 *Rotenone-induced caspase-9 activity*

Rotenone at 10nM had no effect on the caspase-9 activity in primary cortical neurons. However, increasing the intensity of the treatment to 20nM caused a significant increase in the measured caspase-9 activity. The important conclusion to be drawn from this part of the study is that there is a threshold concentration of rotenone treatment, above which early apoptotic events can be detected.

Ideally, several more measures of apoptosis would be made, eg. LDH distribution, Hoechst staining. However, the yield of neurons from each preparation was extremely restricted, and the caspase-9 and cytochrome *c* measurements alone were sufficient to limit the titration to three rotenone concentration points. Caspase-9 activity was chosen as the most useful measurement of apoptosis for several reasons: Firstly, the only recognised means by which procaspase-9 is activated is via the

mitochondrial pathway.[2] Caspases later in the cascade eg. caspase-3, can be activated through the cell surface receptor route also. Therefore the use of caspase-9 activity as an apoptotic marker simplifies the model, and makes it easier to draw conclusions from the data. Secondly, caspase-9 is an 'initiator' caspase. It is the first one to be activated via the cytochrome *c*-induced pathway (Zou *et al*, 1999), and therefore is a marker of the early stages of apoptosis. This enabled a very sensitive analysis of the pro-apoptotic properties of cytochrome *c*, since cells which have not yet progressed to the later, more traditional markers of apoptosis, may nonetheless have committed to the pathway. Also, considering the amplification involved in the caspase cascade (Creagh & Martin, 2001), the activity of an early caspase such as –9 gives a purer indication of the direct effect of any released cytochrome *c*.

6.4.3 *Rotenone-induced cytochrome c release*

The benefits of modelling the recognised disease pathology rather than recreating downstream events were discussed in 5.1.1. Here, the same principle has been applied. Rather than microinjecting cytochrome *c* into cells, an approach often followed (Deshmukh *et al*, 2002; Li *et al*, 1997; Zhivotovsky *et al*, 1998), the experiment was carried out using a model of an underlying disease cause, ie. complex I deficiency (Perier *et al*, 2003).

A discrepancy was observed in the data resulting from 10nM rotenone treatment. A significant increase in CCR was detected at 10nM rotenone, whereas a significant

[2] *(Footnote: an extremely recent publication has reported cytochrome c-independent procaspase-9 activation – McDonnell et al, 2003. This is obviously yet to be confirmed or refuted by subsequent work).*

increase in caspase-9 activity was not detected until the rotenone treatment was raised to 20nM.

6.4.4 *The discrepancy between caspase-9 activity and cytochrome c release*

As discussed (1.3.6), there are a number of recognised post-mitochondrial mechanisms for regulating the commitment to apoptosis. Of these, the IAPs have featured heavily in the literature. Crucially, in the context of this study, it has been demonstrated that XIAP can inhibit the activation of procaspase-9 (Shiozaki *et al*, 2003). The authors demonstrate that XIAP sequesters procaspase-9 in a monomeric state. Since homodimerisation drives the activation of procaspase-9 (Renatus *et al*, 2001), this mechanism serves to inhibit progression down the caspase cascade. It can therefore be hypothesised that the discrepancy in rotenone concentrations required for increased caspase-9 activity and CCR might be explained by this action of XIAP and perhaps other IAP family members.

It is likely that the other post-mitochondrial regulatory mechanisms might also contribute to the caspase-9 activity versus CCR discrepancy observed. However, as yet, there is insufficient understanding of the mechanism of sequestration of cytochrome *c* by Hsps, or the prevention of apoptosome formation by K^+ to be able to conclude whether or not the immunoassay would detect cytochrome *c* which had fallen subject to these regulatory processes. Provided that the monoclonal antibody binding site on cytochrome *c* had not been altered or obstructed, the assay would still detect the protein, but it cannot at this stage be concluded that this is the case.

As discussed previously (5.3.4), cytochrome *c* which is released in response to complex I inhibition will be primarily in the ferri state. According to the hypothesis presented by Hancock *et al* (2001), this cytochrome *c* has pro-apoptotic potential due to its redox state, but can be made 'safe' by the action of cytosolic GSH, which will reduce the cytochrome *c* to the ferro form. This could also help to explain the 'delayed' increase in caspase-9 activity. It is interesting to note that the neuronal culture method uses media which has been 'conditioned' by incubating with astrocytes for 24 hours. It has been suggested that astrocytes lend important support to their neuronal neighbours in the form of transmitted GSH (Gegg *et al*, 2003), and this would have been modelled by the use of conditioned media. It would be interesting to determine the level of protection afforded by astrocytic GSH with respect to maintaining the cytosolic cytochrome *c* pool in a reduced state.

It could be argued that the discrepancy at 10nM rotenone is due to a difference in sensitivity of the two assays. However, both methods are highly quantitative. Conclusions regarding caspase activation have been drawn in the literature using data from Western blotting (eg. Gu *et al*, 1999), which has limited quantitative value, as has been discussed (3.1.2). A sensitive activity assay, as has been used in this study, is preferable for determining very small changes. An explanation of insufficient sensitivity is therefore unlikely to be valid, but is worth taking into consideration.

6.4.5 *Implications of the effect of rotenone on neurons*

This experiment has demonstrated that when CCR is induced by rotenone-induced complex I inhibition, there is a threshold rotenone concentration at which the

apoptotic pathway is triggered. It would appear that below this threshold, caspase activity is not induced.

In contrast to this apparent threshold effect for rotenone-induced caspase-9 activation, it has been shown using experiments on isolated mitochondria (3.3.2) that rotenone-induced CCR shows no such threshold effect. Rather, CCR is increased in proportion to complex I inhibition. It can therefore be concluded that low levels of cytochrome *c* present in the cytosol can be buffered, and 'made safe' with respect to caspase activation. This conclusion is relevant to CCR induced by complex I inhibition, but may not apply to CCR induced by other mechanisms, which may perhaps be more detrimental to mitochondrial integrity.

The findings are particularly relevant in the understanding of the pathology of Parkinson's disease. In early disease states, where complex I activity would be expected to be only marginally reduced, it is likely that the cytochrome *c* signal is already being increased. However, the cells' natural defences are able to buffer its pro-apoptotic activity up to a point. Only once these defences are overcome does neurodegenerative cell loss ensue.

It would appear to be the case that it is primarily the amplitude of the cytochrome *c* signal which is the important factor. Rotenone is known to be capable of inducing apoptosis provided that the concentration is sufficient (Gao *et al*, 2002; Pei *et al*, 2003). From our preliminary blotting data, it would appear that Smac is not required to induce this death, in contrast to the claim of Deshmukh *et al* (2002). However, direct measurement of Smac levels in the cytosol of treated neurons would be

required to confirm this suggestion because it is difficult to equate the strength of rotenone treatment between the isolated mitochondria and the cultured cell experiments. It is intuitive that Smac should only be required in the initiation of apoptosis if the cytochrome *c* signal is too weak to overwhelm the IAP inhibition alone.

Taking account of these considerations, the IAP system presents itself as a very promising therapeutic target. If this family of proteins could be clinically exploited, the threshold level of CCR could be raised to effectively delay onset of neurodegenerative symptoms in Parkinson's disease patients.

6.5 Conclusions

This final section to the study has lent considerable support to the hypothesis that CCR induced by complex I inhibition need not necessarily lead to apoptosis. Neuronal cells appear to be able to tolerate a low level of CCR without undergoing a detectable increase in the activity of the first caspase to be affected by cytochrome *c*. Further investigation would ideally include a number of other assays for apoptotic markers, to confirm this conclusion.

There are a number of possible mechanisms by which cytosolic cytochrome *c* can be made 'safe'. It would be interesting to investigate further in order to determine the relative importance of such mechanisms. The IAP system, in particular, is of potential therapeutic use with respect to early treatment for Parkinson's disease and

perhaps other neurodegenerative diseases. Work in this area is already providing some interesting results (Crocker et al, 2003; Kugler *et al*, 2000).

CHAPTER 7

General Discussion

The discovery of the role which cytochrome *c* plays in the apoptotic pathway has opened up a huge field of research. There has been considerable interest in the mechanism by which the protein is liberated, with recent advances increasingly claiming release via channels in the mitochondrial OM. Another rapidly emerging field is that of post-mitochondrial mechanisms for regulation of apoptosis, such as the IAP system.

These two advances in particular are consistent with the hypothesis that CCR need not be complete within a cell, but may occur at low levels. CCR of small amplitude is often described as 'accidental'. If this occurs, there are mechanisms in place to prevent the amplifying caspase cascade from being induced.

The data in this study provide the first complete demonstration that CCR can be induced in proportion to the severity of an insult to the mitochondria, and that low levels of release induced by a minor insult do not appear to induce apoptosis. This low amplitude release is probably not 'accidental' as often described, but instead a weak pro-apoptotic signal, which appears to be sub-threshold with respect to the activation of procaspase-9.

These findings can be attributed largely to the careful selection of methods for the study. It was vital to the hypothesis that the stimulus used to induce CCR was a recognised model of a naturally-occuring pathology, and that the severity could be titrated. This 'bottom-up' approach was used to determine the dynamics of CCR in a disease state. This is in contrast to the often used approach which uses a stimulus

chosen because of its recognised ability to cause the CCR event, but with little or no relevance to the underlying cause. Comparatively, this is much less useful with respect to determining mechanisms of disease.

The second methodological advantage was the immunoassay used for measuring CCR. There were no published reports using an ELISA assay for this purpose when this study commenced. This method has now been used in published work on a number of occasions (Brustovetsky *et al*, 2003b, Jemmerson *et al*, 2002), and cytochrome *c* ELISA kits are now available from several manufacturers. The method affords significant advantages over the more traditional means for measuring CCR, such as Western blotting or fusion with green fluorescent protein. The former method has comparatively little quantitative value; even using densitometry readings, the data is subject to background variation. Use of the GFP fusion protein is claimed to have quantitative value, but it has been shown that when fused to GFP, cytochrome *c* displays altered properties with respect to release from mitochondria due to the size increase (Roucou *et al*, 2000). The immunoassay method, in contrast, is highly quantitative, can be used to measure large numbers of samples simultaneously and is not subject to the same experimental variation as other methods. These advantages probably underlie the recent surge in utilisation of the technique.

This study was carried out primarily on isolated brain mitochondria. The use of isolated mitochondria enabled a sensitive and accurate determination of CCR, eliminating the effects of cytosolic regulation mechanisms, which would be very difficult to quantify. Brain mitochondria were used due to the particular importance of controlling the induction of apoptosis in mature neurons. Apoptosis is a major

mechanism of neurodegenerative cell loss, and the incidence of 'unnecessary' apoptosis in neurons clearly has severe implications.

There is no immediately obvious reason that proportional release of cytochrome *c*, in response to an insult which is increasing in severity, should be a phenomenon restricted to the brain. The gradient of the respiratory inhibition versus CCR curve may exhibit tissue variation due to the extent of ETC-mediated ROS generation or pro:anti-apoptotic Bcl-2 protein ratio for example. However, the proportional relationship itself does not present any clear basis for tissue specificity.

However, even if this proportional relationship were true of mitochondria in general, there is considerable potential for tissue heterogeneity with respect to the threshold cytochrome *c* concentration required for apoptosis. It might be expected that neurons would exhibit a higher threshold than hepatocytes, for example, which are highly proliferative cells. It is interesting to note that there is a neuronal specific IAP, NAIP (1.3.6.1). This protein could convey added security onto a neuron to raise the threshold for apoptosis.

Crucial to the conclusion that low amplitude CCR need not lead to apoptosis were the features of the release mechanism. The retained integrity of the IM and lack of non-specific rupture of the OM would leave the mitochondria energetically viable, and therefore capable of supporting a host cell if it were to survive. These findings cannot however be extended to situations beyond those tested in this study. It is likely that MPT is responsible for CCR in other situations, for example in response to raised intracellular calcium levels. The mechanism of CCR induced by complex I inhibition

is however of great interest in isolation from other apoptotic scenarios due to the implications for the pathology of Parkinson's disease.

This study has demonstrated that primary cortical neurons can tolerate low levels of CCR which result from inhibition of complex I activity, implying that there is a threshold level at which CCR becomes sufficient to induce caspase-9 activity. Considering heterogeneity between neurons, this could cause a gradually increasing proportion of the cells to commit to apoptosis, underlying the slow progression of Parkinson's disease or other neurodegenerative disorders. This could be mediated by the age-related increase in ROS generation resulting from mitochondrial DNA mutations (Lee & Wei, 1997), given the suggestion that CCR is induced by mitochondrially-generated ROS (5.4.3.1).

Possibly the most important implication of this study concerns potential directions for therapy in neurodegenerative disorders. The threshold effect described for cytochrome *c*-mediated induction of apoptosis reinforces the considerable interest in IAPs as therapeutic targets. Bearing in mind the uncertainty regarding the molecular details of the CCR mechanism, it is important to have determined that cytochrome *c* presence in the cytosol need not be eliminated completely for therapy to be effective. (Indeed if low levels of CCR are in fact a defensive anti-oxidant mechanism in response to ETC-generated ROS – see 3.4.2.2, 5.4.3.1 – then complete elimination of cytosolic cytochrome *c* may actually be detrimental). Rather, from the apparent threshold effect, it would seem feasible to aim to increase the threshold at which caspase activity is induced. The findings from this study imply that this strategy would be sufficient to prolong onset of neurodegenerative symptoms without

additional problems arising from mitochondrial deficiencies. Indeed it has been shown previously that substantial complex I inhibition is possible before ATP synthesis is compromised (Davey & Clark, 1996; Davey *et al*, 1998).

The therapeutic potential of IAPs is already being probed for use in conditions where dysregulation of apoptosis is a primary part of the pathology. This includes cancer, as well as neurodegenerative disorders. Of particular interest with respect to this study is the finding that over-expression of XIAP can protect CA1 hippocampal neurons from ischaemia-induced apoptosis (Xu *et al*, 1999). The protection was of both a histological and, importantly, a functional nature. Surprisingly, perhaps, over-expressed XIAP has also been shown to be capable of rescuing retinal ganglion cells from apoptosis induced by axotomy of the optic nerve, even when the therapy was only applied subsequent to the insult (Kugler *et al*, 2000). Use of XIAP or other IAPs in gene therapy may therefore be of real therapeutic value in delaying the symptoms of neurodegenerative disorders.

A major hindrance in therapy for neurodegenerative diseases is the lack of official diagnosis until post mortem. Symptoms only become apparent once significant 'inappropriate' apoptosis has occurred. Therefore, therapy would initially be aimed at delaying further degeneration rather than preventing onset of the disease. However, screening for individuals at risk, and methods for early detection of these diseases would be of considerable benefit for this strategy.

There are of course potential complications associated with using up-regulation of IAPs as a therapeutic strategy. Upsetting the balance of pro- and anti-apoptotic

proteins carries huge risks in terms of tumourigenesis. Normal apoptotic potential is also essential for development, although this is less likely to be of concern in the treatment of neurodegenerative diseases, which are associated with aging. However, if these complications can be overcome, the strategy of raising the threshold for cytochrome *c* mediated induction of apoptosis could prove extremely fruitful. The support lent to this line of research by this study is extremely important. The study has demonstrated on a number of levels using the relevant subject material (brain mitochondria and primary neurons) and a recognised model of the disease pathology (complex I inhibition to model Parkinson's disease) that the strategy is feasible.

The data reported here have highlighted the sophisticated mechanisms employed by a cell to regulate commitment to apoptosis. Consistent with the tightly controlled apoptotic program, whereby cellular contents are neatly packaged and damage limitation is paramount, the initial 'decision' as to whether or not to commit to the program is not made rashly. However, the considerable amplification and positive feedback loops involved in the caspase cascade ensure that apoptosis itself is a definite all-or-none event. This contrast between the 'reluctance' to commit to apoptosis and the amplification of an initially small pro-apoptotic signal is an intriguing feature of the cell death program, and one which needs to be carefully considered when attempting to regulate the incidence of apoptosis for therapeutic benefit.

Future work

Given the considerable implications of the data from this study, it would be interesting to extend the project in a number of directions.

1 This study was carried out using isolated mitochondria and cultured cells from rat brain, the reasons for which were described in 3.1.3. As described in Chapter 7, there is no clear reason that CCR occurring in proportion to complex I inhibition should be a feature restricted to mitochondria from brain. However, the amplitude of the signal might be expected to vary.

It would therefore be interesting to repeat this part of the study using mitochondria isolated from tissues other than brain. Given the readiness of hepatocytes to undergo apoptosis, liver mitochondria would be particularly useful subjects.

2 There are a number of other inhibitors which could be used to further elucidate the CCR mechanism discussed in Chapter 4. Bonkrekic acid is a more specific inhibitor of the MPT, acting on the IM ANT. There are considerably fewer reports in the literature of the effects of this inhibitor, and it has only recently become readily commercially available. The use of this tool would, however, provide information on whether additional components of the PTP are involved in this case. It would also be interesting to investigate the role of other Bcl-2 proteins, eg. Bax.

3 Further investigation is required to conclusively demonstrate whether ETC-generated ROS are responsible for inducing the observed CCR. Use of exogenous GSH in isolated mitochondrial incubations would demonstrate whether this was the case.

4 The preliminary data obtained in Chapter 6 from cultured neurons would benefit from more extensive investigation. In particular, markers of apoptosis additional to increased caspase-9 activity would add to the validity of the conclusions. Control experiments could also be carried out to confirm the manufacturer's claim that the effect of the lysis buffer is limited to the cell membrane and does not disrupt mitochondrial integrity. The very limited yield of neurons from each preparation prevented these experiments from being done in the course of this study.

5 Affinity chromatography could be used to identify new candidates for cytochrome *c*-binding proteins in the cytosol. This study has yielded results highly consistent with the concept of cytosolic 'buffering' of low levels of cytochrome *c* in the cytosol, and so provides a good basis for such an investigation.

6 In the same vein, it would be extremely interesting to determine the 'buffering power' of cytosols from different cell types. It might be determined that CCR occurs in proportion to complex I inhibition in tissues other than brain (see point 1). However, it is known that there is a neuronal specific IAP (NAIP), and this could contribute to a higher

cytosolic buffering capacity in neurons than other cells from other tissues. This might be expected as an evolutionary adaptation considering the critical implications of neuronal apoptosis in mature brain. Determination of the relative level of IAPs, HSPs, etc. in neurons and other cell types would demonstrate whether the threshold cytosolic cytochrome *c* concentration required for apoptosis exhibits tissue heterogeneity.

References

Adachi S, Gottlieb RA & Babior BM (1998) Lack of release of cytochrome *c* from mitochondria into cytosol early in the course of Fas-mediated apoptosis of Jurkat cells. *J. Biol. Chem.* **273**: 19892-4

Adrain C, Creagh EM & Martin SJ (2001) Apoptosis-associated release of Smac/DIABLO from mitochondria requires active caspases and is blocked by Bcl-2. *EMBO J.* **20**: 6627-36

Almeida A, Brooks KJ, Sammut I, Keelan J, Davey GP, Clark JB & Bates TE (1995) Postnatal development of the complexes of the electron transport chain in synaptic mitochondria from rat brain. *Dev. Neurosci.* **17**: 212-8

Almeida A, Delgado-Esteban M, Bolanos JP & Medina JM (2002) Oxygen and glucose deprivation induces mitochondrial dysfunction and oxidative stress in neurones but not in astrocytes in primary culture. *J. Neurochem.* **81**: 207-17

Almeida A & Medina JM (1998) A rapid method for the isolation of metabolically active mitochondria from rat neurons and astrocytes in primary culture. *Brain Res. Protocols* **2**: 209-14

Andreyev AY, Fahy B & Fiskum G (1998) Cytochrome *c* release from brain mitochondria is independent of the mitochondrial permeability transition. *FEBS Lett.* **439**: 373-6

Anglade P, Vyas S, Hirsch EC & Agid Y (1997) Apoptosis in dopaminergic neurons of the human substantia nigra during normal aging. *Histol. Histopathol.* **12**: 603-10

Antonsson B, Montessuit S, Lauper S, Eskes R & Martinou JC (2000) Bax oligomerization is required for channel-forming activity in liposomes and to trigger cytochrome *c* release from mitochondria. *Biochem. J.* **345**: 271-8

Aon MA, Cortassa S, Marban E & O'Rourke B (2003) Synchronized whole-cell oscillations in mitochondrial metabolism triggered by a local release of reactive oxygen species in cardiac myocytes. *J. Biol. Chem.* published online ahead of print, 10.1074/jbc.M302673200

Arends MJ & Wyllie AH (1991) Apoptosis: mechanisms and roles in pathology. *Int. Rev. Exp. Pathol.* **32**: 223-54

Aschner M (2000) Neuron-astrocyte interactions: implications for cellular energetics and antioxidant levels. *Neurotoxicology* **21**: 1101-7

Babcock GT & Wikstrom M (1992) Oxygen activation and the conservation of energy in cell respiration. *Nature* **356**: 301-9

Bachmair A, Finley D & Varshavsky A (1986) In vivo half-life of a protein is a function of its amino-terminal residue. *Science* **234**: 179-186

Barbu A, Welsh N & Saldeen J (2002) Cytokine-induced apoptosis and necrosis are preceded by disruption of the mitochondrial membrane potential in pancreatic RINm5F cells: prevention by Bcl-2. *Mol. Cell Endocrinol.* **190**: 75-82

Bartalesi I, Bertini I & Rosato A (2003) Structure and dynamics of reduced *Bacillus pasteurii* cytochrome *c*: a fingerprint of the cytochrome *c* fold. *Biochemistry* **42**: 10923-30

Basanez G, Nechushtan A, Drozhinin O, Chanturiya A, Choe E, Tutt S, Wood KA, Hsu Y, Zimmerberg J & Youle RJ (1999) Bax, but not Bcl-xL, decreases the lifetime of planar phospholipid bilayer membranes at subnanomolar concentrations. *Proc. Natl. Acad. Sci. USA* **96**: 5492-7

Battino M, Bertoli E, Formiggini G, Sassi S, Gorini A, Villa RF & Lenaz G (1991) Structural and functional aspects of the respiratory chain of synaptic and nonsynaptic mitochondria derived from selected brain regions. *J. Bioenerg. Biomembr.* **23**: 345-63

Beavis AD (1992) Properties of the inner membrane anion channel in intact mitochondria. *J. Bioenerg. Biomembr.* **24**: 77-90

Bertrand R, Solary E, O'Connor P, Kohn KW & Pommier Y (1994) Induction of a common pathway of apoptosis by staurosporine. *Exp. Cell Res.* **211**: 314-21

Beutner G, Ruck A, Riede B, Welte W, Brdiczka D (1996) Complexes between kinases, mitochondrial porin and adenylate translocator in rat brain resemble the permeability transition pore. *FEBS Lett* **396**: 189-195

Blokhuis GG & Veldstra H (1970) Heterogeneity of mitochondria in rat brain. *FEBS Lett.* **11**: 197-9

Bolanos JP, Peuchen S, Heales SJ, Land JM & Clark JB (1994) Nitric oxide-mediated inhibition of the mitochondrial respiratory chain in cultured astrocytes. *J. Neurochem.* **63**: 910-6

Boldin MP, Goncharov TM, Golstev YV & Wallach D (1996) Involvement of MACH, a novel MORT1/FADD-interacting protease, in Fas/APO-1- and TNF receptor-induced cell death. *Cell* **85**: 803-15

Borutaite V, Jekabsone A, Morkuniene R & Brown GC (2003) Inhibition of mitochondrial permeability transition prevents mitochondrial dysfunction, cytochrome *c* release and apoptosis induced by heart ischaemia. *J. Mol. Cell Cardiol.* **35**: 357-66

Bossy-Wetzel E, Newmeyer DD & Green DR (1998) Mitochondrial cytochrome *c* release in apoptosis occurs upstream of DEVD-specific caspase activation and independently of mitochondrial transmembrane depolarization. *EMBO J.* **17**: 37-49

Bota DA & Davies KJA (2001) Protein degradation in mitochondria: implications for oxidative stress, aging and disease. *Mitochondrion* **1**: 33-49

Boveris A, Oshino N & Chance B (1972) The cellular production of hydrogen peroxide. *Biochem. J.* **128**: 617-30

Brand M (1995) Measurement of mitochondrial protonmotive force. In Bioenergetics: A Practical Approach. Brown GC & Cooper CE (eds.): 39-62. IRL Press, Oxford.

Bret C, Roth M, Norager S, Hatchikian EC & Field MJ (2002) Molecular dynamics study of *Desulfovibrio africanus* cytochrome *c*3 in oxidised and reduced forms. *Biophys. J.* **83**: 3049-65

Brown GC (1995) Nitric oxide regulates mitochondrial respiration and cell functions by inhibiting cytochrome oxidase. *FEBS Lett.* **369**: 136-9

Brown GC & Cooper CE (1994) Nanomolar concentrations of nitric oxide reversibly inhibit synaptosomal respiration by competing with oxygen at cytochrome oxidase. *FEBS Lett.* **356**: 295-8

Brustovetsky N, Brustovetsky T, Jemmerson R & Dubinsky JM (2002) Calcium-induced cytochrome *c* release from CNS mitochondria is associated with the permeability transition and rupture of the outer membrane. *J. Neurochem.* **80**: 207-18

Brustovetsky N, Brustovetsky T, Purl KJ, Capano M, Crompton M & Dubinsky JM (2003a) Incresaed susceptibility of striatal mitochondria to calcium-induced permeability transition. *J. Neurosci.* **23**: 4858-67

Brustovetsky N, Dubinsky JM, Antonsson B & Jemmerson R (2003b) Two pathways for tBID-induced cytochrome *c* release from rat brain mitochondria: BAK- versus BAX-dependence. *J. Neurochem.* **84**: 196-207

Buckman JF & Reynolds IJ (2001) Spontaneous changes in mitochondrial membrane potential in cultured neurons. *J. Neurosci.* **21**: 5054-65

Cacic M, Wilichowski E, Mejaski-Bosnjak V, Fumic K, Lujic L, Marusic Della Marina B & Hanefield F (2001) Cytochrome *c* oxidase partial deficiency-associated Leigh disease presenting as an extrapyramidal syndrome. *J. Child Neurol.* **16**: 616-9

Cain K, Bratton SB & Cohen GM (2002) The Apaf-1 apoptosome: a large caspase-activating complex. *Biochimie* **84**: 203-14

Cain K, Bratton SB, Langlais C, Walker G, Brown DG, Sun XM & Cohen GM (2000) Apaf-1 oligomerizes into biologically active approximately 700-kDa and inactive approximately 1.4-Mda apoptosome complexes. *J. Biol. Chem.* **275**: 6067-70

Cain K, Langlais C, Sun XM, Brown DG & Cohen GM (2001) Physiological concentrations of K^+ inhibit cytochrome *c*-dependent formation of the apoptosome. *J. Biol. Chem.* **276**: 41985-90

Calvert JF, Hill JL & Dong A (1997) Redox-dependent conformational changes are common structural features of cytochrome *c* from various species. *Arch. Biochem. Biophys.* **346**: 287-93

Candé C, Cohen I, Daugas E, Ravagnan L, Larochette N, Zamzami N & Kroemer G (2002) Apoptosis-inducing factor (AIF): a novel caspase-independent death effector released from mitochondria. *Biochimie* **84**: 215-22

Capano M, Virji S & Crompton M (2002) Cyclophilin A is involved in excitotoxin-induced caspase activation in rat neuronal B50 cells. *Biochem. J.* **363**: 29-36

Cardone MH, Roy N, Stennicke HR, Salvesen GS, Franke TF, Stanbridge E, Frisch S & Reed JC (1998) Regulation of cell death protease caspase-9 by phosphorylation. *Science* **282**: 1318-21

Carroll J, Shannon RJ, Fearnley IM, Walker JE & Hirst J (2002) Definition of the nuclear encoded composition of bovine heart mitochondrial complex I. *J. Biol. Chem.* **52**: 50311-7

Chance B & Williams GR (1956) The respiratory chain and oxidative phosphorylation. *Adv. Enzymol.* **17**: 65-134

Chappell JB (1964) The oxidation of citrate, isocitrate and cis-aconitate by isolated mitochondria. *Biochem. J.* **90**: 225-37

Chen L, Smith L, Wang Z & Smith JB (2003) Preservation of caspase-3 subunits from degradation contributes to apoptosis evoked by lactacystin: any single lysine of lysine pair of the small subunit is sufficient for ubiquitination. *Mol. Pharmacol.* **64**: 334-45

Colombini M, Yeung CL, Tung J & Konig T (1987) The mitochondrial outer membrane channel, VDAC, is regulated by a synthetic polyanion. *Biochim. Biophys. Acta* **905**: 279-86

Concannon CG, Orrenius S & Samali A (2001) Hsp27 inhibits cytochrome *c*-mediated caspase activation by sequestering both pro-caspase-3 and cytochrome *c*. *Gene Expr.* **9**: 195-201

Cortese JD, Voglino AL & Hackenbrock CR (1998) Multiple conformations of physiological membrane-bound cytochrome *c*. *Biochemistry* **37**: 6402-9

Creagh EM & Martin SJ (2001) Caspases: cellular demolition experts. *Biochem. Soc. Trans.* **29**: 696-702

Crocker SJ, Wigle N, Liston P, Thompson CS, Lee CJ, Xu D, Roy S, Nicholson DW, Park DS, MacKenzie A, Korneluk RG & Robertson GS (2001) NAIP protects the

nigrostriatal dopamine pathway in an intrastriatal 6-OHDA rat model of Parkinson's disease. *Eur. J. Neurosci.* **14**: 391-400

Crompton M (2000) Mitochondrial intermembrane junctional complexes and their role in cell death. *J. Physiol.* **529**: 11-21

Crompton M, Barksby E, Johnson N & Capano M (2002) Mitochondrial intermembrane junctional complexes and their involvement in cell death. *Biochimie* **84**: 143-52

Crook NE, Clem RJ & Miller LK (1993) An apoptosis-inhibiting baculovirus gene with a zinc finger-like motif. *J. Virol.* **67**: 2168-74

Crouser ED, Gadd ME, Julain MW, Huff JE, Broekemeier KM, Robbins KA & Pfeiffer DR (2003) Quantitation of cytochrome *c* release from rat liver mitochondria. Anal. Biochem. **317**: 67-75

Davey GP & Clark JB (1996) Threshold effects and control of oxidative phosphorylation in nonsynaptic rat brain mitochondria. *J. Neurochem.* **66**: 1617-24

Davey GP, Peuchen S & Clark JB (1998) Energy thresholds in brain mitochondria: Potential involvement in neurodegeneration. *J. Biol. Chem.* **273**: 12753-7

de Giorgi F, Lartigue L, Bauer MK, Schubert A, Grimm S, Hanson GT, Remington SJ, Youle RJ & Ichas F (2002) The permeability transition pore signals apoptosis by directing Bax translocation and multimerization. *FASEB J.* **16**: 607-9

de Jong D, Prins FA, Mason DY, Reed JC, van Ommen GB & Kluin PM (1994) Subcellular localization of the bcl-2 protein in malignant and normal lymphoid cells. *Cancer Res.* **54**: 256-60

Deng Y, Lin Y & Wu X (2002) TRAIL-induced apoptosis requires Bax-dependent mitochondrial release of Smac/DIABLO. *Genes Dev.* **16**: 33-45

Deshmukh M, Du C, Wang X & Johnson EM Jr. (2002) Exogenous smac induces competence and permits caspase activation in sympathetic neurons. *J. Neurosci.* **22**: 8018-27

Deveraux QL, Leo E, Stennicke HR, Welsh K, Salvesen GS & Reed JC (1999) Cleavage of human inhibitor of apoptosis protein XIAP results in fragments with distinct specificities for caspases. *EMBO J.* **18**: 5242-51

Deveraux QL, Takahashi R, Salveson GS & Reed JC (1997) X-Linked IAP is a direct inhibitor of cell-death proteases. *Nature* **388**: 300-4

Diekert K, de Kroon AI, Ahting U, Niggermeyer B, Neupert W, de Kruijff B & Lill R (2001) Apocytochrome *c* requires the TOM complex for translocation across the mitochondrial outer membrane. *EMBO J.* **20**: 5626-35

Doran E & Halestrap AP (2000) Cytochrome *c* release from isolated rat liver mitochondria can occur independently of outer-membrane rupture: possible role of contact sites. *Biochem. J.* **348**: 343-50

Dringen R, Pfeiffer B & Hamprecht B (1999) Synthesis of the antioxidant glutathione in neurons: supply by astrocytes of CysGly as precursor for neuronal glutathione. *J. Neurosci.* **19**: 562-9

Du C, Fang M, Li Y, Li L & Wang X (2000) Smac, a mitochondrial protein that promotes cytochrome *c* dependent caspase activation by eliminating IAP inhibition. *Cell* **102**: 33-42

Duckett CS, Li F, Wang Y, Tomaselli KJ, Thompson CB & Armstrong RC (1998) Human IAP-like protein regulates programmed cell death downstream of Bcl-xL and cytochrome *c*. *Mol. Cell Biol.* **18**: 608-15

Eden D, Matthew JB, Rosa JJ & Richards FM (1982) Increase in apparent compressibility of cytochrome *c* upon oxidation. *Proc. Nat. Acad. Sci. USA* **79**: 815-9

Eskes R, Antonsson B, Osen-Sand A, Montessuit S, Richter C, Sadoul R, Mazzei G, Nichols A & Martinou JC (1998) Bax-induced cytochrome *c* release from mitochondria is independent of the permeability transition pore but highly dependent on Mg^{2+} ions. *J. Cell. Biol.* **143**: 217-24

Ferranti R, da Silva MM & Kowaltowski AJ (2003) Mitochondrial ATP-sensitive K^+ channel opening decreases reactive oxygen species generation. *FEBS Lett.* **536**: 51-5

Ferreira GC (1995) Heme biosynthesis: biochemistry, molecular biology, and relationship to disease. *J. Bioenerg. Biomembr.* **27**: 147-50

Finucane DM, Waterhouse NJ, Amarante-Mendes GP, Cotter TG & Green DR (1999) Collapse of the inner mitochondrial transmembrane potential is not required for apoptosis of HL60 cells. *Exp. Cell Res.* **251**: 166-74

Forman HJ & Azzi A (1997) On the virtual existence of superoxide anions in mitochondria: thoughts regarding its role in pathophysiology. *FASEB J.* **11**: 374-5

Friedrich T, van Heek P, Leif H, Ohnishi T, Forche E, Kunze B, Jansen R, Trowitzsch-Kienast W, Hofle G & Reichenbach H (1994) Two binding sites of inhibitors in NADH: ubiquinone oxidoreductase (complex I). Relationship of one site with the ubiquinone-binding site of bacterial glucose:ubiquinone oxidoreductase. *Eur. J. Biochem.* **219**: 691-8

Gao HM, Hong JS, Zhang W & Liu B (2002) Distinct role for microglia in rotenone-induced degeneration of dopaminergic neurons. *J. Neurosci.* **22**: 782-90

Gardner MT, Deinum G, Kim Y, Babcock GT, Scot MJ & Holm RH (1996) Vibrational analysis of a molecular heme-copper assembly with a nearly linear

Fe(III)-CN-Cu(II) bridge: insight into cyanide binding to fully oxidised cytochome *c* oxidase. *Inorg. Chem.* **35**: 6878-84

Gegg ME, Beltran B, Salas-Pino S, Bolanos JP, Clark JB, Moncada S & Heales SJ (2003) Differential effect of nitric oxide on glutathione metabolism and mitochodnrial function in astrocytes and neurones: implications for neuroprotection/neurodegeneration? *J. Neurochem.* **86**: 228-37

Genova ML, Ventura B, Giulaino G, Bovina C, Formiggini G, Parenti Castelli G & Lenaz G (2001) The site of superoxide radical in mitochondrial Complex I is not a bound ubisemiquinone but presumably iron-sulfur cluster N2. *FEBS Lett.* **505**: 364-8

Gnaiger E, Mendez G & Hand SC (2000) High phosphorylation efficiency and depression of uncoupled respiration in mitochondria under hypoxia. *Proc. Natl. Acad. Sci. USA* **97**: 11080-5

Gogvadze V, Robertson JD, Zhivotovsky B & Orrenius S (2001) Cytochrome *c* release occurs via Ca^{2+}-dependent and Ca^{2+}-independent mechanisms that are regulated by Bax. *J. Biol. Chem.* **276**: 19066-71

Goldstein JC, Waterhouse NJ, Juin P, Evan GI & Green DR (2000) The coordinate release of cytochrome *c* during apoptosis is rapid, complete and kinetically invariant. *Nat. Cell Biol.* **2**: 156-62

Gray CW, Ward RV, Karran E, Turconi S, Rowles A, Viglienghi D, Southan C, Barton A, Fantom KG, West A, Savopoulos J, Hassan NJ, Clinkenbeard H, Hanning C, Amegadzie B, Davis JB, Dingwall C, Livi GP & Creasy CL (2000) Characterization of human HtrA2, a novel serine protease involved in the mammalian cellular stress response. *Eur. J. Biochem.* **267**: 5699-710

Gray EG & Whittaker VP (1962) The isolation of nerve endings from brain: an electron-microscopic study of cell fragments derived by homogenisation and centrifugation. *J. Anat. (London)* **96**: 79-88

Gu C, Casaccia-Bonnefil P, Srinivasan A & Chao M (1999) Oligodendrocyte apoptosis mediated by caspase activation. *J. Neurosci.* **19**: 3043-9

Gu M, Gash MT, Mann VM, Javoy-Agid F, Cooper JM & Schapira AHV (1996) Mitochondrial defect in Huntington's disease caudate nucleus. *Ann. Neurol.* **39**: 385-9

Hampton MB, Zhivotovsky B, Slater AFG, Burgess DH & Orrenius S (1998) Importance of the redox state of cytochrome *c* during caspase activation in cytosolic extracts. *Biochem. J.* **329**: 95-9

Hancock JT, Desikan R & Neill SJ (2001) Does the redox status of cytochrome *c* act as a fail-safe mechanism in the regulation of programmed cell death? *Free Radic. Biol. Med.* **31**: 697-703

Hausladen A & Fridovich I (1994) Measuring nitric oxide and superoxide: rate constants for aconitase reactivity. *Methods Enzymol.* **269**: 37-41

Heales SJR, Gegg ME & Clark JB (2002) Oxidative phosphorylation: structure, function, and intermediary metabolism. *Int. Rev. Neurobiol.* **53**: 25-56

Hengartner MO (2000) The biochemistry of apoptosis. *Nature* **407**: 770-6

Hirsch EC, Hunot S, Faucheux B, Agid Y, Mizuno Y, Mochizuki H, Tatton WG, Tatton N & Olanow WC (1999) Dopaminergic neurons degenerate by apoptosis in Parkinson's disease. *Mov. Disord.* **14**: 383-5

Hofmann K, Bucher P & Tschopp J (1997) The CARD domain: a new apoptotic signalling motif. *Trends Biochem. Sci.* **22**: 155-6

Holcik M, Gibson H & Korneluk RG (2001) XIAP: apoptotic brake and promising therapeutic target. *Apoptosis* **6**: 253-61

Huang H, Joazeiro CA, Bonfoco E, Kamada S, Leverson JD & Hunter T (2000) The inhibitor of apoptosis, cIAP2, functions as a ubiquitin-protein ligase and promotes *in vitro* monoubiquitination of caspases 3 and 7. *J. Biol. Chem.* **275**: 26661-4

Hughes FM Jr. Bortner CD, Purdy GD & Cidlowski JA (1997) Intracellular K^+ suppresses the activation of apoptosis in lymphocytes. *J. Biol. Chem.* **272**: 30567-76

Hunte C, Palsdottir H & Trumpower BL (2003) Protonmotive pathways and mechanisms in the cytochrome bc_1 complex. *FEBS Lett.* **545:** 39-46

Hunter DR & Haworth RA (1979) The Ca^{2+}-induced membrane transition in mitochondria. I. The protective mechanisms. *Arch. Biochem. Biophys.* **195**: 453-9

Igney FH & Krammer PH (2002) Death and anti-death: tumour resistance to apoptosis. *Nat. Rev. Cancer* **2**: 277-88

Jaattela M, Wissing D, Bauer PA & Li GC (1992) Major heat shock protein hsp70 protects tumor cells from tumor necrosis factor cytotoxicity. *EMBO J.* **11**: 3507-12

Jansen B, Schlagbauer-Wadl H, Brown BD, Bryan RN, van Elsas A, Muller M, Wolff K, Eichler HG & Pehamberger H (1998) bcl-2 antisense therapy chemosensitizes human melanoma in SCID mice. *Nat. Med.* **4**: 232-4

Jemmerson R, LaPlante B & Treeful A (2002) Release of intact, monomeric cytochrome *c* from apoptotic and necrotic cells. *Cell Death Differ.* **9**: 538-48

Jiang X & Wang X (2000) Cytochrome *c* promotes caspase-9 activation by inducing nucleotide binding to Apaf-1. *J. Biol. Chem.* **275**: 31199-31203

Jordi W, Hergersberg C & de Kruijff B (1992) Bilayer-penetrating properties enable apocytochrome *c* to follow a special import pathway into mitochondria. *Eur. J. Biochem.* **204:** 841-6

Joza N, Susin SA, Daugas E, Stanford WL, Cho SK, Li CYJ, Sasaki T, Elia AJ, Cheng HYM, Ravagnan L, Ferri KF, Zamzami N, Wakeham A, Hakem R, Yoshida H, Kong YY, Zuniga-Pflucker JC, Kroemer G & Penninger JM (2001) Essential role of the mitochondrial apoptosis-inducing factor in programmed cell death. *Nature* **410**: 549-54

Jürgensmeier JM, Xie Z, Deveraux Q, Ellerby L, Bredesen D & Reed JC (1998) Bax directly induces release of cytochrome *c* from isolated mitochondria. *Proc. Nat. Acad. Sci. USA* **95**: 4997-5002

Kadenbach B (2003) Intrinsic and extrinsic uncoupling of oxidative phosphorylation. *Biochim. Biophys. Acta* **1064**: 77-94

Kandasamy K, Srinivasula SM, Alnemri ES, Thompson CB, Korsmeyer SJ, Bryant JL & Srivastava RK (2003) Involvement of proapoptotic molecules Bax and Bak in tumor necrosis factor-related apoptosis-induced ligand (TRAIL)-induced mitochondrial disruption and apoptosis: differential regulation of cytochrome *c* and Smac/DIABLO release. *Cancer Res.* **63**: 1712-21

Keane MM, Ettenberg SA, Nau MM, Russell EK & Lipkowitz S (1999) Chemotherapy augments TRAIL-induced apoptosis in breast cell lines. *Cancer Res.* **59**: 734-41

Kerr JFR, Wyllie AH & Currie AR (1972) Apoptosis: a basic biological phenomenon with wide-ranging implications in tissue kinetics. *Br. J. Cancer* **26**: 239-57

Kim JA, Kang YS & Lee YS (2003) Role of Ca^{2+}-activated Cl^- channels in the mechanism of apoptosis induced by cyclosporin A in a human hepatoma cell line. *Biochem. Biophys. Res. Commun.* **309**: 291-7

Kim SH, Vlkolinsky R, Cairns N, Fountoulakis M & Lubec G (2001) The reduction of NADH ubiquinone oxidoreductase 24- and 75-kDa subunits in brains of patients with Down syndrome and Alzheimer's disease. *Life Sci.* **68**: 2741-50

Kim JS, He L & Lemasters JJ (2003) Mitochondrial permeability transition: a common pathway to necrosis and apoptosis. *Biochem. Biophys. Res. Commun.* **304**: 463-70

Kluck RM, Esposti MD, Perkins G, Renken C, Kuwana T, Bossy-Wetzel E, Goldberg M, Allen T, Barber MJ, Green DR & Newmeyer DD (1999) The pro-apoptotic proteins, Bid and Bax, cause a limited permeabilization of the mitochondrial outer membrane that is enhanced by cytosol. *J. Cell Biol.* **147**: 809-822

Knight VA, Wiggins PM, Harvey JD & O'Brien JA (1981) The relationship between the size of mitochondria and the intensity of light that they scatter in different energetic states. *Biochim. Biophys. Acta* **637**: 146-51

Komachi K, Redd MJ & Johnson AD (1994) The WD repeats of Tup1 interact with the homeodomain protein α2. *Genes Dev.* **8**: 2857-67

Korshunov SS, Krasnikov BF, Perevernez MO & Skulachev VP (1999) The antioxidant functions of cytochrome *c*. *FEBS Lett.* **462**: 192-8

Kowaltowski AJ, Castilho RF & Vercesi AE (2001) Mitochondrial permeability transition and oxidative stress. *FEBS Lett.* **495**: 12-5

Krajewski S, Tanaka S, Takayama S, Schibler MJ, Fenton W & Reed JC (1993) Investigation into the subcellular distribution of the bcl-2 oncoprotein: residence in the nuclear envelope, endoplasmic reticulum, and outer mitochondrial membranes. *Cancer Res.* **53**: 4701-14

Kristiàn T, Gertsch J, Bates TE & Siesjo BK (2000) Characteristics of the calcium-triggered mitochondrial permeability transition in nonsynaptic brain mitochondria: effect of cyclosporin A and ubiquinone O. *J. Neurochem.* **74**: 1999-2009

Kugler S, Straten G, Kreppel F, Isenmann S, Liston P & Bahr M (2000) The X-linked inhibitor of apoptosis (XIAP) prevents cell death in axotomized CNS neurons in vivo. *Cell Death Differ.* **7**: 815-24

Lai JC & Clark JB (1989) Isolation and characterization of synaptic and non-synaptic mitochondria from mammalian brain. Neuromethods, Vol. 11: Carbohydrates and

Energy Metabolism (Boulton AA & Baker GB, eds.): 43-97. Humana Press, Clifton, NJ.

Lai JC, Leung TK & Lim L (1994) Heterogeneity of monoamine oxidase activities in synaptic and non-synaptic mitochondria derived from three brain regions: some functional implications. *Metab. Brain Dis.* **9**: 53-66

Lee HC & Wei YH (1997) Mutation and oxidative damage of mitochondrial DNA and defective turnover of mitochondria in human aging. *J. Formas. Med. Assoc.* **96**: 770-8

Lehninger AL, Nelson DL & Cox MM (1993) Principles of Biochemistry. Second Edition. Worth Publishers, New York, USA.

Li P, Nijhawan D, Budihardjo I, Srinivasula SM, Ahmad M, Alnemri ES & Wang X (1997) Cytochrome *c* and dATP-dependent formation of Apaf-1/caspase-9 complex initiates an apoptotic protease cascade. *Cell* **91**: 479-89

Lill R & Neupert W (1996) Mechanisms of protein import across the mitochondrial outer membrane. *Trends Cell Biol.* **6**: 56-61

Liu Y, Fiskum G & Schubert D (2002) Generation of reactive oxygen species by the mitochondrial electron transport chain. *J. Neurochem.* **80**: 780-7

Liu X, Kim CN, Yang J, Jemmerson R & Wang X (1996) Induction of apoptotic program in cell-free extracts: requirement for dATP and cytochrome *c*. *Cell* **86**: 147-57

Liu J, Yeo HC, Overvik-Douki E, Hagen T, Doniger SJ, Chyu DW, Brooks GA, Ames BN & Chu DW (2000) Chronically and acutely exercised rats: biomarkers of oxidative stress and endogenous antioxidants. *J. Appl. Physiol.* **89**: 21-8

Lowry OH, Rosebrough NJ, Farr AL & Randall RJ (1951) Protein measurement with the Folin phenol reagent. *J. Biol. Chem.* **193**: 265-75

MacFarlane M, Merrison W, Bratton SB & Cohen GM (2002) Proteasome-mediated degradation of Smac during apoptosis: XIAP promotes Smac ubiquitination *in vitro*. *J. Biol. Chem.* **277**: 11345-51

Madesh M, Antonsson B, Srinivasula SM, Alnemri ES & Hajnoczky G (2002) Rapid kinetics of tBID-induced cytochrome *c* and Smac/DIABLO release and mitochondrial depolarization. *J. Biol. Chem.* **277**: 5651-9

Madesh M & Hajnoczky G (2001) VDAC-dependent permeabilization of the outer mitochondrial membrane by superoxide induces rapid and massive cytochrome *c* release. *J. Cell. Biol.* **155**: 1003-1016

Maier JK, Lahoua Z, Gendron NH, Fetni R, Johnston A, Davoodi J, Rasper D, Roy S, Slack RS, Nicholson DW & MacKenzie AE (2002) The neuronal apoptosis inhibitory protein is a direct inhibitor of caspases 3 and 7. *J. Neurosci.* **22**: 2035-43

Mannella CA (1998) Conformational changes in the mitochondrial channel protein, VDAC, and their functional implications. *J. Struct. Biol.* **121**: 207-218

Margulis, L (1981) Symbiosis in Cell Evolution, (W.H. Freeman & Co., San Fransisco)

Marshansky V, Wang X, Bertrand R, Hongyu L, Duguid W, Chinnadurai G, Kanaan N, Vu MD & Wu J (2001) Proteasomes modulate balance among proapoptotic and antiapoptotic Bcl-2 family members and compromise functioning of the electron transport chain in leukemic cells. *J. Immunol.* **166**: 3130-3142

Marzo I, Brenner C, Zamzami N, Jurgensmeier JM, Susin SA, Vieira HL, Prevost MC, Xie Z, Matsuyama S, Reed JC & Kroemer G (1998) Bax and adenine nucleotide translocator cooperate in the mitochondrial control of apoptosis. *Science* **281**: 2027-31

Matsubara H & Smith EL (1962) The amino acid sequence of human heart cytochrome *c*. *J. Biol. Chem.* **237**: 3575-6

Mayer A, Neupert W & Lill R (1995) Translocation of apocytochrome *c* across the outer membrane of mitochondria. *J. Biol. Chem.* **270**: 12390-7

McDonnell MA, Wang D, Khan SM, Vander Heiden MG & Kelekar A (2003) Caspase-9 is activated in a cytochrome *c*-independent manner early during TNFalpha-induced apoptosis in murine cells. *Cell Death Differ.* **10**: 1005-15

McEnery MW, Snowman AM, Trifiletti RR & Snyder SH (1992) Isolation of the mitochondrial benzodiazepine receptor: association with the voltage-dependent anion channel and the adenine nucleotide carrier. *Proc. Nat. Acad. Sci. USA* **89**: 3170-4

Mitchell P (1961) Coupling of phosphorylation to electron and hydrogen transfer by chemiosmotic type of mechanism. *Nature* **191**: 193-216

Miwa S & Brand MD (2003) Mitochondrial matrix reactive oxygen species production is very sensitive to mild uncoupling. *Biochem. Soc. Trans.* **31**: 1300-1

Monaghan P, Robertson D, Amos TA, Dyer MJ, Mason DY & Greaves MF (1992) Ultrastructural localization of bcl-2 protein. *J. Histochem. Cytochem.* **40**: 1819-25

Montessuit S, Mazzei G, Magnenat E & Antonsson B (1999) Expression and purification of full-length human Bax alpha. *Protein Expr. Purif.* **15**: 202-206

Mootha VK, Wei MC, Buttle KF, Scorrano L, Panoutsakopoulou V, Mannella CA & Korsmeyer SJ (2001) A reversible component of mitochondrial respiratory dysfunction in apoptosis can be rescued by exogenous cytochrome *c*. *EMBO J.* **20**: 661-71

Mosser DD, Caron AW, Bourget L, Denis-Larose C & Massie B (1997) Role of the human heat shock protein hsp70 in protection against stress-induced apoptosis. *Mol. Cell Biol.* **17**: 5317-27

Murphy BM, O'Neill AJ, Adrain C, Watson RW & Martin SJ (2003) The apoptosome pathway to caspase activation in primary human neutrophils exhibits dramatically reduced requirements for cytochrome *c*. *J. Exp. Med.* **197**: 625-32

Mutisya EM, Bowling AC & Beal MF (1994) Cortical cytochrome oxidase activity is reduced in Alzheimer's disease. *J. Neurochem.* **63**: 2179-84

Nakano M (1990) Determination of superoxide radical and singlet oxygen based on the chemiluminescence of luciferin analogs. *Methods Enzymol.* **186**: 585-91

Nakashio A, Fujita N, Rokudai S, Sato S & Tsuruo T (2000) Prevention of phosphatidylinositol 3'-kinase-Akt survival signalling pathway during topotecan-induced apoptosis. *Cancer Res.* **60**: 5303-9

Nakatomi H, Kuriu T, Okabe S, Yamamoto S, Hatano O, Kawahara N, Tamura A, Kirino, T & Nakafuku M (2002) Regeneration of hippocampal pyramidal neurons after ischaemic brain injury by recruitment of endogenous neural progenitors. *Cell* **110**: 429-41

Narita M, Shimizu S, Ito T, Chittenden T, Lutz RJ, Matsuda H & Tsujimoto Y (1998) Bax interacts with the permeability transition pore to induce permeability transition and cytochrome *c* release in isolated mitochondria. *Proc. Natl. Acad. Sci. USA* **95**: 14681-6

Neame SJ, Rubin LL & Philpott KL (1998) Blocking cytochrome *c* activity within intact neurons inhibits apoptosis. *J. Cell Biol.* **142**: 1583-93

Newmeyer DD, Farschon DM & Reed JC (1994) Cell-free apoptosis in Xenopus egg extracts: inhibition by Bcl-2 and requirement for an organelle fraction enriched in mitochondria. *Cell* **79**: 353-64

Niemenen AL, Saylor AK, Tesfai SA, Herman B & Lemasters JJ (1995) Contribution of the mitochondrial permeability transition to lethal injury after exposure of hepatocytes to t-butylhydroperoxide. *Biochem. J.* **307**: 99-106

Nicholls P (1974) Cytochrome *c* binding to enzymes and membranes. *Biochim. Biophys. Acta* **346**: 261-310

Oppenheim RW (1991) Cell death during development of the nervous system. *Annu. Rev. Neurosci.* **14**: 453-501

Oster G & Wang H (2000) Reverse engineering a protein: the mechanochemistry of ATP synthase. *Biochim. Biophys. Acta* **1458**: 482-510

Ott M, Robertson JD, Gogvadze V, Zhivotovsky B & Orrenius S (2002) Cytochrome *c* release from mitochondria proceeds by a two-step process. *Proc. Nat. Acad. Sci. USA* **99**: 1259-63

Pan G, Humke EW & Dixit VM (1998) Activation of caspases triggered by cytochrome *c in vitro*. *FEBS Lett.* **426**: 151-4

Pan Z, Voehringer DW & Meyn RE (1999) Analysis of redox regulation of cytochrome *c*-induced apoptosis in a cell-free system. *Cell Death Differ.* **6**: 683-8

Pandey P, Saleh A, Nakazawa A, Kumar S, Srinivasula SM, Kumar V, Weichselbaum R, Nalin C, Alnemri ES, Kufe D & Kharbanda S (2000) Negative regulation of cytochrome *c*-mediated oligomerization of Apaf-1 and activation of procaspase-9 by heat shock protein 90. *EMBO J.* **19**: 4310-22

Pei W, Liou AK & Chen J (2003) Two caspase-mediated apoptotic pathways induced by rotenone toxicity in cortical neuronal cells. *FASEB J.* **17**: 520-2

Perier C, Bove J, Vila M & Przedborski S (2003) The rotenone model of Parkinson's disease. *Trends Neurosci.* **26**: 345-6

Petit PX, Goubern M, Diolez P, Susin SA, Zamzami N & Kroemer G (1998) Disruption of the outer mitochondrial membrane as a result of large amplitude swelling: the impact of irreversible permeability transition. *FEBS Lett.* **426**: 111-6

Pettmann B & Henderson CE (1998) Neuronal cell death. *Neuron* **20**: 633-47

Pickart CM (2001) Mechanisms underlying ubiquitination. *Annu. Rev. Biochem.* **70**: 503-33

Polster BM, Kinnally KW & Fiskum G (2001) BH3 death domain peptide induces cell type-specific mitochondrial outer membrane permeability. *J. Biol. Chem.* **276**: 37887-94

Ragan CI, Wilson MT, Darley-Usmar VM & Lowe PN (1987) Sufractionation of mitochondria and isolation of the proteins of oxidative phosphorylation. In Mitochondria: A Practical Approach (Darley-Usmar VM, Rickwood D & Wilson MT, eds.): 79-112. IRL Press, London.

Ramasarma T, Radsheed BK, Vijaya S, Puranam RS, Shivaswamy V, Gaikwad AS & Kurup CK (1992) Functions of cytochrome *c* in regulation of electron transfer and protein folding. *Indian J. Biochem. Biophys.* **29**: 173-8

Ramsay RR & Singer TP (1992) Relation of superoxide generation and lipid peroxidation to the inhibition of NADH-Q oxidoreductase by rotenone, piericidin A, and MPP^+. *Biochem. Biophys. Res. Comm.* **189**: 47-52

Rehm M, Dussmann H & Prehn JH (2003) Real-time single cell analysis of Smac/DIABLO release during apoptosis. *J. Cell Biol.* **162**: 1031-43

Renatus M, Stennicke HR, Scott FL, Liddington RC & Salvesen GS (2001) Dimer formation drives the activation of the cell death protease caspase 9. *Proc. Nat. Acad. Sci. USA* **98**: 14250-5

Riederer P, Sofic E, Rausch WD, Schmidt B, Reynolds GP, Jellinger K & Youdim MBH (1989) Transition metals, ferritin, glutathione and ascorbic acid in Parkinsonian brains. *J. Neurochem.* **52**: 515-20

Riedl SJ, Renatus M, Schwarzenbacher R, Zhou Q, Sun C, Fesiz SW, Liddington RC & Salvesen GS (2001) Structural basis for the inhibition of caspase-3 by XIAP. *Cell* **104**: 791-800

Rodriguez J & Lazebnik Y (1999) Caspase-9 and APAF-1 form an active holoenzyme. *Genes Dev.* **13**: 3179-84

Rolfe DF, Hulbert AJ & Brand MD (1994) Characteristics of mitochondrial proton leak and control of oxidative phosphorylation in the major oxygen-consuming tissues of the rat. *Biochim. Biophys. Acta* **1188**: 405-16

Roucou X, Prescott M, Devenish RJ & Nagley P (2000) A cytochrome *c*-GFP fusion is not released from mitochondria into the cytosplasm upon expression of Bax in yeast cells. *FEBS Lett.* **471**: 235-9

Ruan Q, Chen Y, Gratton E, Glaser M & Mantulin WW (2002) Cellular characterization of adenylate kinase and its isoform: two-photon excitation

fluorescence imaging and fluorescence correlation spectroscopy. *Biophys. J.* **83**: 3177-87

Saleh A, Srinivasula SM, Balkir L, Robbins PD & Alnemri ES (2000) Negative regulation of the Apaf-1 apoptosome by Hsp70. *Nat. Cell Biol.* **2**: 476-83

Samartsev VN, Simonyan RA, Markova OV, Mokhova EN & Skulachev VP (2000) Comparative study on uncoupling effects of laurate and lauryl sulfate on rat liver and skeletal muscle mitochondria. *Biochim. Biophys. Acta.* **1459**: 179-90

Sanchez H, N'Guessan B, Ribera F, Ventura-Clapier R & Bigard X (2003) Cyclosporin A treatment increases rat soleus muscle oxidative capacities. *Muscle Nerve* **28**: 324-9

Scarlett JL & Murphy MP (1997) Release of apoptogenic proteins from the mitochondrial intermembrane space during the mitochondrial permeability transition. *FEBS Lett.* **418**: 282-286

Scarpulla RC, Agne KM & Wu R (1981) Isolation and structure of a rat cytochrome *c*. *J. Biol. Chem.* **256**: 6480-6

Schapira AH, Cooper JM, Dexter D, Clark JB, Jenner P & Marsden CD (1990) Mitochondrial complex I deficiency in Parkinson's disease. *J. Neurochem.* **54**: 823-7

Scheffler IE (1999) Mitochondria. Wiley-Liss, New York, USA.

Seidl R, Bajo M, Bohm K, LaCasse EC, MacKenzie AE, Cairns N & Lubec G (1999) Neuronal apoptosis inhibitory protein (NAIP)-like immunoreactivity in brains of adult patients with Down syndrome. *J. Neural Transm. Suppl.* **57**: 283-91

Shepherd D & Garland PB (1969) The kinetic properties of citrate synthase from rat liver mitochondria. *Biochem. J.* **114**: 597-610

Shimizu S, Ide T, Yanagida T & Tsujimoto Y (2000) Electrophysiological study of a novel large pore formed by Bax and the voltage-dependent anion channel that is permeable to cytochrome *c*. *J. Biol. Chem.* **275**: 12321-12325

Shimizu S, Narita M & Tsujimoto Y (1999) Bcl-2 family proteins regulate the release of apoptogenic cytochrome *c* by the mitochondrial channel VDAC. *Nature* **399**: 483-7

Shiozaki EN, Chai J, Rigotti DJ, Reidl SJ, Li P, Srinivasula SM, Alnemri ES, Fairman R & Shi Y (2003) Mechanism of XIAP-mediated inhibition of caspase-9. *Mol. Cell* **11**: 519-27

Sipos I, Tretter L & Adam-Vizi V (2003) Quantitative relationship between inhibition of respiratory complexes and formation of reactive oxygen species in isolated nerve terminals. *J. Neurochem.* **84**: 112-8

Siskind LJ, Kolesnik RN & Colombini M (2002) Ceramide channels increase the permeability of the mitochondrial outer membrane to small proteins. *J. Biol. Chem.* **277**: 26796-803

Skulachev VP (1996) Why are mitochondria involved in apoptosis? Permeability transition pores and apoptosis as selective mechanisms to eliminate superoxide-producing mitochondria and the cell. *FEBS Lett.* **397**: 7-10

Slee EA, Harte MT, Kluck RM, Wolf BB, Casiano CA, Newmeyer DD, Wang HG, Reed JC, Nicholson DW, Alnemri ES, Green DR & Martin SJ (1999) Ordering the cytochrome *c*-initiated caspase cascade: hierarchical activation of caspases-2, -3, -6, -7, -8 and –10 in a caspase-9-dependent manner. *J. Cell Biol.* **144**: 281-92

Smale G, Nichols NR, Brady DR, Finch CE & Horton WE Jr. (1995) Evidence for apoptotic cell death in Alzheimer's disease. *Exp. Neurol.* **133**: 225-30

Sokolik CW & Cohen RE (1992) Ubiquitin conjugation to cytochromes *c*. Structure of the yeast iso-1 conjugate and possible recognition determinants. *J. Biol. Chem.* **267**: 1067-71

Srinivasula SM, Ahmed M, Fernandez_Alnemri T & Alnemri ES (1998) Autoactivation of procaspase-9 by Apaf-1-mediated oligomerization. *Mol. Cell* **1**: 949-57

Srinivasula SM, Hegde R, Saleh A, Datta P, Shiozaki E, Chai J, Lee RA, Robbins PD, Fernandes-Alnemri T, Shi Y & Alnemri ES (2001) A conserved XIAP-interaction motif in caspase-9 and Smac/DIABLO regulates caspase activity and apoptosis. *Nature* **410**: 112-6

Stennicke HR, Deveraux QL, Humke EW, Reed JC, Dixit VM & Salvesen GS (1999) Caspase-9 can be activated without proteolytic processing. *J. Biol. Chem.* **274**: 8359-62

Stennicke HR & Salvesen GS (1998) Properties of the caspases. *Biochim. Biophys. Acta* **1387**: 17-31

Stewart VC, Sharpe MA, Clark JB & Heales SJ (2000) Astrocyte-derived nitric oxide causes both reversible and irreversible damage to the neuronal mitochondrial respiratory chain. *J. Neurochem.* **75**: 694-700

St-Pierre J, Buckingham JA, Roebuck SJ & Brand MD (2002) Topology of superoxide production from different sites in the mitochondrial electron transport chain. *J. Biol. Chem.* **277**: 44784-90

Suzuki Y, Imai Y, Nakayama H, Takahashi K, Takio K & Takahashi R (2001) A serine protease, HtrA2, is released from the mitochondria and interacts with XIAP, inducing cell death. *Mol. Cell* **8**: 613-21

Suzuki Y, Nakabayashi Y & Takahashi R (2001b) Ubiquitin-protein ligase activity of X-linked inhibitor of apoptosis protein promotes proteasomal degradation of caspase-3 and enhances its anti-apoptotic effect in Fas-induced cell death. *Proc. Nat. Acad. Sci. USA* **98**: 8662-7

Thomas LB, Gates DJ, Richfield EK, O'Brien TF, Schweiotzer JB & Steindler DA (1995) DNA end labelling (TUNEL) in Huntington's disease and other neuropathological conditions. *Exp. Neurol.* **133**: 265-72

Thompson CB (1995) Apoptosis in the pathogenesis and treatment of disease. *Science* **267**: 1456-62

Thornberry NA & Lazebnik Y (1998) Caspase: enemies within. *Science* **281**: 1312-6

Tsujimoto Y & Shimizu S (2000) VDAC regulation by the Bcl-2 family of proteins. *Cell Death Differ.* **7**: 1174-81

Tuominen Ek, Zhu K, Wallace CJ, Clark-Lewis I, Craig DB, Rytomaa M & Kinnunen PK (2001) ATP induces a conformational change in lipid-bound cytochrome *c*. *J. Biol. Chem.* **276**: 19356-62

Turrens JF, Alexandre A & Lehninger AL (1985) Ubisemiquinone is the electron donor for superoxide formation by complex III of heart mitochondria. *Arch. Biochem. Biophys.* **237**: 408-14

Turrens JF & Boveris A (1980) Generation of superoxide anion by the NADH dehydrogenase of bovine heart mitochondria. *Biochem. J.* **191**: 421-7

van Gurp M, Festjens N, van Loo G, Saelens X & Vandenbeele P (2003) Mitochondrial intermembrane proteins in cell death. *Biochem. Biophys. Res. Commun.* **304**: 487-97

van Loo G, van Gurp M, Depuydt B, Srinivasula SM, Rodriguez I, Alnemri ES, Gevaert K, Vandekerckhove J, Declercq W & Vandenbeele P (2002) The serine protease Omi/HtrA2 is released from mitochondria during apoptosis. Omi interacts with caspase-inhibitor XIAP and induces enhanced caspase activity. *Cell Death Differ.* **9**: 20-6

Vander Heiden MG & Thompson CB (1999) Bcl-2 proteins: regulators of apoptosis or of mitochondrial homeostasis? *Nat Cell Biol* **1**: E209-E216

Vassault A (1983) L-Lactate dehydrogenase. UV method with pyruvate and NADH. In Methods of Enzymatic Analysis (Bergmeyer J & Grassl M, eds.): 118-26. Verlag Chemie GmbH, Weinheim.

Verhagen AM, Coulson EJ & Vaux DL (2001) Inhibitor of apoptosis proteins and their relatives: IAPs and other BIRPs. *Genome Biol.* **2**: reviews 3009.1-3009.10

Verhagen AM, Ekert PG, Pakush M, Silke J, Connolly LM, Reid GE, Moritz RL, Simpson RJ & Vaux DL (2000) Identification of DIABLO, a mammalian protein that promotes apoptosis by binding to and antagonizing IAP proteins. *Cell* **102**: 43-53

Von Ahsen O, Renken C, Perkins G, Kluck RM, Bossy-Wetzel E & Newmeyer DD (2000) Preservation of mitochondrial structure and function after Bid- or Bax-mediated cytochrome *c* release. *J. Cell. Biol.* **150**: 1027-36

Walz W & Mukerji S (1998) Lactate release from cultured astrocytes and neurons: a comparison. *Glia* **1**: 366-70

Waterhouse NJ, Goldstein JC, von Ahsen O, Schuler M, Newmeyer DD & Green DR (2001) Cytochrome *c* maintains mitochondrial transmembrane potential and ATP generation after outer membrane permeabilization during the apoptotic process. *J. Cell Biol.* **153**: 319-28

Waterhouse NJ, Ricci JE & Green DR (2002) And all of a sudden it's over: mitochondrial outer-membrane permeabilization in apoptosis. *Biochimie* **84**: 113-21

Wharton DC & Tzagoloff A (1967) Cytochrome oxidase from beef heart mitochondria. *Methods Enzymol.* **10**: 245-50

Więckowski MR, Vyssokikh M, Dymkowska D, Antonsson B, Brdiczka D & Wojtczak L (2001) Oligomeric C-terminal truncated Bax preferentially releases

cytochrome c but not adenylate kinase from mitochondria, outer membrane vesicles and proteoliposomes. *FEBS Lett.* **505**: 453-9

Wolter KG, Hsu YT, Smith CL, Nechushtan A, Xi XG & Youle RJ (1997) Movement of Bax from the cytosol to mitochondria during apoptosis. *J. Cell Biol.* **139**: 1281-1292

Woolley GA & Wallace BA (1992) Model ion channels: gramicidin and alamethicin. *J. Membr. Biol.* **129**: 109-136

Xu D, Bureau Y, McIntyre DC, Nicholson DW, Liston P, Zhu Y, Fong WG, Crocker SJ, Korneluk RG & Robertson GS (1999) Attenuation of ischaemia-induced cellular and behavioural deficits by X chromosome-linked inhibitor of apoptosis protein overexpression in the rat hippocampus. *J. Neurosci.* **19**: 5026-33

Yang JC & Cortopassi GA (1998) Induction of the mitochondrial permeability transition causes release of the apoptogenic factor cytochrome *c*. *Free Radic. Biol. Med.* **24**: 624-31

Yang QH, Church-Hajduk R, Ren J, Newton ML & Du C (2003) Omi/HtrA2 catalytic cleavage of inhibitor of apoptosis (IAP) irreversibly inactivates IAPs and facilitates caspase activity in apoptosis. *Genes Dev.* **17**: 1487-96

Yang Y, Fang SY, Jensen JP, Weissman AM & Ashwell JD (2000) Ubiquitin protein ligase activity of IAPs and their degradation in proteasomes in response to apoptotic stimuli. *Science* **288**: 874-7

Yang J, Liu X, Bhalla K, Kim C, Ibrado A, Cai J, Peng T, Jones DP & Wang X (1997) Prevention of apoptosis by Bcl-2: release of cytochrome *c* blocked. *Science* **275**: 1129-32

Yang Y & Yu X (2003) Regulation of apoptosis: the ubiquitous way. *FASEB J.* **17**: 790-9

Yuan J & Yanker BA (2000) Apoptosis in the nervous system. *Nature* **407**: 802-9

Zamzami N, Marchetti P, Castedo M, Zanin C, Vayssiere JL, Petit PX & Kroemer G (1995) Reduction in mitochondrial potential constitutes an early irreversible step of programmed lymphocyte death *in vivo*. *J. Exp. Med.* **181**: 1661-72

Zeiss CJ (2003) The apoptosis-necrosis continuum: insights from genetically altered mice. *Vet. Pathol.* **40**: 481-95

Zhang H, Heim J & Meyhack B (1998) Redistribution of Bax from cytosol to membranes is induced by apoptotic stimuli and is an early step in the apoptotic pathway. *Biochem. Biophys. Res. Commun.* **251**: 454-459

Zhivotovsky B, Orrenius S, Brustugun OT & Doskeland SO (1998) Injected cytochrome ***c*** causes apoptosis. *Nature* **391**: 449-50

Zhu Y, Xu H & Huang K (2002) Mitochondrial permeability transition and cytochrome *c* release induced by selenite. *J. Inorg. Biochem.* **90**: 43-50

Zou H, Li Y, Liu X & Wang X (1999) An Apaf-1.cytochrome *c* multimeric complex is a functional apoptosome that activates procaspase-9. *J. Biol. Chem.* **274**: 11549-56